Exploring the role of local glucocorticoid metabolism in osteoblasts during chronic inflammation

By: **Syeda Fareed**

A thesis submitted to the University of Birmingham for the degree

of

Masters (MSc) by Research in Metabolism and Systems Research

Supervisor: **Dr Rowan Hardy**

Institute of Metabolism and Systems Research

College of Medical and Dental Sciences

University of Birmingham

October 2021

Abstract

Glucocorticoids (GCs) are extensively utilised in the management of chronic inflammatory polyarthritides, such as rheumatoid arthritis (RA) due to profound anti-inflammatory properties. However, their prolonged use results in the development of adverse effects, which limit their therapeutic application. Such adverse effects include systemic bone loss, which may be mediated by 11β-hydroxysteroid dehydrogenase type 1 (11β-HSD1) – an enzyme which works bidirectionally to convert inactive GCs to their active counterparts. 11β-HSD1 is highly expressed in osteoblasts (OBs) and potently induced by combinations of GCs and inflammatory factors. Hence, inhibiting 11β-HSD1 may be an effective mechanism by which the side effect profile of GCs can be managed. This thesis studied the role local steroid metabolism has on the inflammatory suppression of osteoblast differentiation, with the aim to provide valuable insights into how endogenous glucocorticoids mediate bone protection in response to inflammation and inform future therapeutic approaches. Primary cultures of human osteoblasts were established and the inflammatory suppression of their differentiation and function was characterised using alizarin red staining, RT-PCR and ELISA. The role of steroid metabolism in this process in response to endogenously derived steroids in combination with selective inhibitors of steroid metabolism was assessed by TLC using radio-labelled steroids. These findings were examined *in vivo* using mouse models of chronic inflammation with osteoblast targeted disruption of steroid metabolism, where the bone phenotype was assessed by micro-CT. Our results validated strong synergistic upregulation of 11β-HSD1 in GC activation in OBs in response to pro-inflammatory mediators and in combination with GCs. This increase in 11β-HSD1 was shown to be functional, where GCs exerted a negative effect on OB formation as they suppressed collagen formation and suppressed osteoblast differentiation. Some suppression of pro-inflammatory mediators was also observed. However, the murine models show limited changes in the architecture of cortical bone following GC treatment, implying that 11β-HSD1 is not influencing cortical bone metabolism over the timeframes studied in this thesis. Whilst limited changes were seen in cortical bone, further analysis of trabecular bone and other bone parameters are required to fully understand the role of therapeutic GCs.

Acknowledgments

I would like to express my heartfelt deepest gratitude to Dr Rowan Hardy for accommodating me in his lab and allowing me to be part of his research group. Rowan, without your continuous support, guidance and understanding, this thesis would not have been possible. You have inspired me to consider Translational Medicine as a career. Frankly speaking, you are the best supervisor that a student can ask for. Thank you for reassuring me in periods of stress and never giving up on me.

I would also like to thank a crucial former member of the Hardy lab: Dr Chloe Fenton, who helped me master all the protocols used as part of my project and the animal work she did, without which I would have no *in vivo* data.

I would also like to thank my friends and house mates for the constant check ins, encouragement, and the daily dose of motivation through memes. Special thanks to my best mates who supported me through all-nighters and did not let me give up.

I would like to thank my parents for their support and encouragement, and my brother for his constant reminders to ‘just get on with it’.

Table of Contents

List of Figures

List of Tables

Abbreviations

11β-HSD	11β-hydroxysteroid dehydrogenase
AC	Adenylate cyclase
ACTH	Adrenocorticotropic hormone
AF-	Activation function-
ALP	Alkaline phosphatase
AP-1	Activating/Activator protein 1
ARE	AU-rich element
ATP	Adenosine triphosphate
AU	Arbitrary units
BMU	basic multicellular unit
BSP	Bone sialoprotein
CAIA	Collagen-antibody-induced arthritis
cAMP	Cyclic adenosine monophosphate
CaSR	Calcium sensing receptor
cbfa1	Core-binding factor A1
CBG	Corticosteroid-binding globulin
CBP	CREB protein binding protein
cDNA	Complementary DNA
CEBP	CCAAT/enhancer-binding protein
CIA	Collagen-induced arthritis
CII	Type II homologous collagen
Col1	Type 1 collagen
COX	Cyclooxygenase
CREB	cAMP-response element binding

CRH	Corticotropin releasing hormone
CT	Cycle threshold
CTSK	Cathepsin K
CTX-1	Carboxy-terminal cross-linked telopeptide of type 1 collagen
DBD	DNA-binding domain
DC-STAMP	Dendritic cell–specific transmembrane protein
DKK-1	Dickkopf-1
DMARD	disease modifying anti-rheumatic drug
DMEM	Dulbecco’s Modified Eagle Medium
DNA	Deoxyribonucleic acid
DUSP1	Dual specificity phosphatase 1
ELISA	Enzyme linked immunosorbent assays
ERK	Extracellular signal-regulated kinase
ESR	erythrocyte sedimentation rate
FBS	Fetal bovine serum
FKBP	FK506 binding protein
FLS	fibroblast like synoviocytes
FZ	Frizzled
GC	Glucocorticoid
GE	Glycyrrhetinic acid
GILZ	Glucocorticoid-induced leucine zipper
GR	Glucocorticoid receptor
GRE	GC response element
H6PDH	Hexose-6-phosphate dehydrogenase
HA	Hydroxyapatite

HCL	Hydrochloric acid
hCOLIA1	Human Pro-Collagen I α1
hIL-6	Human IL-6
HPA	Hypothalamic pituitary adrenal
HRP	Horseradish peroxidase
HSCs	haematopoietic stem cells
HSP	Heat shock protein
ICAM-1	Intercellular adhesion molecule 1
IFN-γ	Interferon-gamma
IGF-1	Insulin-like growth factor-1
IL-	Interleukin-
IL-	Interleukin-
Iκβ	Inhibitor of nuclear factor kappa B
iNOS	Inducible nitric oxidase synthase
KO	Knockout
LBD	Ligand-binding C-terminal domain
LDL	Low-density lipoprotein
LPS	Lipopolysaccharides
LRP	Low-density lipoprotein-related protein
MAPK	Mitogen-activated protein kinase
MCP-1	Monocyte chemoattractant protein-1
M-CSF	Macrophage-colony stimulating factor
MHC	Major histocompatibility complex
MIP-2	Macrophage inflammatory protein 2
MKP-1	Mitogen-activated protein kinase phosphatase-1

MR	Mineralocorticoid receptor
mRNA	Messenger RNA
NADPH	Nicotinamide adenine dinucleotide phosphate
NFAT	Nuclear factor of activated T cell
NF-κB	Nuclear factor kappa B
nGRE	Negative GRE
NTD	Amino-terminal domain
OD	Optical density
OPG	Osteoprotegerin
OPN	Osteopontin
OSC	Osteocalcin
P38MAPK	p38 mitogen-activated protein kinase
PBS	Phosphate buffer saline
PDGF	Platelet-derived growth factor
PGE_2	Prostaglandin E_2
pGRE	Positive GRE
PI3K	Phosphoinositide 3-kinase
PK	Protein kinase
PLC	Phospholipase C
POMC	Proopiomelanocortin
PTH	parathyroid hormone
PTH1R	PTH type 1 receptor
PVN	Paraventricular nucleus
qRT-PCR	Quantitative reverse transcription PCR
RA	Rheumatoid arthritis

RANKL	receptor activator for NF-κβ ligand
RUNX2	Runt-related transcription factor 2
RXR	Retinoid X receptor
SCN	Suprachiasmatic nuclei
SLPI	Secretory leukocyte protease inhibitor
SOST	sclerostin
StAR	Steroidogenic acute regulatory
Stat3	Signal transduction and activator of transcription 3
SWI/SNF	SWItch/Sucrose Non-Fermentable
T2DM	Type 2 diabetes mellitus
TGF-β1	Transforming growth factor-β1
Th-	T-helper
TLC	Thin layer chromatography
TMB	Tetramethylbenzidine
TNF-Tg	TNF-transgenic
TNF-α	Tumour necrosis factor-α
TNF-α	Tumour necrosis factor-α
TRAF	TNF-receptor associated factor
TRAP	Tartrate-resistant acid phosphatase
T-reg	T-regulatory
TTP	Tristetraprolin
UTR	Untranslated region
VDR	Vitamin D receptor
WNT	Wingless
WT	Wildtype

Chapter 1: Introduction

1.1. Glucocorticoids in the management of chronic inflammation

Chronic inflammatory polyarthritides such as rheumatoid arthritis (RA) are conditions characterised by dysregulated inflammatory processes in the synovial joints, which are accompanied by cartilage damage, juxta-articular bone loss and extra-articular features including inflammatory osteoporosis and muscle atrophy (Van Staa et al., 2006; Gullick and Scott, 2011; Hafez et al., 2011). The profound anti-inflammatory properties of glucocorticoids (GCs) have made them the first choice of therapeutics for the management of chronic inflammatory diseases. However, their prolonged use results in the development of adverse off target effects, which limit their therapeutic application (Silverstein et al., 2000; Smolen et al., 2016; Littlejohn and Monrad, 2018). In this thesis, we explore the role of GCs and their local metabolism and activation within bone forming cells known as osteoblasts, in mediating the adverse off target actions of GCs in the context of chronic inflammatory polyarthritis.

1.2. Discovery of glucocorticoids

The physiological and biochemical discovery of GCs began in the early 20th century with Philip Hench and Edward Kendall who investigated the ability of GCs to suppress the clinical manifestations of inflammation-associated conditions, particularly rheumatoid arthritis (RA) (Hench et al., 1949). In 1950, Hench and Kendall in tandem with Tadeusz Reichstein, a Swiss scientist who also independently isolated cortisone from the adrenal glands, were presented the Nobel Prize in Physiology and Medicine. Since their discovery, GCs have been the focal point of many studies due to their anti-inflammatory therapeutic potential in human disease.

At present, synthetic GCs form the basis for the management of numerous inflammatory and autoimmune diseases, with around 1% of the UK and US adult population receiving GCs (van Staa et al., 2002; Overman et al., 2013; Laugesen et al., 2019). Despite their success, the use of systemic GC therapy is hampered due to the occurrence of adverse reactions in approximately 70% of patients. These include abdominal obesity, diabetes, hypertension, muscle wasting and osteoporosis (van Staa et al., 2002; Curtis et al., 2006; Fardet et al., 2007). Hence, there is a clear need for the development of targeted GC therapies where the therapeutic outcome is optimised, and the risk of adverse effects is minimised.

1.2.1. Physiological functions of endogenous glucocorticoids

Endogenous glucocorticoids are a class of steroid hormones which constitute an integral component of glucose homeostasis in both the resting state and the stress response. Cortisol, widely known as the stress hormone, is the principal GC in humans along with its inactive metabolite, cortisone (Arlt and Stewart, 2005; Nicolaides et al., 2015).

GCs also function to suppress glucose uptake and utilisation in skeletal muscle and adipose tissue (Di Dalmazi et al., 2012; Kuo et al., 2013). Moreover, GCs increase hepatic glycogen storage, and suppress insulin-mediated glycogen synthesis (Stalmans and Laloux, 1979; Ruzzin et al., 2005). GCs can also impact the function of pancreatic α-cells to increase the secretion of glucagon, which in turn increases the blood glucose levels (Wise et al., 1973; Rafacho et al., 2014). The resulting rise in serum glucose can be used to fuel the brain so that maximal function can be promoted during stress. Further effects of GCs on glucose homeostasis in peripheral tissues are outlined in illustrated form in figure 1.1.

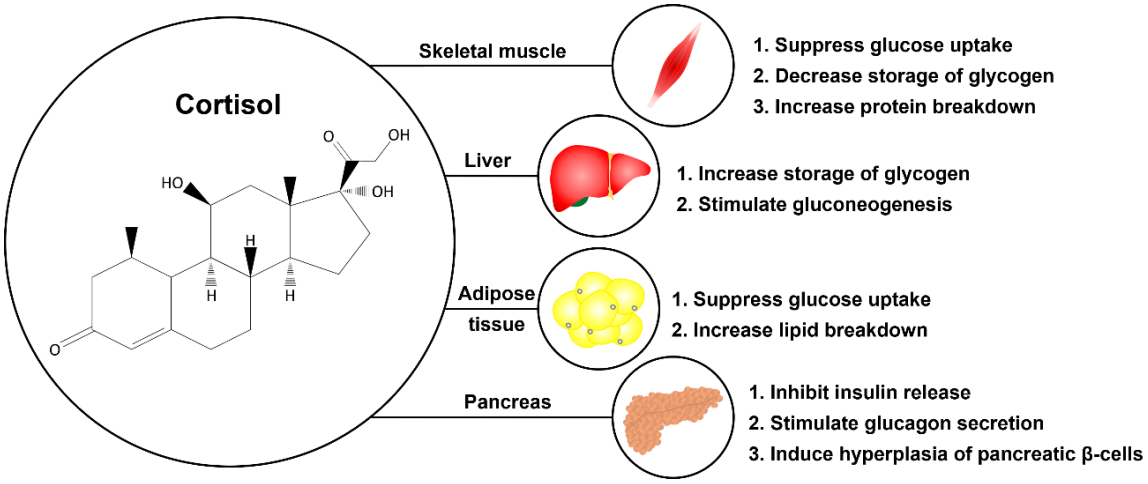

Figure 1.1: Actions of glucocorticoids (GCs) on glucose homeostasis in peripheral tissues

In stressful conditions, GCs regulate physiological process to ensure a constant glucose supply is available for the brain. To ensure this sustained supply, GCs regulate glucose metabolism in different organs. This is achieved by decreasing glucose uptake peripherally and stimulating hepatic gluconeogenesis. More specifically, in skeletal muscle, GCs suppress insulin-mediated glucose uptake and storage of glycogen, and induce protein degradation (through muscle wasting), which provides substrates for gluconeogenesis. In the liver, GCs stimulate glycogen storage, increase gluconeogenesis, and suppress rate-limiting enzymes regulated by insulin. The latter results in inhibition of insulin-mediated glycogen synthesis. In adipose tissue, GCs exert similar effects to those seen in skeletal muscle, i.e., decreasing glucose uptake and increasing lipolysis to generate precursors for gluconeogenesis. The function of pancreatic β-cells is inhibited by GCs, resulting in suppression of insulin secretion, whilst α-cells are stimulated to increase production of glucagon.

Glucocorticoids are essential to life. Deficiencies in the endogenous GC, cortisol, result in Addisonian crisis and death secondary to low blood glucose, loss of permissive blood pressure and elevated potassium levels (Bornstein et al., 2016; Oprea et al., 2019). GCs are also necessary for the neonatal development and function of many organs, with the heart, lungs and bone being the principal targets. The importance of glucocorticoids in lung development have been highlighted through studies using global glucocorticoid receptor (GR) deficient mice, which die within a few hours post-birth because of respiratory failure (Cole et al., 1995). Similarly, endogenous GR signalling is vital for development and function of

cardiomyocyte and vascular smooth muscle with GR deletion resulting in short, disorganised myofibrils, and an inability to induce genes required for contraction, calcium handling and energy metabolism (Rog-Zielinska et al., 2013; Oakley and Cidlowski, 2015). GCs are also critical for bone homeostasis (described in section 1.4.6.).

1.2.2. Suppression of inflammation by endogenous GCs

Endogenous GCs possess potent anti-inflammatory and immunosuppressive properties through the suppression of a wide array of pro-inflammatory signalling pathways, (including NF-ĸB, AP-1 and p38MAPK) and induction of resolving factors mediators (such as annexins, IL-10, GILZ and DUSP-1) (Yang-Yen et al., 1990; Nissen, 2000; Nelson et al., 2003; Miller et al., 2005; Hoppstädter and Ammit, 2019). These pathways are discussed in greater detail in section 1.3.

1.2.3. Regulation of glucocorticoid synthesis

The hypothalamic pituitary adrenal (HPA) axis mediates the systemic release of GCs in response to various basal circadian factors and physiological stressors (see figure 1.2). Under basal (unstressed) conditions, the adrenal glands synthesise and release GCs into the blood in a circadian rhythm, with GC levels peaking in the morning in humans upon wakening. This peak is observed in the beginning of the night in rodents and other nocturnal animals.

During stressful conditions, increased circulating GCs are glucose mobilising, inhibiting protein synthesis, stimulating proteolysis within the muscle, and promoting gluconeogenesis in the liver (Exton, 1979; Kraus-Friedmann, 1984).

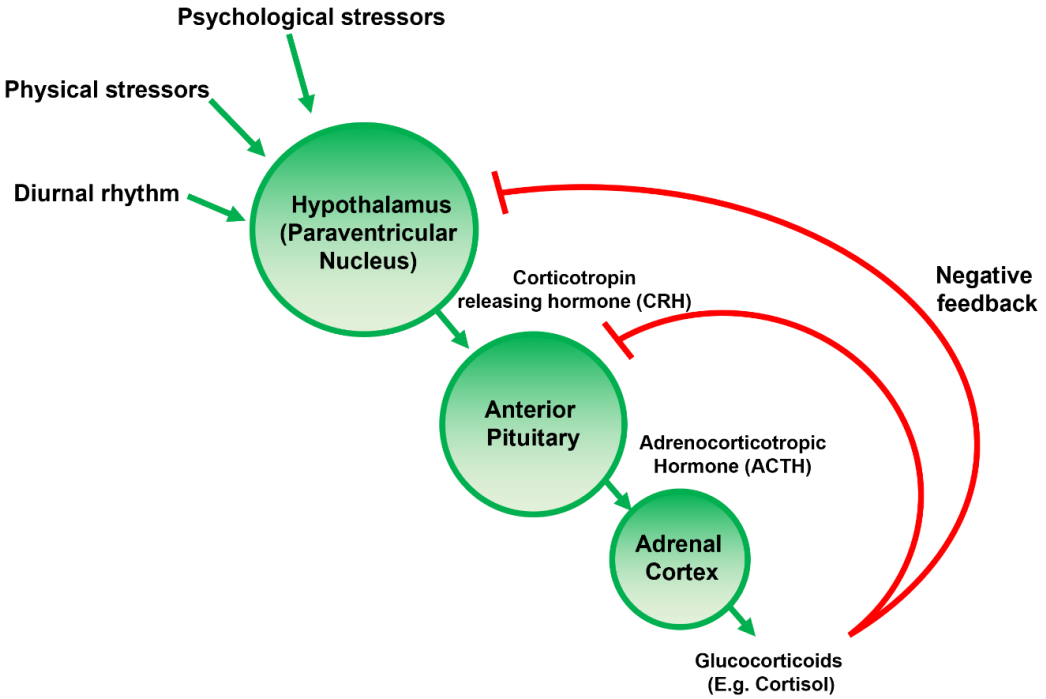

Figure 1.2: The hypothalamic pituitary adrenal (HPA) axis

The HPA axis contains different cell types which secrete distinct hormones. HPA axis is activated by diurnal rhythm, psychological and physical stressors. Neurones in the paraventricular nucleus (PVN) of the hypothalamus are responsible for the synthesis and secretion of corticotropin releasing hormone (CRH). CRH stimulates the anterior pituitary gland to produce adrenocorticotropic hormone (ACTH). ACTH is released into the general circulation, which in turn, triggers the synthesis and release of glucocorticoids (GCs) from the cortex of the adrenal gland GC, such as cortisol which generate a stress response. Cortisol also exerts negative feedback on endocrine cells of the anterior pituitary and on the CRH neurones of the hypothalamic PVN to prevent its overproduction.

Activation of the HPA axis invokes the production of corticotrophin-releasing hormone (CRH) from the hypothalamic paraventricular nucleus (PVN) neurons, which project to the median eminence where CRH is secreted into the hypophyseal portal circulation. CRH then travels to the anterior pituitary gland, where CRH binds to G-protein coupled receptors on corticotroph cells. CRH-cognate receptor interaction activates adenylate cyclase (AC) release and stimulates the transcription of the proopiomelanocortin (POMC) gene, which encodes adrenocorticotropic hormone (ACTH) (Aguilera, 1994). ACTH is then packaged into secretory vesicle

and released into the systemic circulation via exocytosis. ACTH vesicles travel to cortex of the adrenal gland. At the adrenal cortex, ACTH binds to the melanocortin 2 receptors in the zona fasciculata (Hadley and Haskell-Luevano, 2006). This interaction results in the activation of AC cascade leading to an increase in cyclic adenosine monophosphate (cAMP) production and the stimulation of cholesterol biosynthesis which precedes GC production (Simpson and Waterman, 1988). Cholesterol is the precursor for GC production, which gets translocated from the intracellular stores to the outer mitochondrial membrane, from where steroidogenic acute regulatory (StAR) proteins promote the movement of cholesterol into the mitochondrial inner membrane. Cholesterol is then converted to an immediate precursor called pregnenolone, from which mineralocorticoids, GCs and androgens can be synthesized via the action of various key enzymes (see figure 1.3). Once synthesized, GCs are released into the circulation and can travel to different targets (see figure 1.1).

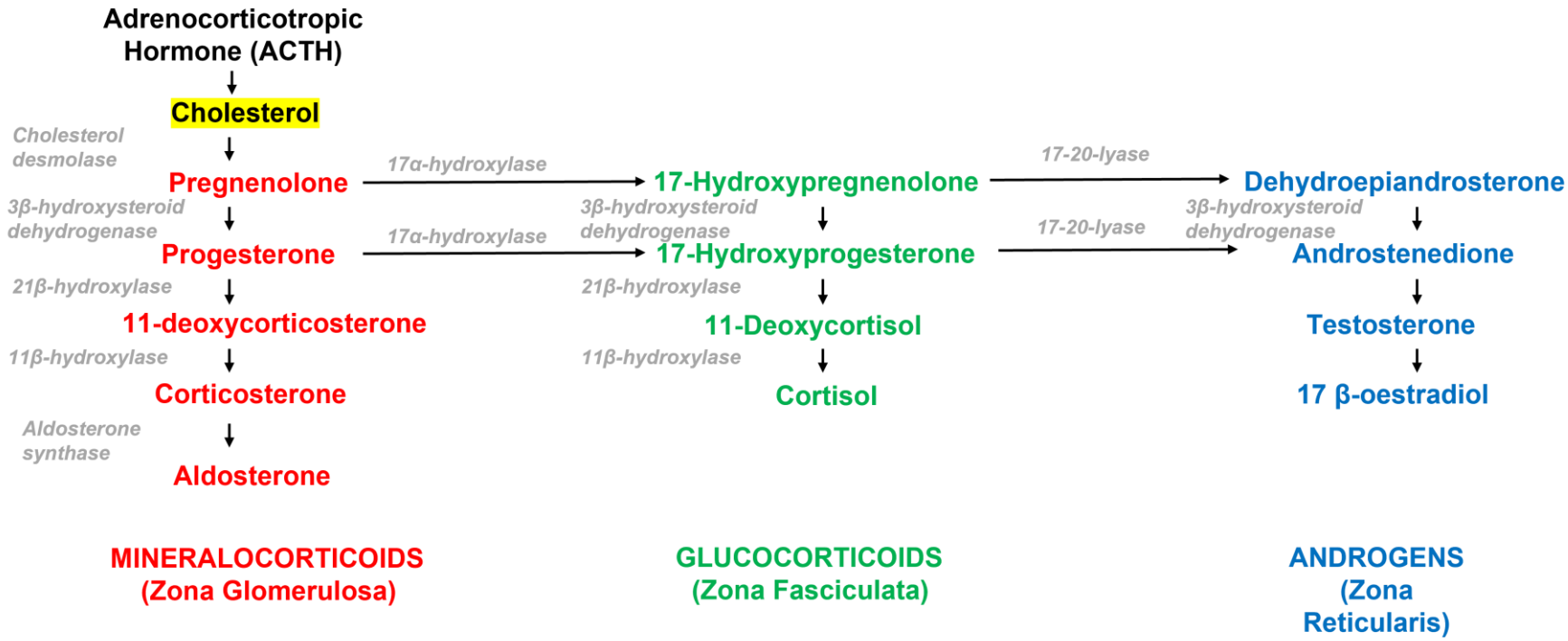

Adrenal steroid hormones are synthesised from cholesterol (highlighted in yellow). In the zona glomerulosa, zona fasciculata and zona reticularis, a number of enzymatic reactions result in the production of mineralocorticoids, glucocorticoids and androgens respectively. These pathways are indicated in red, green and blue respectively. Enzymes are indicated in grey italics.

Corticosteroids have the capacity to regulate their own synthesis by a negative feedback mechanism, stopping the HPA axis from becoming overstimulated. To achieve this, GCs use both non-genomic (fast) and genomic (delayed) mechanisms. Non-genomic mechanisms induce endocannabinoid signalling which causes a reduction in the release of hypothalamic CRH, thereby decreasing the activity of CRH-containing hypothalamic neurones (Evanson et al., 2010). However, genomic mechanisms work by directly suppressing the expression of CRH and POMC in the parvocellular neurones and pituitary corticotropic cells respectively (Erkut et al., 1998; Parvin et al., 2017).

1.2.3.1. The HPA axis and circadian CLOCK system

The HPA axis secretory activity is regulated by a complex crosstalk between the HPA axis and the circadian CLOCK system which is the suprachiasmatic nuclei (SCN) of the hypothalamus (see figure 1.4). This central component receives light/ dark signal via afferent neurones from the retina through the retino-hypothalamic tract and stimulates the diurnal release of GCs from the adrenal glands. The central component communicates with the HPA axis via efferent neurones which project from the SCN to the PVN. The peripheral CLOCKs, found in the adrenal glands, are modulated by the central CLOCK via the activation of sympathetic nervous system contributing to GC secretion. Circulating GCs influence the circadian rhythm by causing reset or delays of the peripheral CLOCKs via the transcription of CLOCK-related genes, thus playing an important role in adjusting the body's activity during periods of stress. The peripheral CLOCKS can impact the production of GCs in local tissues, creating a local feedback system which counter regulates the influence of the circadian CLOCKs on the HPA axis (Ulrich-Lai et al., 2006).

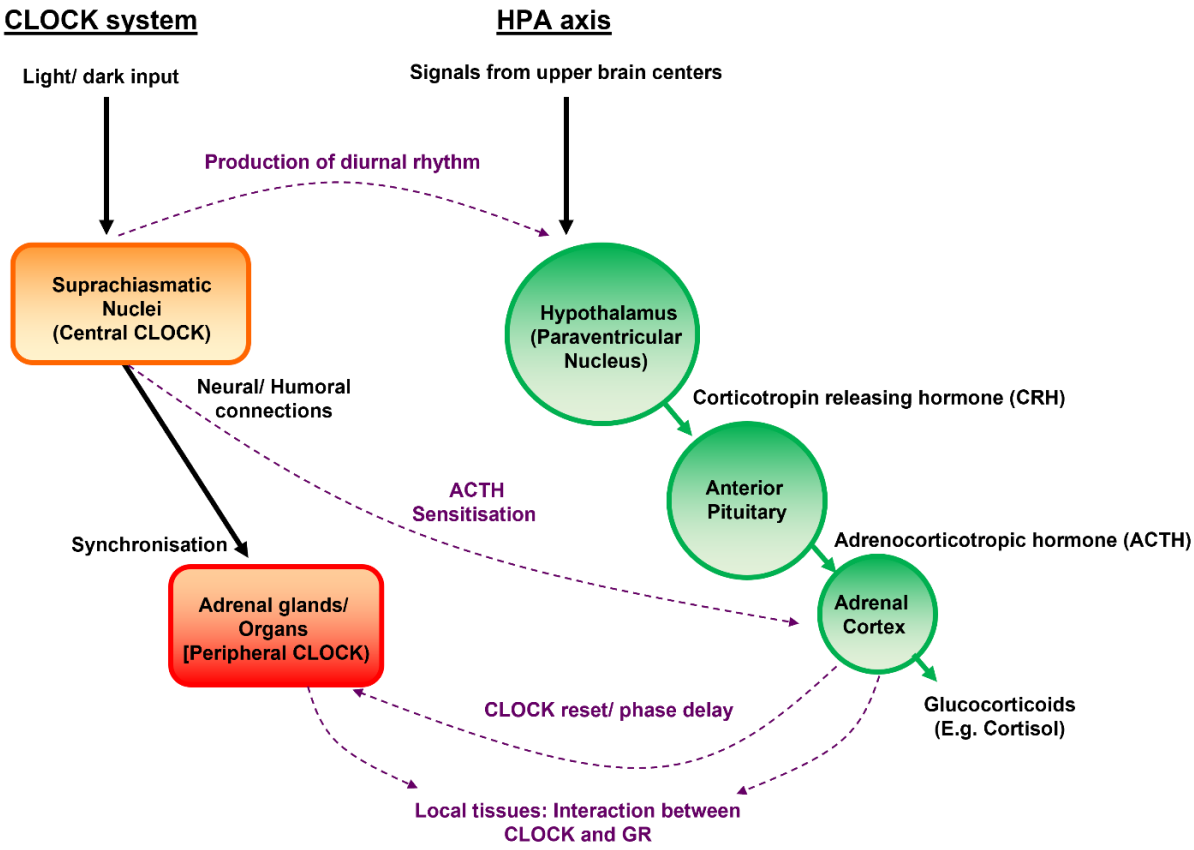

Figure 1.3: Circadian regulation of the HPA axis

The suprachiasmatic nuclei (SCN), known as the central CLOCK, receives light/dark input and stimulates diurnal release of glucocorticoids (GCs) from the adrenal glands. The SCN, through the sympathetic nervous system, regulates the adrenal glands and other organs of the HPA axis which contain peripheral CLOCKs. These peripheral CLOCKs also contribute to the rhythmic production of GCs in local tissues, which can counteract the role of the central CLOCK on the HPA axis. The circulating GCs stimulate synthesis of CLOCK-related genes, which reset and delay the circadian sequence of the peripheral CLOCKs. This helps to adjust how the body responds to stress.

1.2.3.2. Inflammatory regulation of the HPA axis

To maintain homeostasis, GCs modulate the inflammatory response and mediate the resolution of inflammation. Cytokines released as part of the innate or adaptive immune response can cause HPA activation. This results in the production of adrenal GCs, which exert a negative feedback action on the immune cells to prevent

further cytokine production and release, thereby preventing tissue damage. To achieve this negative feedback regulation, cytokines interact with multiple brain regions involved in the HPA axis. Several studies have demonstrated that IL-1, IL-6 and TNF-α can induce CRH production by acting on parvocellular neurones of the hypothalamic PVN, causing HPA axis to be stimulated (Berkenbosch et al., 1987; Bernardini et al., 1990; Navarra et al., 1991; Spinedi et al., 1992). Intravenous TNF-α injections in rats have been shown to cause a dose-dependent rise in plasma ACTH and corticosterone levels (Bernardini et al., 1990). Similarly, studies using a murine AtT-20 cell line has reported that IL-1 and IL-6 can upregulate the expression of POMC to increase ACTH synthesis and release (Woloski et al., 1985; Brown et al., 1987; Fukata et al., 1989; Katahira et al., 1998). Studies have reported that cytokines are able to cause a direct effect on the production of GCs by acting on the adrenal gland. IL-1 and IL-6 have been shown to induce corticosterone release in cultured adrenal cells either independently or in synergy with ACTH (Tominaga et al., 1991; O'Connell et al., 1994; Barney et al., 2000; Salas et al., 2008).

1.2.4. Glucocorticoids in the circulation

Once GCs are released into the circulation, GCs are transported bound to plasma proteins which function to keep the GCs inactive. The principal GC-binding protein present in the plasma is called corticosteroid-binding globulin (CBG). Around 80-90% of GCs are bound by CBG in the bloodstream, whilst only 10% is bound by albumin (Lewis et al., 2005; Hammond, 2016). Albumin binds to GCs with less affinity compared with CBG and acts to buffer changes where the plasma GC concentration fluctuates transiently (Dunn et al., 1981). The remaining 5% of the GCs circulate freely and can interact with receptors. Several proteases, such as

neutrophil elastase, can cleave CBG and disrupt the protein's steroid binding ability resulting in irreversible destruction (Hammond, 2016). This cleavage allows the release of CBG-bound GCs, causing an accumulation of free, active GCs at sites of inflammation. Studies have suggested that when CBG is inactivated or congenitally absent, around 75% of GCs becomes albumin bound and the percentage of biologically active GCs in the circulation rises to 25% (Lewis et al., 2005).

1.2.5. Glucocorticoid receptor signalling

The effects of GCs are mediated in a range of cell types via activation of the ubiquitously expressed GRs (Ray et al., 2006; Heitzer et al., 2007; Huang et al., 2010). These are ligand-regulated transcription factors which belong to the superfamily of *NR3C1* encoded nuclear receptors and are modular in structure (Evans, 1988; Smoak and Cidlowski, 2004; Heitzer et al., 2007; Beck et al., 2011). GRs are composed of three functional domains: amino-terminal domain (NTD), a central DNA-binding domain (DBD) and a ligand-binding C-terminal domain (LBD) (Kumar and Thompson, 2003). The highly variable NTD is encoded by exon 2 and contains the ligand independent activation function-1 (AF-1). AF-1 is central to attaining maximal transcriptional activation of the GR, by interacting with co-factors, chromatin modulators and transcriptional machinery (O'Malley, 1990; Dieken and Miesfeld, 1992; Kumar and Thompson, 2003). The DBD, encoded by exons 3 and 4, plays an important role in DNA binding the GR dimerization (Hard et al., 1990). In between the DBD and the LBD is a hinge region which acts to provide flexibility and a regulatory interface. Embedded within the LBD is a ligand-dependent transcriptional AF-2 domain, which also interacts with coactivators (Bledsoe et al., 2002).

Five isoforms of GR termed GRα, GR-A, GR-P, GRβ and GRγ have been identified through alternative splicing of GR precursor messenger RNA, though the predominant mediator of GC action is GRα (Hollenberg et al., 1985; Lu and Cidlowski, 2005; Turner et al., 2007). GRα functions as a conventional ligand-activated transcription factor, activity of which may be regulated by GR-A and GR-P. GRβ is expressed at levels lower than GRα and in contrast, it does not bind to ligands (Bamberger et al., 1995; de Castro et al., 1996; Pujols et al., 2002). Instead of ligand binding, GRβ affects gene expression and transcription by functioning as a dominant negative inhibitor and antagonizes the activity of GRα. Similarly, the transcriptional profile of GRγ is distinct and lower than that of GRα (Rivers et al., 1999; Oakley and Cidlowski, 2013).

Within the GR are two nuclear localisation signals, one of which is in the DBD, and the other is found within the LBD. When unbound, GRs reside primarily within the cytoplasm in the inactive state as a multimeric chaperone complex. This complex contains heat shock protein (HSP) 90, immunophilins, p23 stabilising proteins and other factors which prevent the nuclear import, degradation of the GR and aid in its maturation (Pratt and Toft, 1997; Cheung and Smith, 2000). Upon GC binding, the chaperone proteins dissociate from the GR allowing the GC-nuclear receptor complex to translocate to the nucleus where it forms a homodimer (Wikström et al., 1986; Picard et al., 1988; Dao-Phan et al., 1997).

1.2.6. Transactivation and Transrepression

Multiple glucocorticoid signalling pathways exist, including monomeric tethering, changes in phosphoinositide 3-kinase (PI3K) signalling and signalling through membrane receptors (Hardy et al., 2020). For the focus of this thesis, a well

characterised GC signalling called the transactivation and transrepression pathway will be highlighted.

In the nucleus, the GC-GR complex bind to specific DNA sequences called GC response elements (GREs), which may be positive or negative (see figure 1.5). If the 5' promoter region of GC-responsive gene contains a positive GRE, transactivation is initiated and transcription of genes encoding anti-inflammatory proteins (annexin-1, IL-10, and the inhibitor of NF-κβ, Iκβ-α) is increased (Beato, 1989; Schaaf and Cidlowski, 2002; Harke et al., 2008). However, binding to a negative GRE result in transrepression of the target genes due to dissociation of active transcription factors. (Sakai et al., 1988; Drouin et al., 1989; Nakai et al., 1991; Subramaniam et al., 1998). GRs, when bound to a ligand may also bind to transcriptional coactivators such as cAMP-response element binding (CREB) protein binding protein (CBP), resulting in enhanced local histone acetyl transferase activity via chromatin modifications. This subsequently increases expression of genes which encode inflammatory proteins, as seen with GC-induced leucine zipper (GILZ) (Govindan, 2010). Conversely, negative GREs binding to GR results in the recruitment of histone deacetylases which closes chromatin. This causes transcriptional silencing, as seen with osteocalcin (OSC). The activity of genes which do not contain GRE can also be modulated by GCs. This involves the GR and transcription factor forming protein-protein interactions, which allows the subsequent binding of histone deacetylases. The latter inhibit gene transcription, as seen with TNF-α (Ito et al., 2000).

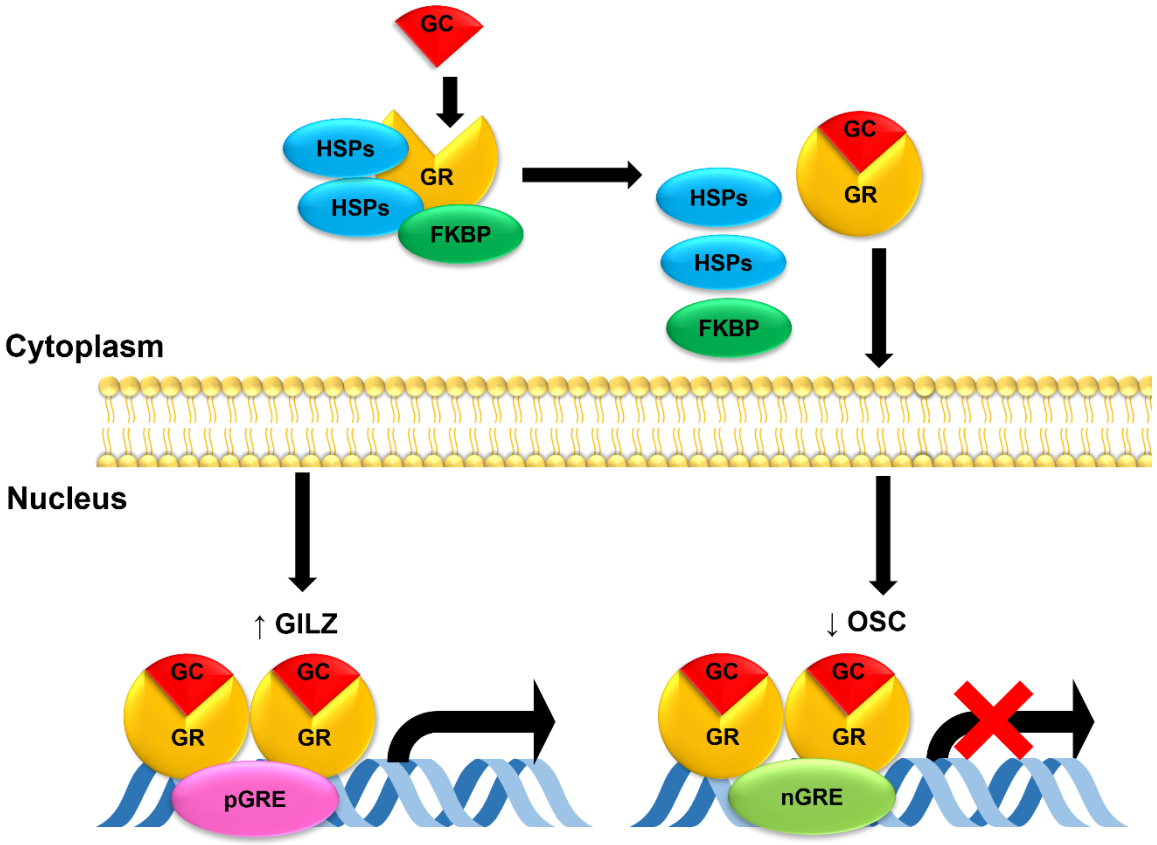

Figure 1.4: Mechanisms of glucocorticoid receptor signalling

When unbound to glucocorticoids (GCs), GR is found in the cytoplasm as a transcriptionally inactive multi-protein complex, which contains molecular chaperones (heat shock proteins [HSPs]) and immunophilins (FKBP). GCs can passively diffuse across the plasma membrane and into the cytoplasm, where GCs bind to GRs. This interaction causes a structural rearrangement which dissociates the chaperone proteins and exposes the nuclear localisation signals. Consequently, the GC-GR complex translocate to the nucleus, where GR binds to glucocorticoid-responsive elements (GREs) and regulates gene expression. Binding to positive GREs (pGREs) stimulates gene transcription (e.g. GILZ), whilst binding to negative GREs (nGREs) suppresses gene transcription (e.g. osteocalcin [OSC]).

1.2.7. Role of 11β-HSD enzymes in pre-receptor GC metabolism

The bioavailability and activity of GCs in the cytoplasm is influenced by the 11β-hydroxysteroid dehydrogenase (11β-HSD) enzymes: type 1 11β-HSD (11β-HSD1) and type 2 11β-HSD (11β-HSD2) (see figure 1.6). 11β-HSD1 is a bidirectional reductase enzyme which catalyses the interconversion of active cortisol with inert cortisone in humans and corticosterone with inert 11-dehydrocorticosterone in

rodents (Brem et al., 1995). This reduction of cortisone to cortisol by 11β-HSD1 is dependent on the availability of the co-factor NADPH generated by the enzyme hexose-6-phosphate dehydrogenase (H6PDH) in the endoplasmic reticulum (Atanasov et al., 2004; (Bujalska et al., 2005; Dzyakanchuk et al., 2009). This interaction results in the transfer of a hydrogen from the H6PDH to reduce a ketone to a hydroxyl group at carbon 11 position to convey activation. H6PDH is critical for NADPH-oxoreductase activity as demonstrated by H6PDH knockout mice, which exhibited a profound switch in 11β-HSD1 activity from active (oxoreductase) to inactive (dehydrogenase) (Lavery et al., 2006). 11β-HSD metabolism is responsible for the conversion of various synthetic GCs, including prednisolone, although some GCs are resistant to reductase metabolism (Homma et al., 1994). Dexamethasone is an example of a GCs that does not undergo reductase metabolism.

In contrast, 11β-HSD2 is a high-affinity, NAD-dependent dehydrogenase which is responsible for the unidirectional conversion of active GCs to their inactive metabolites. Conversion is achieved by the oxidation of a hydroxyl group at the carbon11 position to form a ketone group. This prevents activation of the mineralocorticoid receptor (MR) by GCs, which is usually capable of binding both mineralocorticoids and active corticosteroids with high affinity, hence, 11β-HSD2 protects MR against inappropriate activation by excess GCs (Homma et al., 1994).

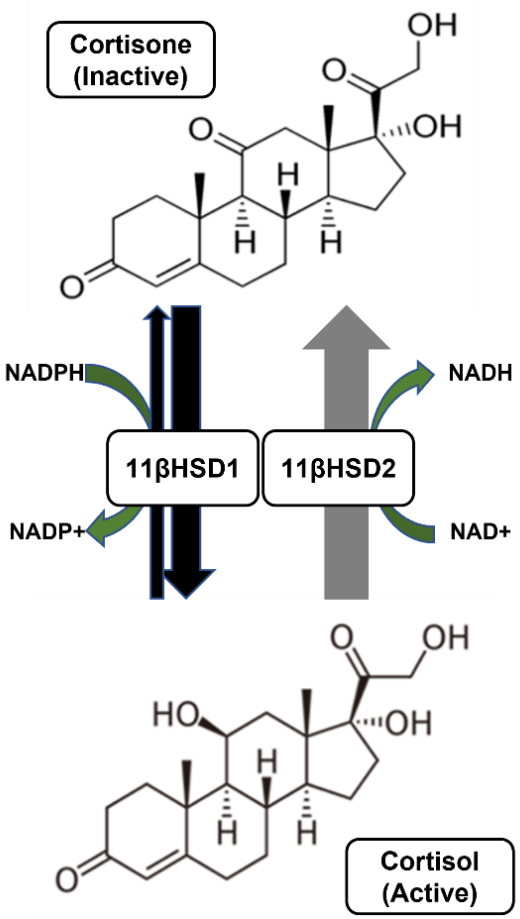

Figure 1.5: The enzymatic actions of 11β-hydroxysteroid dehydrogenase (11β-HSD) enzymes in glucocorticoid (GC) metabolism

The activity of GCs is regulated by 11β-HSD enzymes found in the endoplasmic reticulum. 11β-HSD1 is a NAPDH-reductase enzyme which works bi-directionally to catalyse the conversion of inactive GCs (e.g., cortisone) to receptor active GCs (e.g., cortisol), whilst 11β-HSD2 is a unidirectional dehydrogenase which converts active GCs to their inactive counterparts. The latter reaction is NAD+-dependent.

1.3. Mechanisms of anti-inflammatory glucocorticoids

The inflammatory and anti-inflammatory effects of GCs are dependent on different molecular mechanisms which include directly affecting gene expression through GR and GRE binding, indirectly affecting gene expression through GR-transcription factor interactions and activation of second messenger cascades, such as kinases (discussed in section 1.2.6) (Ayroldi et al., 2012; Busillo and Cidlowski, 2013; Oakley and Cidlowski, 2013; Uhlenhaut et al., 2013). Whilst direct effects of

therapeutic GCs involve the suppression of pro-inflammatory genes, indirect effects of synthetic GCs are mediated via the induction of anti-inflammatory genes. The latter are upregulated via GC signalling, which is achieved post GR-GRE interaction. Such anti-inflammatory genes include GC-induced leucine zipper (GILZ), secretory leukocyte protease inhibitor (SLPI) and mitogen-activated protein kinase phosphatase-1 (MKP-1) (De Bosscher and Haegeman, 2009).

GCs also induce the synthesis of an anti-inflammatory protein called tristetraprolin (TTP), which via a negative feedback mechanism suppresses the pro-inflammatory response, and consequently, chronic inflammation. TTP does this by decreasing the mRNA stability of pro-inflammatory cytokines which targets them for degradation, thus preventing their translation (Dreyfuss et al., 2002; Carrick et al., 2004). Such cytokines include TNF-α, which acts upstream of other pro-inflammatory mediators, such as IL-1β and IL-6 and initiates the pro-inflammatory cytokine cascade (Carballo, 1998). Hence, TNF-α blockade inhibits the production of IL-1β and IL-6. TTP is also directly involved in the destabilisation of mRNA transcripts encoding IL-1β and IL-6, amongst other inflammatory mediators (Anderson, 2010; Terrando et al., 2010).

As previously discussed, GCs suppress inflammation by regulating the inflammatory response at the cellular and transcriptional level, where the latter involves the repression of pro-inflammatory cytokine synthesis. This is achieved by inhibiting the transcriptional activity of AP-1 and NF-KB through GR repression, which in turn prevents the transcription of TNF-α, IL-1 and IL-6. GCs upregulate the gene expression and protein synthesis of Iκ-B, which is a NF-κB antagonist. Iκ-B binds to NF-κB and sequesters it in the cytosol, thereby preventing its nuclear

translocation. This leads to a decline in NF-κB mediated pro-inflammatory gene expression (Auphan et al., 1995; Scheinman et al., 1995).

GCs can exert either, direct or indirect effect on various immune cells. For instance, glucocorticoid exposure can suppress maturation of dendritic cells (Moser et al., 1995; Piemonti et al., 1999). This results in impaired antigen presentation, significant reduction in the expression level of class II major histocompatibility complex (MHC) and costimulatory molecules, as well as suppression of pro-inflammatory cytokine production (Sacedón et al., 1999; Pan et al., 2001; Mirenda, 2004; Rozkova et al., 2006).

Glucocorticoids also limit the capacity of dendritic cells to stimulate helper T-cells, specifically Th1 cells, which cause increased synthesis of IL-10 positive immunosuppressive regulatory T (T-reg) cells (Matyszak et al., 2000). Although, GCs trigger T-cell apoptosis, T-regs are reported to be relatively resistant to GC-mediated cell death which results in an increase T-regs cells population (Chen et al., 2004; Prenek et al., 2020). Additionally, GCs prevent neutrophil activation and adhesion to the blood vessels by inhibiting the leucocyte-endothelial cell interactions via decreased expression of adhesion molecules. Examples of such molecules include L-selectin and intercellular adhesion molecule-1 (ICAM-1). The reduced expression of adhesion molecules favours neutrophil detachment and prevents neutrophil recruitment to the site of inflammation (Watanabe et al., 1991; Cronstein et al., 1992).

GCs activate the M2 subset of macrophages which exert an anti-inflammatory profile and inhibit the pro-inflammatory M1 phenotype. The critical role of the GR in mediating GC actions in myeloid cells was investigated using murine models of

contact allergy. This showed that in the absence of GR in macrophages and neutrophils, GCs were unable to inhibit the inflammatory response. The study also reported that GR deletion in myeloid cells resulted in increased infiltration of leucocytes into the site of inflammation and inability of GCs to decrease secretion of pro-inflammatory cytokines (e.g., IL-1) and chemokines (e.g. MIP-2, MCP-1) (Tuckermann et al., 2007). GCs also have been shown to impact phagocytosis, with GC-treated macrophages possessing an increased capacity to engulf apoptotic cells and release pro-resolution/ anti-inflammatory mediators (Liu et al., 1999; Van der Goes et al., 2000; Giles et al., 2001).

1.3.1. Synthetic glucocorticoids in the management of inflammation

Due to their immunosuppressive effects, GCs are extensively utilised for the treatment of immune and inflammatory conditions, such as allergy, asthma, RA and multiple sclerosis. Additionally, adrenal GCs are used in immunosuppressive regimes to prevent organ transplant rejection and can also be used in treatment of lymphoid malignancies (Rhen and Cidlowski, 2005). The potent anti-inflammatory activity of endogenous GCs has been exploited and lead to the development of synthetic GC derivatives, which are used in the treatment of both acute and chronic inflammatory conditions (Beaulieu and Morand, 2011).

A recent meta-analysis reviewing the disease-modifying properties of GCs in early RA has reported that when given in conjunction with disease modifying anti-rheumatic drugs (DMARDs), low dose GCs cause a significant reduction in the progression rate of cartilage and bone erosion relative to DMARD only controls (Kirwan et al., 2004). Similarly, another study investigating the effects of GC administration on synovial tissue, the principal target of chronic arthritidies, revealed

that oral GC treatment causes a marked reduction in synovial tissue infiltration and expression of pro-inflammatory cytokines (Klint et al., 2005). GC therapy reduces joint inflammation and tenderness, and the expression of inflammation markers whilst improving the disease activity score in patients with RA (Kirwan et al., 2004; Wolf et al., 2008).

The most widely used synthetic GCs include synthetic preparations of cortisol called hydrocortisone, prednisolone, and dexamethasone (Karssen and de Kloet, 2007). The structure of all GC analogues is related to cortisol, although structural changes affect the activity, potency, and the clearance of each derivative (Cevc and Blume, 2004). For instance, prednisone is a biologically inert GC which is converted to prednisolone in the liver. This conversion to the active form involves the addition of a double bond between carbon positions 1 and 2 of cortisol. Prednisolone has a longer duration of action of 12-36 hours relative to hydrocortisone's shorter biological half-life of 8-12 hours. Prednisolone is also 4 times more potent than hydrocortisone (Zoorob and Cender, 1998). For prednisolone to become activated, the 11-keto group requires reduction. Methylprednisolone is synthesised following the incorporation of methoxycarbonyl group to the 6^{th} carbon of prednisolone and has 5 times more potent anti-inflammatory activity compared to hydrocortisone (Diederich et al., 2002). Methylprednisolone also produces fewer systemic adverse effects relative to hydrocortisone. Dexamethasone, a long-acting synthetic GC with a duration of action of 36-72 hours, is formed following the introduction of a methyl group on carbon 16 and a fluoro group on carbon 9α on prednisone (Cevc and Blume, 2004). These additions result in dexamethasone being 25-fold more potent than hydrocortisone (Zoorob and Cender, 1998). Dexamethasone is more

commonly used to treat acute conditions and avoided as a long-term treatment due to its ability to significantly suppress the HPA axis (Liu et al., 2013).

Specifically, 11β-HSD1 reduces prednisone more effectively to generate prednisolone compared to the reduction of cortisone to cortisol, causing there to be increased potency and greater systemic availability of prednisolone (Jenkins and Sampson, 1967). However, variation in the metabolism of other GC derivatives by 11β-HSD enzymes has also been noted. For instance, 11β-HSD1 oxidation and 11β-HSD2 reduction of dexamethasone is diminished, whereas 11β-HSD2 can reduce 9-fluorinated GCs such as 11-dehydrodexamethasone to dexamethasone, resulting in the long half-life of dexamethasone *in vivo* (Diederich et al., 1996; Diederich et al., 1997; Obeyesekere et al., 1997; Diederich et al., 2002) (see figure 1.7)

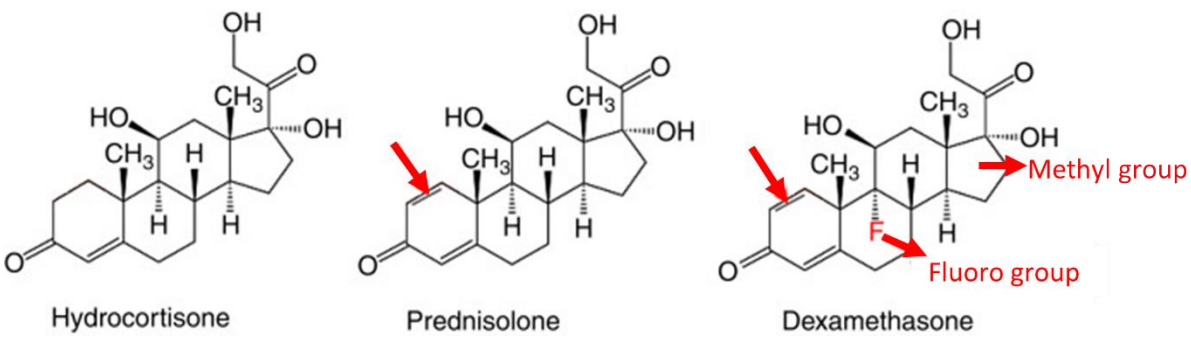

Figure 1.6: Chemical structures of GC analogues - prednisolone and dexamethasone

All synthetic GCs are structurally related to endogenous cortisol. The chemical structure of synthetic hydrocortisone is identical to physiological cortisol. The insertion of a double bone between carbon positions 1 and 2 of cortisol yields prednisolone. To generate dexamethasone, hydrocortisone requires incorporation of a double bond, a methyl group and a fluoro group. Modifications to the chemical structure of synthetic GCs are illustrated in red.

1.3.2. Glucocorticoid excess and Cushing's syndrome

Due to the diverse pleotropic actions of endogenous GCs, their therapeutic application in for the management of inflammatory disease is associated with a diverse range of systemic side effects. Collectively, these are termed Cushing's syndrome and represent a considerable health burden. GC excess can be due to chronic use of exogenous GCs or a pathological endogenous increase, both of which result in the same phenotype referred to as Cushing's syndrome (Sato et al., 2018). The latter more commonly presents as Cushing's disease which is a pituitary-dependent Cushing's syndrome and is less common relative to iatrogenic Cushing's syndrome (Newell-Price et al., 2006). The traditional stigmata of Cushing's syndrome include truncal obesity, muscle weakness, myopathy, hypertension, rounded 'moon' face, osteoporosis, and glucose intolerance – all of which overlap with the side effect profile of GC treatment in those with chronic inflammatory condition, as seen in around 70% of patients receiving GC therapy (Giraldi et al., 2003; Fardet et al., 2007; Pivonello et al., 2015).

1.4. 11β-HSD1 and glucocorticoid excess

To investigate the role of 11β-HSD1 metabolism in GC-excess induced adverse effects, a murine model with global transgenic deletion of 11β-HSD1 has been created. In a recent study by Morgan et al., 2014, 11β-HSD1 KO and WT control mice were given corticosterone (100 μg/mL) infused drinking water for five weeks. Following treatment with the supraphysiological concentration of GC, WT mice developed Cushingoid features. Such features included glucose intolerance, hypertension, hepatic steatosis, myopathy, and increased adiposity. In contrast, 11β-HSD1 KO mice were protected against the deleterious side effects associated

with circulatory GC excess. Interestingly, in both GC-treated mice groups, adrenal atrophy was observed together with an elevated level of serum corticosterone, confirming that both groups were exposed to the same level of corticosterone. These results deduced that 11β-HSD1 reactivated GCs play a significant role in the development of metabolic side effects linked to GC use, and that the deletion of type 1 11β-HSD results in amelioration of GC-induced adverse effects regardless of increased level of circulating GCs. Together, the data proposes the prospect of using 11β-HSD1 inhibitors to limit the GC-excess induced side effects (Morgan et al., 2014).

1.4.1. 11β-HSD1 and clinical research

The inhibition of 11β-HSD1 offers a therapeutic means of treating metabolic disorders, such as obesity, polycystic ovary syndrome and type 2 diabetes mellitus (T2DM). The contribution of 11β-HSD1 in mitigating the detrimental effects caused by GC excess on metabolic parameters has been investigated by several research groups, which started with the development of a prototypic 11β-HSD antagonist called carbenoxolone (Walker et al., 1995; Andrews et al., 2003). Treatment with carbenoxolone downregulated glycogenolysis and hepatic gluconeogenesis in those with T2DM, but not in healthy subjects. However, carbenoxolone reduced cholesterol levels in in healthy patients, but not in those with diabetes. Whilst these findings reinforced the potential of carbenoxolone in managing the metabolic complications of diabetes, being a non-selective compound, carbenoxolone also suppressed 11β-HSD2 in the kidneys. Inhibition of renal 11β-HSD2 lead to the development of hypernatremia, high blood pressure and hypokalaemia, thus demonstrating the limitations of carbenoxolone as a therapy for metabolic syndrome and the need for isozyme selective inhibitor (Bujalska et al., 1997; Schuster et al.,

2006). Consequently, a selective inhibitor of 11β-HSD1 called INCB13739 was developed. INCB13739, when used as an adjunct to metformin in type 2 diabetics, produces significant reduction in average glycaemic levels, fasting plasma glucose and insulin resistance hence proving to be an efficacious treatment. Other beneficial effects produced by INCB13739 include an improved lipid profile (lower plasma cholesterol and LDL levels) in those with hyperlipidaemia (Rosenstock et al., 2010). Similar results were shown by another selective antagonist of 11β-HSD1 called MK-0916 (Feig et al., 2011). Therefore, 11β-HSD1 inhibition offers a new potential approach to manage different components of metabolic syndrome.

1.4.2. 11β-HSD1 and inflammation

The expression of 11β-HSD1 is upregulated in the inflamed tissue, primarily due to the actions of pro-inflammatory mediators. 11β-HSD1 is expressed by many immune cells and by those cell types found in the synovium of patients with inflammatory arthritis (Chapman et al., 2009). Such cells include T-lymphocytes, dendritic cells, endothelial cells, fibroblasts, and macrophages (Hardy et al., 2006). A significant positive correlation between the activity of 11β-HSD1, GC activation and the expression of inflammatory markers in serum have been reported (Hardy et al., 2007). Such inflammatory markers include erythrocyte sedimentation rate (ESR). Pro-inflammatory cytokines, such as TNF-α and IL-1, also promote the expression and the activity of type 1 11β-HSD in mesenchymal cells (Ahasan et al., 2012). These cells include osteoblasts, adipocytes, and fibroblasts. When present in combination with pro-inflammatory mediators, GCs exert a synergistic effect on 11β-HSD1 and positively modulate the enzyme's activity (Kaur et al., 2009). The synergistic surge in 11β-HSD1 expression results in the accumulation of active GCs in bone and in surrounding tissues, which amplifies the anti-inflammatory response

(Sun and Myatt, 2003; Rae et al., 2004; Li et al., 2006; Kaur et al., 2009). Although, non-stimulated monocytes lack 11β-HSD1, their differentiation into resting or naive macrophages induces 11β-HSD1 expression. M1 polarisation of macrophages by LPS and interferon-γ (IFN-γ) has been shown to further increase 11β-HSD1 expression levels, however little effect on 11β-HSD1 expression was shown when macrophages were polarised to the M2 phenotype by IL-4 (Martinez et al., 2006).

1.4.3. Contribution of 11β-HSD1 metabolised corticosteroids in inflammation

The functional consequences of 11β-HSD1 have been investigated by several studies, particularly during inflammation where enzyme activity is regulated by pro-inflammatory cytokines. Such studies have focused on, for example, the impact of 11β-HSD1 in regulating physiological GCs during chronic inflammatory disease. To achieve this, a TNF-transgenic murine model of chronic inflammatory arthritis (TNF-Tg) lacking 11β-HSD1 (TNF-Tg$^{11\beta KO}$) both globally or specifically in mesenchymal-derived cell populations were used. Global 11β-HSD1 deletion resulted in a severe exacerbation of polyarthritis, as shown by increased swelling, greater paw deformities, significantly more pannus invasion into subchondral bone and synovitis, and exacerbated systemic bone loss (Hardy et al., 2018). Similarly, greater muscle wasting was also observed during chronic inflammation in the TNF-Tg$^{11\beta KO}$ mouse, highlighting the important role that 11β-HSD1 activated local GCs play in suppressing inflammation (Hardy et al., 2016).

To explore the role of fibroblast like synoviocytes (FLS) and osteoblastic 11β-HSD1 in an inflammatory phenotype, a murine model with a targeted mesenchymal 11β-HSD1 deletion was used. These animals showed similar patterns of synovitis, destructive bone lesions and arthritic scores to TNF-Tg mice, indicating that

although 11β-HSD1 has a catabolic role within the mesenchyme, exacerbation of the inflammatory phenotype is not mediated by 11β-HSD1 in mesenchymal-derived cells (Hardy et al., 2016).

A greater degree of synovitis was seen in TNF-Tg$^{11\beta KO}$, as demonstrated by the marked increase in infiltration of leucocytes (T-cells, macrophages, and neutrophils) into the joint relative to TNF-Tg mice. A shift in macrophage polarisation from M2 to M1 phenotype was also observed in TNF-Tg$^{11\beta KO}$ mouse, highlighting the supporting role 11β-HSD1 plays in M2 polarisation, and consequently in the phagocytic removal of apoptotic and damaged cells in inflammation. Another study investigating the contribution of 11β-HSD1 in the inflammatory response using mice lacking 11β-HSD1 reported that in the absence of 11β-HSD1, phagocytic clearance of apoptotic neutrophils is significantly delayed. Hence, suggesting the need of 11β-HSD1 to be present for M2 macrophages to perform their anti-inflammatory function. This finding was reinforced by *in vitro* experiments on murine macrophages, where an 11β-HSD1 inhibitor in the presence of endogenous GCs antagonised the phagocytic capacity of macrophages for apoptotic and damaged leucocytes (Gilmour et al., 2006).

These studies suggest that although 11β-HSD1 is a key regulator of adverse effects associated with GC excess (as outlined in 1.3.3), further detrimental effects may also be seen with the use of 11β-HSD1 inhibitors for the treatment of chronic inflammatory states. This may be attributable to the enzyme antagonists inhibiting the beneficial 11β-HSD1-produced anti-inflammatory actions.

Together these studies reveal that 11β-HSD1 plays a role in both GC-induced and inflammatory-induced osteoporosis. Whether this is mediated by changes in

disease severity, or due to GC metabolism by 11β-HSD1 within bone remains poorly defined. To better understand how GC metabolism by 11β-HSD1 influences bone remodelling in chronic inflammatory disorders and in therapeutic GC application, it is important to understand normal physiological bone remodelling.

1.5. Bone

Bone is a highly specialised and dynamic tissue which is constantly undergoing a process called remodelling, through which up to 10% of the adult skeleton is renewed every year (Manolagas, 2000). Bone exerts multiple important functions in the body. These include movement and locomotion, providing structural support and soft tissue protection, being a harbour of bone marrow and acting as a calcium and phosphate reservoir (Robling et al., 2006; Datta et al., 2008). Cortical bone accounts for 80% of the skeletal mass, whilst trabecular (cancellous) bone only makes up 20% of the skeleton. Cortical bone is dense and surrounds the medullary cavity, whereas trabecular bone contains a honeycomb-like meshwork of trabecular rods interspersed alongside bone marrow cells (Clarke, 2008). Bone is composed of three main cells, which include osteoblasts, osteoclasts, and osteocytes. Osteoblasts are bone forming cells which originate from mesenchymal stromal cells whilst osteoclasts are bone resorbing cells which are myeloid lineage derived. Osteocytes are terminally differentiated cells which have a mechanotransduction and regulatory function (Teitelbaum, 2007; Clarke, 2008; Karsenty et al., 2009; Bonewald, 2011).

1.5.1. Gross anatomy of bones

Bones can be divided into five distinct types: long, short, sesamoid, flat and irregular bones. A long bone can be divided into two main regions: the diaphysis and the epiphysis (see figure 1.8). The diaphysis refers to the hollow shaft which runs from the proximal to the distal end of the bone, whilst the epiphyseal plates are found on either end of the bone. Located between the diaphysis and epiphysis is an area called metaphysis, which encompasses the growth plate. The diaphysis is made up primarily of cortical bone which surrounds the medullary cavity, in which yellow bone marrow (fat) is contained. Fatty yellow marrow progressively replaces haemopoietic red marrow over the course of life (Moore and Dawson, 1990). Conversely, the epiphysis and the metaphysis are made up of thin cortical bone surrounding a trabecular bone.

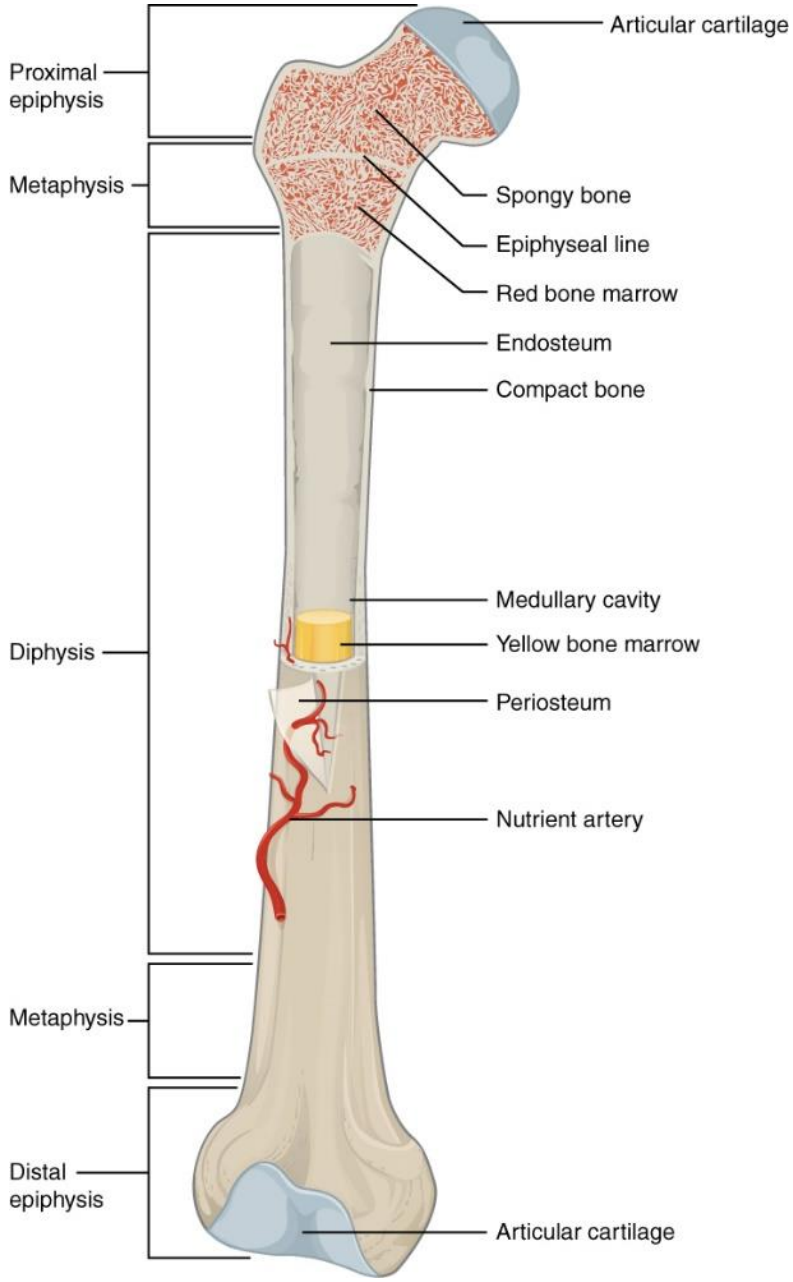

Figure 1.7: Gross anatomical characteristics of a long bone

A long bone can be divided into two parts: diaphysis and epiphysis. The diaphysis is a tubular shaft which is composed of dense and hard compact bone. The diaphysis houses a medullar cavity, in which yellow bone marrow is contained. Epiphysis refers to the wider section found on either side of the bone. The epiphysis is made up of spongy (trabecular) bone. This spongy bone is filled with red bone marrow. Connecting the diaphysis and epiphysis is an area termed metaphysis which has the epiphyseal growth plate.

1.5.1.1. Structure of cortical bone

Cortical bone is composed of cylindrical osteons. An osteon, the chief structural unit of compact bone, is made up of concentric layers of lamellar bone which surround an inner cavity referred to as a Haversian canal (see figure 1.9). The Haversian canal contains nerves, lymph vessels and small blood vessels which are responsible for blood supply and nourishment to the osteocytes residing in lacunae within mineralized bone (Clarke, 2008).

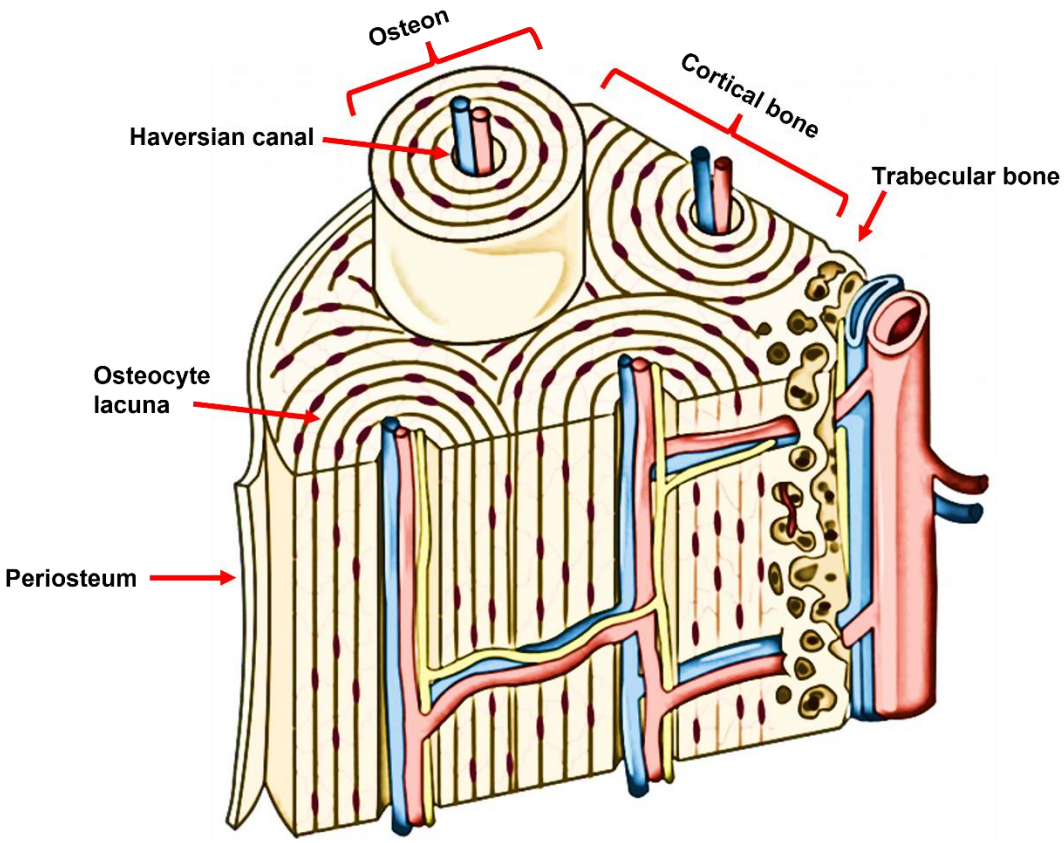

Figure 1.8: Gross characteristics of cortical bone

The functional units of cortical bone are called osteons. Osteons are composed of layers of bone matrix called lamellae, which are organised in concentric rings around a central Harversian canal. This canal harbours blood vessels and nerves from the periosteum. Osteocytes are embedded in the cortical bone and are found residing in the lacunae.

The inner surface of the cortical bone is lined by a thin vascular membrane of connective tissue referred to as the endosteum. The endosteum is in contact with a

range of cells, which include osteoblasts, osteoclasts, adipocytes, and mesenchymal stem cells. A study has suggested that the endosteal niche has an important function in inducing vascular remodelling in the bone marrow during development and in maintaining quiescent haematopoietic stem cells (HSCs) (Nakamura et al., 2010). The outer cortical surface of bone consists of 2 layers, collectively termed the periosteum. The outer fibrous surface of the periosteum is made up of collagen, elastin, and fibroblasts alongside a nerve and microvascular network, whilst inner cellular layer houses progenitor cells that mature into osteoblasts (Allen et al., 2004). Another study has reported that periosteum is central to bone regeneration and acts as a reservoir for chondrocytes during endochondral ossification (Colnot, 2009). The periosteum envelops all outer bone surfaces, except in regions where epiphyses connect with other bones to form joints. These articulating surfaces are covered by a thin layer of smooth hyaline cartilage called articular cartilage, which function to absorb shock reduce friction (Servaty et al., 2001; Clarke, 2008).

1.5.2. The bone remodelling process

The process of bone remodelling is highly complex and tightly regulated. It aims to repair fatigue microdamage (via targeted remodelling), replace old bone with fresh new units and maintains mineral homeostasis of calcium and phosphorus (Mori and Burr, 1993; Bentolila et al., 1998; Dallas et al., 2013). In the remodelling process, osteoblastic formation and osteoclastic resorption are coupled to ensure that an equal quantity of resorbed bone has been replaced. The remodelling cycle is composed of five co-ordinated phases: activation, resorption, reversal, formation and finally, termination (Kenkre and Bassett, 2018) (see figure 1.10). Bone

remodelling occurs asynchronously at anatomical sites called the basic multicellular unit (BMU), which is composed of osteoblasts, osteoclasts and a capillary blood supply. BMU is enclosed in a circulatory canopy formed from bone lining cells (Frost, 1990; Hauge et al., 2001). BMU's structure and function differs greatly based on whether it is located within cortical or trabecular bone. Cortical BMUs are organised in a cutting cone lined with osteoclasts and is responsible for remodelling bone by osteoclastic tunnelling. This tunnel gets refilled by osteoblasts, to give rise to an osteon (Agerbæk et al., 1991).

Activation phase is initiated when osteocytes sense an activation stimulus and transduce it as a biochemical signal to other cells via dendritic processes. Such activation signals include mechanical strain, chemical signals (i.e., hormones) and structural damage. When an activation signal is not available, osteocytes secrete factors which antagonise osteogenesis. These factors include the Wingless (WNT) signalling pathway inhibitors, sclerostin (SOST) and Dickkopf-1 (DKK-1) which inhibit osteoblast activity, and specific factors which promote local osteoclastogenesis (Bonewald and Johnson, 2008; Moriishi et al., 2012). Osteocyte apoptosis, induced by microdamage to bone matrix due to osteocyte canaliculi disruption results in further recruitment of osteoblast and osteoclast precursor cells, thereby promoting osteoclastogenesis (Atkins and Findlay, 2012; Chen et al., 2015). *In vitro* studies investigating osteoclast migration and differentiation in the presence of conditioned media from apoptotic osteocytes and non-apoptotic osteocytes have reported that apoptotic media stimulates the migration of osteoclast precursors by 64% and formation of osteoclasts by 450% (Al-Dujaili et al., 2011; McCutcheon et al., 2020). These effects have shown to be mediated by receptor activator for NF-κβ ligand (RANKL), which acts as chemotactic signal for the osteoclasts (Al-Dujaili

et al., 2011; McCutcheon et al., 2020). The next stage to occur is resorption which is initiated following osteocyte recruitment and osteoclast differentiation.

The resorption phase comprises of multiple steps which begin with the polarised, multinucleated osteoclasts attaching to the extracellular matrix of the bone. This adherence results in the osteoclasts reorganising their actin cytoskeleton to form four unique domains: the sealing zone and the ruffled border which are in contact with the bone matrix, and the functional apical secretory domain and the basolateral domain which are not in contact with the bone matrix. In the presence of growth factors, osteoclasts synthesise dynamic adhesion structures called podocytes, which are made up of a membrane domain. This domain houses an actin filament-rich core (Itzstein et al., 2011). It has been previously reported that the sealing zone is composed of densely packed actin-rich podosomes, and that the β3-integrin is responsible for the organisation of the cytoskeleton during sealing zone formation as it mediates the adherence of the podosomes to the mineralised matrix (Faccio et al., 2003; Luxenburg et al., 2007; Roy and Roux, 2018). This attachment prevents the catalytic enzymes from leaking from the ruffled border into the surrounding tissue. Osteoclasts contain high levels of carbonic anhydrase, which is a source for bicarbonate and protons, where the latter is pumped across the ruffled border with chloride ions, into the functional secretory domain. This endocytosis is carried out by a vacuolar-type H+-ATPase and is needed to acidify the resorption lacuna and break down the inorganic hydroxyapatite crystals of the bone (Silver, 1988; Tolar et al., 2004). A chloride/ bicarbonate exchanger at the basolateral domain exchanges chloride ions for bicarbonate ions, to maintain cytoplasmic pH homeostasis (Teti et al., 1989).

The organic matrix of the bone is composed of collagenous proteins, primarily type 1 collagen, and is degraded by proteases which are released into the resorption space. In order to function, proteolytic enzymes require an acidic environment, a H+-ATPase, and an anion exchanger on the lysosomal membrane. These lysosomal enzymes include cathepsin K and matrix metalloproteinases. Cathepsin K accounts for one of the most potent proteases found within the lysosome, the key function of which is to enable bone resorption which it does so by efficiently breaking down type 1 collagen (Garnero et al., 1998; Kafienah et al., 1998). Cathepsin K is also responsible for excising the inhibitor loop domain which represses the function of a phosphatase called tartrate-resistant acid phosphatase (TRAP) (Ljusberg et al., 2005). TRAP is selectively expressed in the ruffled border and intracellular vesicles of osteoclasts (Hollberg et al., 2005; Reinholt et al., 2009). Although, the precise mechanism of TRAP remains ambiguous, it is thought that TRAP generates highly destructive reactive oxygen species, such as hydroxyl radicals, to catalyse the resorption of the bone matrix (Halleen et al., 1999). The degraded matrix is shuttled in transcytotic vesicles through the functional secretory domain into the extracellular space. These transcytotic vesicles also contain TRAP, which enables further break down of the resorbed products.

The reversal phase follows the resorption phase, during which an osteogenic environment is generated. This allows for bone resorption to be coupled to bone formation. Although several osteogenic molecules which aid in this coupling have been identified, the precise coupling mechanism remains unclear. It has been proposed that this bone resorption and formation coupling occurs when growth factors are released from the bone matrix during resorption. Such growth factors include insulin-like growth factor-1 (IGF-1), transforming growth factor-β1 (TGF-β1)

and platelet-derived growth factor (PDGF). These osteotropic factors recruit mesenchymal stem cells from the bone marrow to the resorption sites of the bone, stimulating osteoblast differentiation (Tang et al., 2009; Xian et al., 2012). Literature has also postulated that the transmembrane proteins EphrinB and tyrosine kinase receptors EphB may be involved in this process. More specifically, EphrinB2 and its receptor Eph4 are found to be strongly expressed in osteoclast membrane and osteoblast membrane respectively. EphrinB2 and Eph4 interact with each other and via bidirectional signalling upregulate osteogenic differentiation and suppress osteoclast formation, ensuring bone homeostasis (Zhao et al., 2006).

Following the commitment of mesenchymal progenitors to an osteoblast lineage and the subsequent differentiation into mature osteoblasts, extracellular matrix proteins are synthesised and secreted. Such molecules include type 1 collagen, OSC, osteopontin and bone sialoprotein; collectively, this unmineralised protein matrix is termed the osteoid (Cowles et al., 1998). Phosphate and calcium ions contained within the matrix vesicles nucleate to generate hydroxyapatite crystals, which express ion transporters calcium and phosphate on their surface. Hydroxyapatite microcrystals are deposited in the osteoid, which then undergoes mineralisation. These hydroxyapatite crystals puncture the vesicles' membranes of the matrix to assemble into a mineralised nodule (Hasegawa et al., 2017). Also contained within the matrix vesicles is the enzyme alkaline phosphatase (ALP), which promotes pyrophosphate hydrolysis to release inorganic phosphate ions to fuel crystal formation and bone mineralisation (Orimo, 2010). In the presence of persistently high phosphate level, osteoblasts and osteoclasts release osteopontin, which localises to the periphery of the mineralised nodules. Osteopontin functions as an inhibitor of excessive or abnormal mineralisation by binding to calcium in

crystal surfaces and inhibiting the generation of hydroxyapatite crystals (Mark et al., 1988; Yuan et al., 2014).

Termination is the last phase of the bone remodelling process which is reached when resorbed bone has been replaced with an equal quantity of newly synthesised bone. Mature osteoblasts either undergo apoptosis, change into a bone-lining phenotype, or undergo terminal differentiation into osteocytes. Osteocytes have a critical role in terminating the bone remodelling process as they express SOST. During the bone remodelling cycle, SOST expression is diminished which allows WNT signalling to promote osteoblast differentiation, however towards the end of remodelling cycle, SOST expression is increased to antagonise osteogenesis. Additionally, further osteoblast differentiation and bone formation is inhibited by newly formed osteocytes which re-express SOST during the termination phase of cycle (Poole et al., 2005).

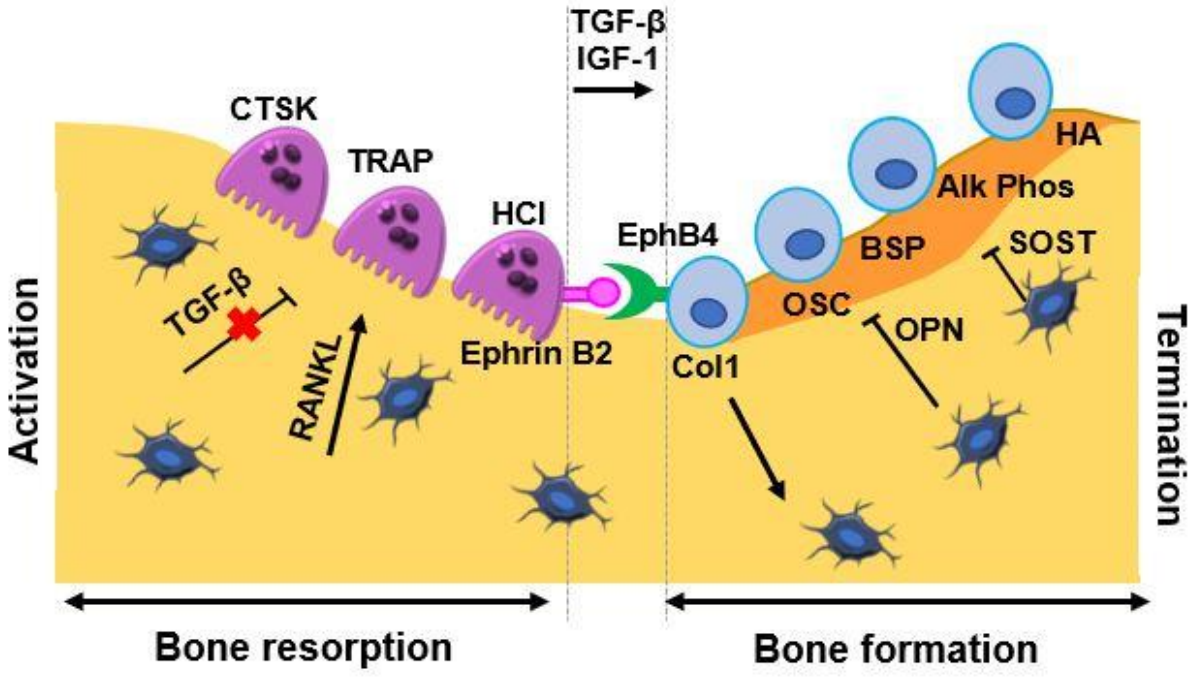

Figure 1.9: The bone remodelling process

The bone remodelling cycle can be divided into five stages: activation, resorption, reversal, formation, and termination. The remodelling cycle is initiated following osteocytes apoptosis, which reduces the local levels of TGF-β and therefore, removes the inhibitory signals on osteoclastogenesis. This enables osteoclast synthesis to occur, which involves the expression of osteoclast marker enzymes called cathepsin K (CTSK) and tartrate-resistant acid phosphatase (TRAP), and the production of hydrochloric acid (HCL) which aid in the resorption of bone matrix. The resorbed bone releases growth factors (insulin-like growth factor-1 (IGF-1), transforming growth factor-β1 (TGF-β1) which activate osteoblasts. Osteoblasts can also be activated following the interaction between transmembrane proteins EphrinB and tyrosine kinase receptors EphB on osteoclast and osteoblast respectively. Activated osteoblasts release hydroxyapatite (HA), alkaline phosphatase (alk phos), bone sialoprotein (BSP), osteocalcin (OSC) and type 1 collagen (Col1). Post completion of the formation phase of the bone remodelling cycle, osteocytes release osteopontin (OPN) and sclerostin (SOST) which serve as inhibitory signals to terminate the remodelling process. The differentiation of osteoblasts into osteocytes can also terminate the process.

1.5.3. Regulation of osteoblast differentiation

The process of bone remodelling is active and dynamic, which is tightly coordinated to ensure that there is a correct balance between bone resorption and bone deposition (Zaidi, 2007). Any imbalances in resorption and formation can result in

abnormal bone remodelling, net bone loss and the development of pathological disorders (Eriksen et al., 1990; Guerrini et al., 2008). Several transcription factors are involved in regulating osteoblast differentiation from mesenchymal cells, from which Runt-related transcription factor 2 (RUNX2) is the master regulator. RUNX2 modulates osteoblast differentiation by affecting the expression of osteoblast-specific proteins including type 1 collagen, OSC, osteopontin and bone sialoprotein (Stein et al., 1996; Roca et al., 2005). RUNX2 is activated following phosphorylation by ERK/MAPK signalling pathway (Ge et al., 2009; Li et al., 2009). This phosphorylation is necessary before RUNX2 can bind to enhancers on target genes. Such enhancers include CCAAT/enhancer-binding protein (C/EBP). CEBP is a key of transactivator of the OSC gene, which when bound to RUNX2 functions to increase the transcription of OSC in osteoblasts. CEBP also recruits chromatin-remodelling proteins, such the ATP-dependent SWI/SNF complexes, to promoters of tissue-specific genes, resulting in transcriptional activation during cell differentiation (Kowenz-Leutz and Leutz, 1999; Gutierrez et al., 2002; Villagra et al., 2006). Hence, osteoblast differentiation is strongly modulated by factors which regulate RUNX2 signalling.

The canonical WNT signalling pathway also plays a key role in influencing the expression of RUNX2 and consequently, underpins osteogenesis. WNT signalling promotes the commitment of mesenchymal stem cells towards osteoblastogenesis, which occurs after WNT proteins bind to its transmembrane receptors; Frizzled (Fz) and low-density lipoprotein-related protein 5/6 (LRP5/6) (Day et al., 2005). This complex results in the transduction of signal through the β-catenin pathway, result of which is increased RUNX2 expression (Gaur et al., 2005). When WNT signalling is antagonised, the differentiation of osteoblasts is also inhibited. DKK-1 is a

secreted glycoprotein which inhibits WNT signalling by forming high affinity bonds with LRP5/6 (Bafico et al., 2001; Semënov et al., 2001). A similar mechanism of inhibition is demonstrated by SOST (as previously discussed), which is expressed by osteocytes (Winkler, 2003; Semënov et al., 2005).

Chemical messengers have been reported as being positive modulators of bone remodelling. These hormones include parathyroid hormone (PTH), which is produced by the chief cells of the parathyroid gland. PTH is found contained within secretory vesicles. PTH promotes the proliferation of mesenchymal progenitors as well as regulating systemic calcium and phosphate homeostasis, thereby influencing the bone remodelling process (Bhandi et al., 2021). PTH exerts both, catabolic and anabolic effects on bone mass, where these effects are governed by the duration and periodicity of exposure to PTH. When administered intermittently, PTH stimulates osteoblast activity whereas, continuous PTH stimulation suppresses osteoblastogenesis (Yang et al., 2009; Chen et al., 2014). PTH influences the cell cycle of osteoblast by upregulating the expression of cyclin D, which induces the proliferation of early osteoblasts (Datta et al., 2007). PTH also stimulates osteoblast activity and differentiation by increasing ALP expression and IGF-1 signalling, where the latter exerts a stimulatory effect on type 1 collagen production (Canalis et al., 1989; Nishida et al., 1994). The parathyroid gland also contains calcium-sensing receptors (CaSR), which act to maintain serum concentration of calcium by activating the secretion of PTH in response to hypocalcaemia (Brown et al., 1993). PTH actions are primarily mediated via an osteoblast G-protein coupled receptor called PTH type 1 receptor (PTH1R). PTH-PTH1R binding activates at least two calcium-dependent intracellular signalling pathways. These cause activation of either G-protein alpha subunit or G-protein

alpha q subunit, which subsequently activate either protein kinase (PK) A through cAMP or PKC through phospholipase C (PLC) (Bhandi et al., 2021). PTH signalling also reduces the expression of DKK-1 whilst increasing the expression of β-catenin, net result of which is the stimulation of the WNT signalling pathway (Kulkarni et al., 2005).

Similarly, Vitamin D can also upregulate β-catenin expression resulting in the promotion of WNT-signalling (Shah et al., 2002; Haussler et al., 2010). Vitamin D also plays a role in mineral homeostasis which is integral in maintaining the skeleton. Specifically, vitamin D stimulates the intestinal absorption of calcium. The effects of vitamin D are facilitated by binding to the nuclear vitamin D receptor (VDR), where the interaction induces a conformational change that enables the VDR to form a heterodimer with the retinoid X receptor (RXR). VDR-RXR heterodimer interacts with vitamin D response elements (VDRE) in the promoter regions of target genes to modulate transcription (Carlberg et al., 1993). An example of such gene is the LRP5 gene, which leads to increased WNT signalling and consequently, increased differentiation of osteoblasts (Fretz et al., 2007). Vitamin D also has a direct effect on the bone-specific transcription factor, RUNX2, which results in increased transcription and hence, expression of OSC (Paredes et al., 2004).

1.5.4. Regulation of osteoclast differentiation

Several systemic and local factors regulate the function and differentiation of osteoclasts, which includes the macrophage-colony stimulating factor (M-CSF). M-CSF has a critical function in the differentiation, survival, and motility of osteoclasts. However, to achieve this, M-CSF relies on RANK/RANKL pathway to provide the

osteoclast lineage signal to early progenitors, and consequently induce osteoclastogenesis (see figure 1.11). Whilst RANK is mainly expressed by osteoclast precursors and mature osteoclasts, RANKL is expressed in the membrane-bound or secreted form by osteoblasts, osteocytes, activated lymphocytes and fibroblasts (Page and Miossec, 2005; Wei et al., 2005; Atkins et al., 2006; Kawai et al., 2006; Nakashima et al., 2011).

Binding of homotrimeric RANKL to its receptor RANK induces receptor oligomerisation, which leads to the recruitment of adapter proteins to the C-terminal cytoplasmic tail of RANK. Such adaptor proteins include TNF-receptor associated factor 6 (TRAF6). TRAF6 recruitment initiates signalling cascades, all of which promote osteoclastogenesis and osteoclast survival (Lomaga et al., 1999; Naito et al., 1999; Yavropoulou et al., 2008). These signalling pathways include the c-Src, MAPK and/or NF-κB pathways. The c-Src protein promotes the activation of an Akt/protein kinase B mediated anti-apoptotic programme and the MAPK pathway induces the translocation of proteins c-Fos and C-Jun into the nucleus along with the NF-κB. Activated NF-κB upregulates the expression of c-Fos which binds to calcium regulated NFATc1. NFATc1, the master activator of RANKL-induced osteoclast differentiation and promotes the expression of osteoclast-specific genes such as TRAP and cathepsin K, and proteins such as DC-STAMP and Atp6v0d2; all of which are important in osteoclast fusion and activation and the production of mature osteoclasts (Zhao et al., 2010; Miyamoto, 2011; Kim and Kim, 2014). The importance of tightly regulating RANK/RANKL signalling has been demonstrated by studies using murine models where RANKL-deficient transgenic mice lack osteoclasts and develop severe osteopetrosis. Hepatic overexpression of soluble RANKL leads to a hyper-resorptive and osteoporotic phenotype and ubiquitous

overexpression of soluble RANKL results in *in utero* death (Kong et al., 1999; Mizuno et al., 2002).

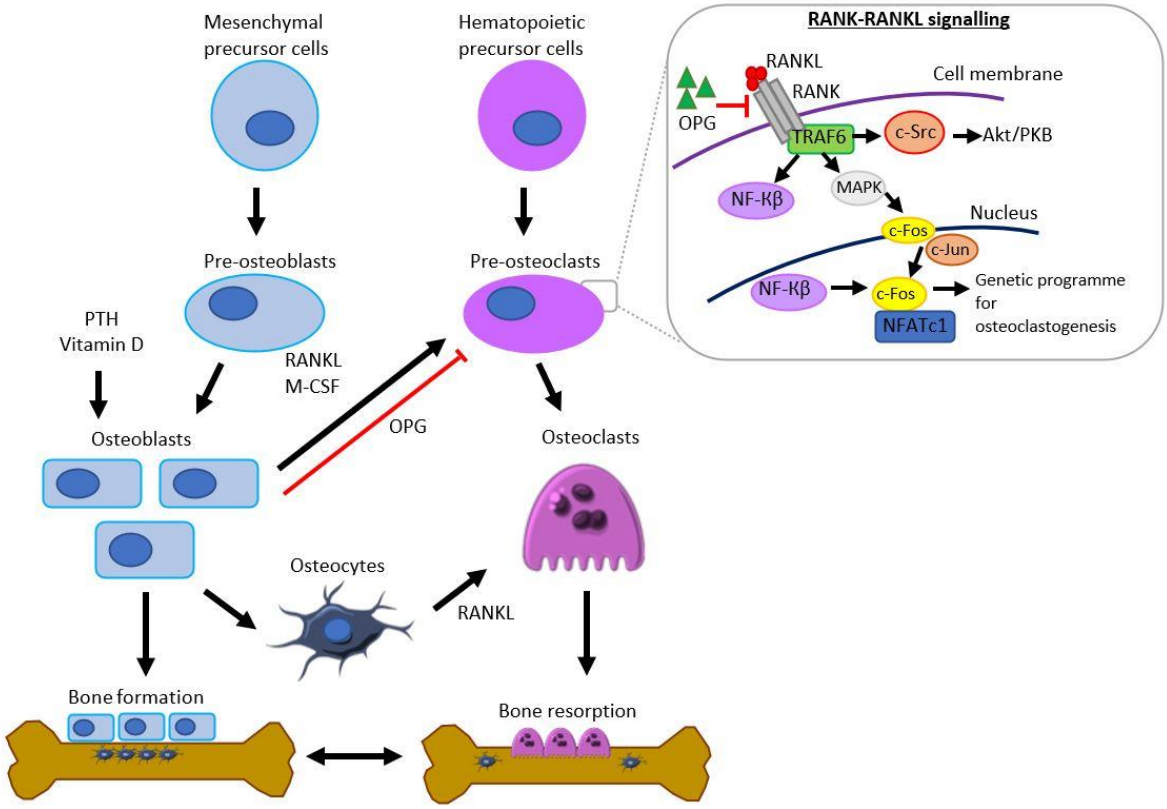

Figure 1.10: RANK-RANKL influence on osteoclastogenesis

Osteoblasts (bone forming cells) can be stimulated by multiple factors, including parathyroid hormone (PTH) and vitamin D. Once activated, osteoblasts present RANKL to osteoclast precursor cells, pre-osteoclasts. Osteoprotegerin (OPG) is a soluble decoy receptor for RANKL which inhibits RANK/RANKL signalling and therefore, osteoclastogenesis. Binding of RANKL to its receptor, RANK, triggers receptor oligomerisation, which in turn, recruit adapter proteins (e.g., TNF-receptor associated factor 6 [TRAF6]), which activate signalling cascades including the c-Src, MAPK and/or NF-κB pathways. c-Src activates an Akt/protein kinase B induced anti-apoptotic pathway and the MAPK pathway induces the translocation of c-Fos and c-Jun into the nucleus along with the NF-κB. The latter induces the expression of c-Fos which interacts with calcium regulated NFATc1, the master activator of RANKL-induced osteoclast differentiation. This interaction upregulates expression of osteoclast-specific genes (e.g., TRAP) and proteins (e.g., DC-STAMP) which play key roles in the fusion and activation of osteoclasts, and consequently in synthesis of mature osteoclast.

Osteoprotegerin (OPG), also known as osteoclastogenesis inhibitory factor, is a secreted glycoprotein produced by osteoblasts. OPG functions as a soluble decoy

receptor for RANKL and negatively regulates the RANK/RANKL signalling pathway, inhibiting osteoclastogenesis. *In vivo* transgenic mice overexpressing OPG develop osteopetrosis (increased bone mass) whereas mice lacking OPG had decreased bone mass (i.e., osteoporotic bones) (Simonet et al., 1997; Bucay et al., 1998). *In vitro* OPG expression has been shown to suppress the bone resorbing function of osteoclasts (Hakeda et al., 1998).

Chemical messengers, such as PTH, can also impact osteoclastogenesis. Continuous PTH exposure promotes bone resorption by upregulating RANKL and M-CSF. PTH can also target osteoblasts and stromal cells where it downregulates OPG expression, which together with the upregulated RANKL expression leads to an increased RANKL/OPG ratio favouring bone resorption (Huang et al., 2003; O'Brien et al., 2008) (See figure 1.11).

1.5.5. Glucocorticoids in bone remodelling

GC signalling also plays a chief part in the regulation of RANK/ RANKL signalling and consequently, the bone remodelling process. Endogenous GCs positively regulate the differentiation and function of MSCs, which in turn promotes bone development and maintenance. *In vitro* studies have demonstrated that abrogation of GC signalling through targeted overexpression of 11β-HSD2 in osteoblasts results in MSCs exhibiting reduced capacity to commit to osteoblastogenesis, and an increased ability to commit to the adipogenic lineage (Zhou et al., 2008). This was attributable to changes in the expression of WNT proteins which are governed by GC levels. Whilst low GC concentrations upregulate WNT 7B and WNT 10B expression in osteoblasts and thus, promote osteoblastogenesis; higher GC levels inhibit the expression of these WNT ligands and instead, increase expression of

WNT signalling inhibitors such as DKK-1 (Mak et al., 2009). Hence, GCs exert both beneficial and adverse effects on bone, with low levels being beneficial and high levels inducing bone loss and osteoporosis (Ishida and Heersche, 1998; O'Brien et al., 2004).

The exact effects of GCs on bone-resorbing osteoclasts are yet to be determined. Previous literature has reported that GCs decrease the number of osteoclast progenitors and inhibit their bone resorptive activity but can prolong their lifespan (Rubin et al., 1998; Weinstein et al., 1998; Jia et al., 2006). The latter is achieved by increased expression of M-CSF. Conversely, discordant results have been stated by other studies investigating the effect of GCs on osteoclastic genes, with one study reporting that GCs increase the mRNA expression of RANK, RANKL and OPG, which consequently increase TRAP and cathepsin K levels and thus, osteoclast activation (Swanson et al., 2006). Conflicting results are reported by further studies which found that GCs either decrease only OPG levels or do not impact RANKL and OPG levels (Hofbauer et al., 1999; Humphrey et al., 2006; Jia et al., 2006). These conflicting results may be attributable to the differences in the stage of osteoclast differentiation or whether an osteoclast is activated or deactivated (Kim, 2006).

1.5.6. Inflammation and bone homeostasis

Inflammation perturbs normal bone remodelling process in favour of resorption, resulting in either impaired bone production or more commonly, net bone loss. This is due to the crosstalk between the activated immune system and bone cells. Chronic inflammation induces a catabolic state where bone loss is promoted by direct communication with cells of the immune system and by synthesis of pro-

inflammatory cytokines. Cytokines can be categorised into two groups according to their ability to influence osteoclastogenesis: osteoclastogenic, if they promote bone resorption and anti-osteoclastogenic, if they inhibit osteoclast activity. Osteoclastogenic cytokines include IL-1, IL-6, IL-8, IL-17, TGF-β and TNF-α. Such cytokines exert their positive regulatory role in osteoclast differentiation by upregulating the expression of RANKL on osteoblasts and fibroblastic stromal cells (Kotake et al., 1999; Palmqvist et al., 2002; Wei et al., 2005; Yoshitake et al., 2008; Ragab et al., 2002). A similar mechanism is exhibited by lymphocytes to stimulate osteoclastogenesis. When activated following contact with antigens, B- and T-cells induce RANKL-dependent osteoclast differentiation as demonstrated by *in vitro* studies (Kawai et al., 2006). The ability of T-cells to induce or suppress osteoclast differentiation varies between the T-helper (Th) subsets. Th17 is the chief osteoclastogenic T-cell which stimulates osteoclast production either directly or indirectly. This is achieved by either expressing RANKL on its surface which binds to RANK on osteoclast precursors, or by producing IL-17 which stimulates osteoblasts and fibroblasts to express RANKL leading to further osteoclastogenesis. Conversely, Th1 possesses anti-osteoclastogenic activity which it executes by secreting IFN-γ which breaks down TRAF6 and so, suppresses osteoclast activity (Takayanagi et al., 2000; Sato et al., 2006). Similarly, Th2 cells secrete IL-4, which negatively regulates osteoclast formation by inhibiting NFATc1 expression and TNF-α signalling (Cheng et al., 2011).

During inflammation, TNF-α inhibits pre-osteoblast differentiation. *In vitro* studies have reported that this inhibition is due to TNF-α suppressing IGF-1, RUNX2 and the DNA-binding ability of core-binding factor A1 (cbfa1), which together reduce the expression of ALP and matrix deposition (Abbas et al., 2003). Both of the latter

markers are important for osteoblast differentiation, as is Cbfa1, which is an essential transcription factor for osteoblastogenesis. TNF-α can also causes apoptosis of osteoblasts, which contributes to inflammation-mediated bone loss (Hill et al., 1997; Jilka et al., 1998). Using transgenic mice overexpressing human TNF-α, a study investigated the effect of TNF blockage on bone loss (Redlich et al., 2004). This was achieved by combining anti-TNF therapy with OPG and/ or PTH. When administered together with OPG, anti-TNF treatment suppressed osteoclastogenesis and therefore, the development of more erosions. But, when combined with both OPG and PTH, anti-TNF treatment arrested bone loss and repaired bone damage. This study therefore suggests that bone damage can be repaired using therapies which can control inflammation whilst driving osteoblastogenesis and inhibiting the bone-resorptive activity of osteoclasts.

IL-6 also negatively regulates osteoblast differentiation by causing a significant reduction in the activity of ALP and in the expression osteoblastic genes, which include RUNX2 and OSC. This inhibition results in reduced bone mineralisation, hence disturbing the balance of normal bone turnover. However, other studies have suggested that IL-6 exerts a stimulatory effect on osteoblast differentiation by activating a transcription factor called signal transduction and activator of transcription 3 (Stat3) and suppressing the TNF-α mediated apoptosis of osteoblasts (Jilka et al., 1998; Itoh et al., 2006). Although, most studies have reported that inflammation drives bone away from the formative state and towards resorption, further research is necessary to establish the exact role of cytokines in inflammation-induced bone loss (Hardy and Cooper, 2009).

1.6. Murine models of bone loss in inflammatory diseases

The use of mouse models has proved to be imperative to the research of the aetiology, pathogenesis, and consequently, in the management of chronic inflammatory arthritides. The most widely used animal models include collagen-induced arthritis (CIA), collagen-antibody-induced arthritis (CAIA), K/BxN mice and TNF-Tg mice (Kannan et al., 2005; Asquith et al., 2009).

1.6.1. Contributions and limitations of murine models

Despite the murine models progressing our knowledge of inflammatory arthritis, each model does present with inherent limitations.

CIA, considered the gold-standard *in vivo* model of RA, shows both, immunological and pathological characteristics of RA. The CIA model involves inoculation with type II homologous collagen (CII) emulsified with total Freund's adjuvant (Holmdahl et al., 1986; Malfait et al., 2001). The resultant synovitis, bone and cartilage erosion, synthesis of CII autoantibodies and CII-specific T-cells mimic the disease progression of human RA (Stuart and Dixon, 1983; Joe et al., 1999). Due to the CIA model being restricted to the DBA/1 strain, it has been challenging to explore the effect of targeted gene deletion or modification as most transgenic models use the CIA-resistant C57BL/6 mouse strain (Pan et al., 2004). However, protocols have been refined to induce CIA in C57BL/6 mice, although this strain develops a variable, milder form of RA, which may yield irreproducible results (Campbell et al., 2000; Inglis et al., 2008).

An extension of the CIA model, the CAIA model which displays acute arthritis has been generated using monoclonal antibodies against CII to achieve more robust and reproducible results. Although clinically, the CAIA model displays symptoms and joint pathology, which is similar to human RA, it lacks B- and T-cell response

thus cannot be used to investigate the role of adaptive immunity in the development of inflammatory arthritis (Yoshino et al., 1990; Nandakumar et al., 2004).

The K/BxN mouse strain, expressing both the MHC class II molecule and a transgenic T-cell receptor recognising specifically an epitope of bovine RNAse (KRN), has been integral to study the autoimmune development of inflammatory arthritis. Serum from these mice (which contains high levels of autoantibodies to the ubiquitous antigen glucose 6-phosphate isomerase) can be injected into recipient mice of any strain to induce a reliable, standardisable, resolving inflammatory arthritis. The induced arthritis is attributable to complement activation, degranulation of mast cells and activation of pro-inflammatory cytokines (namely IL-1 and TNF-α) (Kouskoff et al., 1996).

1.6.2. TNF-Tg murine model of inflammatory arthritis

Transgenic mice overexpressing the human version of the pro-inflammatory cytokine, TNF-α are termed TNF-Tg (Keffer et al., 1991). These mice develop erosive polyarthritis, the chronic progressive nature of which closely mirrors RA. Generally, TNF-α production is tightly regulated, with the AU-rich element (ARE) containing 3′ untranslated region (UTR) implicated in the breakdown of TNF-α transcripts in resting cells (Han et al., 1990; Pauli, 1994). However, in the TNF-Tg mice, the human TNF-α transgene is modified in the ARE containing 3′ UTR and replaced with 3′ UTR from the β-globin gene, which lacks ARE elements and is therefore more stable and less prone to enzymatic degradation mediated by ARE-binding proteins. As a result, increased levels of soluble and membrane-bound TNF-α are present (Keffer et al., 1991). This has led to the generation of various TNF-Tg mouse lines, all of which develop inflammatory arthritis. Such lines include

the 3647 and the 197 lines. Whilst Tg-3647 contains only one transgene copy and the mice develop mild arthritis, Tg-197 mice contain five copies of the transgene and develop severe arthritis. The phenotype displayed by Tg197 more closely resembles human RA, but like with CAIA model, lacks adaptive immune pathway in RA development (Douni et al., 1995). The TNF-Tg model has been pivotal in understanding the cytokine hierarchy in the pathogenesis of RA, and has consequently led to the development anti-TNF-α biological agents (Keffer et al., 1991)

1.6.2.1. TNF-Tg murine model: TNF impact on bone and muscle

As previously mentioned, TNF-α negatively regulates osteogenic differentiation, whilst upregulating osteoclast activation and expression of ubiquitin ligases – net result of which is bone loss and muscle atrophy (Lam et al., 2000; Wang et al., 2014). Hence, TNF-Tg model also mirrors the extra-articular manifestations of RA.

In a recent study, we reported that when compared with WT mice, the bone volume, trabecular number, and thickness was significantly reduced in TNF-Tg mice (Fenton et al., 2019). Using histochemistry and subsequent quantification, the study showed that the number of osteoclasts stained with TRAP was increased in the bones of TNF-Tg mice. The gene expression of osteoblast markers, ALP and OSC, was also significantly reduced. Lastly, more significant muscle atrophy was observed in TNF-Tg mice when compared with WT mice, with the TNF-Tg mice having lower muscle weight and smaller fibre size (Fenton et al., 2019).

1.7. Summary

In inflammatory conditions and glucocorticoid use, systemic bone loss accounts for a significant complication. In this context, 11β-HSD1 is potently upregulated within bone cells, such as osteoblasts, where it may mediate the detrimental actions of endogenous and therapeutic GCs in human disease.

1.8. Hypothesis

We predict that in response to inflammation, the induction of 11β-HSD1 increases local exposure to active GCs and results in reduced bone formation. Here the application of 11β-HSD1 inhibitors will prevent activation of GCs and protect bone.

In this study, we will examine the inflammatory regulation and expression of 11β-HSD1 in bone forming osteoblasts and determine its contribution to the suppression of bone formation during inflammation and in response to therapeutic GCs.

1.9. Aims

The specific aims for this project are:

- Establish primary human osteoblast cultures to investigate the expression and regulation of 11β-HSD1 in the presence of GCs, and GCs and inflammation
- Characterise the activity and GC activation of 11β-HSD1 in osteoblasts
- Examine the functional consequences of GCs activated by 11β-HSD1 on bone formation by osteoblasts using primary cultures and animal models

Chapter 2: Methods

All *in vitro* experiments and quantitative analysis of animal work has been done by me [Syeda Fareed]. However, biopsies from murine models were obtained by and provided to me by Dr Chloe Fenton. A brief overview of how Dr Fenton obtained these is stated in my thesis.

2.1. Primary human osteoblast cell culture

Trabecular bone chips were obtained from patients with hip osteoarthritis (age 69 ± 3 years) (collaboration with Simon Jones (UK National Research Ethics Committee 14/ES/1044) approval date: 17/9/2016) and stored in phosphate buffer saline (PBS) prior to being used. Trabecular chips were cultured in high-glucose Dulbecco's Modified Eagle Medium (DMEM, Sigma, Gillingham). To each bottle of high-glucose DMEM, the following were added: 50 ml of 10% fetal bovine serum (FBS); 5 ml each of 1% non-essential amino acids, 1% sodium-pyruvate and 1% penicillin-streptomycin; and 500 µl each of 50 μg/ml ascorbic acid and 2 mM β-glycerophosphate. Hereafter, this mixture referred to as osteoblast differentiation media, which enables osteoblasts to be released. For the pre-osteoblasts (also obtained from bone chips), growth media was used (high-glucose DMEM, 50 ml of 10% FBS, 5 ml each of 1% non-essential amino acids, 1% sodium-pyruvate and 1% penicillin-streptomycin). Osteoblasts were grown in incubators at 37°C under a 5% CO_2 atmosphere until they reached a confluency of 80%, after which the bone chips were removed. Cell media was replaced every 2 days. The cells were trypsinised until 90% of the cells were detached. These were then placed into either T25 flasks, 12-well or 96-well plates. The cells were passaged once a confluency of 80% was reached (around day 21) prior to being plated in 12-well or 96-well plates for the relevant experiments (passage 0) or grown to confluence again (passage 1) (see figure 2.1). Depending on the aim of the experiment, osteoblasts were then allowed to differentiate for three weeks in osteoblast media containing different combinations of TNF (10 ng/ml), cortisol (5, 10, 50, 100, 500, 1000 nM), cortisone (100 ng/ml) and the 11β-HSD1 inhibitor (1 µM): glycyrrhetinic (GE) acid. Control osteoblasts were grown in media alone alongside the treated osteoblasts. For 12-

well plates, the treatments were repeated in 3 wells, whilst for 96-well plates, 5 wells were designated to each treatment. Treatments were replaced three times per week, with extra care taken to ensure the cells were not disrupted.

2.1.1. Thawing and plating of cryopreserved osteoblasts

Cryopreserved osteoblasts were removed from liquid nitrogen and thawed in 37°C water for 1 minute by gentle swirling. Caution was taken to make sure that the vial was not completely submerged in the water. The cryovial was removed and wiped with ethanol before placement in a sterile hood. The cells in the vial were resuspended and transferred into a falcon tube. Warm media was added to the falcon tube, which was then centrifuged for 5 minutes at 1,600 rpm to yield a cell pellet at the bottom of the tube. The supernatant was decanted. The resultant cell pellet was resuspended in fresh media and transferred to a T75 flask containing fresh osteoblast media. The flask was capped and rocked gently to ensure even distribution of cells, prior to placement in a 5% CO_2 humidified 37°C incubator for osteoblasts to grow. Media was replaced every 2 days and cells were grown until reaching 80% confluence, after which the osteoblasts were placed in either T25 flasks, 12-well or 96-well plates (see figure 2.1). The same method was used to plate cells with treatment to monitor cell differentiation as mentioned in section 2.1.

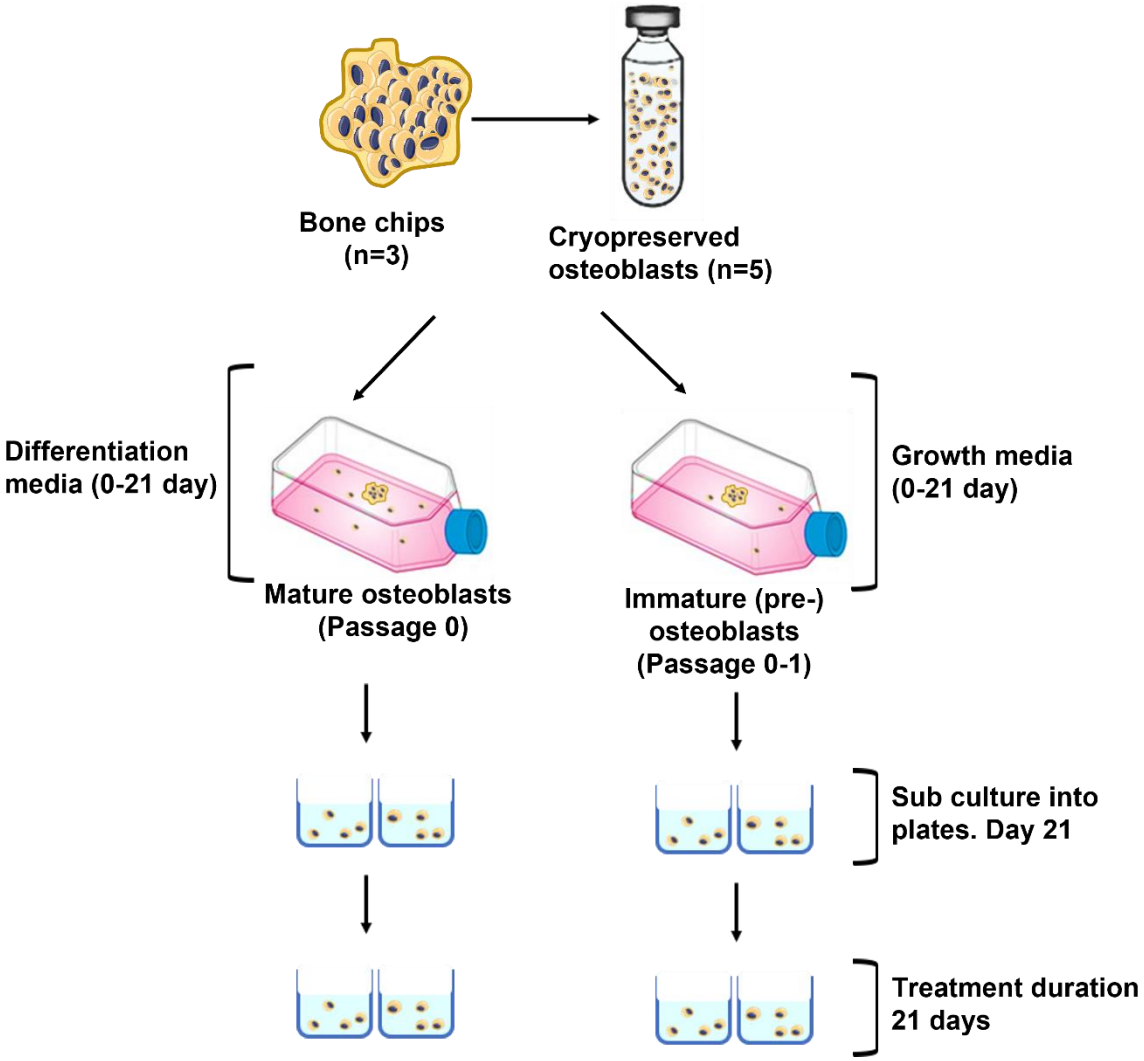

Figure 2.1: Cell culture set up

For cell culture experiments, 2 sources were used: trabecular bone chips from 3 patients (n=3) or cryopreserved osteoblasts (n=5).

Initially, both were cultured in differentiation media or growth media, and incubated at 37°C and 5% CO_2. The cells were allowed to reach a confluency of 80% (around day 21), after which their differentiation status was confirmed. Once the cells were confirmed as being mature (via alizarin red staining and mRNA expression levels [not illustrated], treatments were added (with the differentiation media) to the mature osteoblasts plated on 12/96-well plate (n=5). Treatment duration: 21 days.

2.1.2. Alizarin Red staining

To evaluate calcium deposits and mineralization of osteoblasts in cell culture, an Alizarin Red S staining quantification assay was utilised. Care was taken to produce the Alizarin Red S staining solution and to correct the pH to 4.1 - 4.3. Once made, the solution was stored in the dark prior to use and discarded within 7 days from the date of production. Media from cell culture was aspirated, after which the cells received a PBS wash. This PBS lacked calcium and magnesium. Precaution was taken when washing to make sure that the cell monolayer was not disrupted. Once washed, Alizarin Red S stain was added to each well and left to incubate for 45 minutes in the dark at room temperature. Post incubation period, the stain was aspirated, and cell monolayer was washed four times with PBS. The stain was then solubilized for 10 minutes with hexadecyl pyridinium chloride monohydrate (Sigma), after which the supernatant was diluted with water (1:10). The plate was read using Victor multilabel plate reader (PerkinElmer, Bucks, UK) at 570 nm.

2.2. RNA extraction and analysis

RNA was isolated from cultured cells and tissues. Extracted RNA was measured and then, reverse transcribed to yield complementary DNA (cDNA). The cDNA was utilised for subsequent analysis by quantitative reverse transcription polymerase chain reaction (qRT-PCR) to ascertain expression levels of specific messenger RNA (mRNA).

2.2.1 RNA extraction

The innuPREP RNA Mini Kit 2.0 (AnalytikJena, Jena, Germany) was used to extract RNA. Mice tibias were dissected from the hind limb, soft tissue removed and then,

homogenized using liquid nitrogen in a sterilised pestle and mortar. Lysis solution RL was added to the resulting homogenate to create a mixture which was centrifuged for 5 minutes at 13,000 rpm. All centrifugation steps of the extraction process were carried out at 4°C. For cells, lysis solution RL was added to the directly to the plate and cells were scraped from the monolayers in each well. The supernatant from the cell culture and tissues was then placed into a receiver tube containing Spin Filter D and centrifuged for 2 minutes at 12,000 rpm. This removes genomic DNA, which binds to Spin Filter D which was then discarded. An identical volume (~400µl) of 70% ethanol was added into the filtrate and mixed to enable ethanol-induced RNA precipitation. The sample was then moved into a receiver tube containing Spin Filter R and centrifuged for 2 minutes at 12,000 rpm. Total RNA is bound to Spin Filter R, to which washing solution HS is added first and centrifuged for 60 seconds at 12,000 rpm. The filtrate is discarded and washing solution LS is added and the centrifugation step (60 seconds at 12,000 rpm) is repeated. The filtrate is removed, and the filter is transferred to a receiver tube. The filtrated containing tube is placed in a centrifuge for 3 minutes at 12,000 rpm. This removes any remaining ethanol, drying the RNA. 30 µl of RNAse-free water is added to the filter, which is placed into an elution tube, and centrifuged for 1 minute at 8,000 rpm. This elutes the purified RNA, concentration of which can be measured by means of a NanoDrop™ 1000 Spectrophotometer (ThermoFisher, Paisley, UK). Following quantification, all RNA samples were stored at -80°C.

2.2.2. Reverse transcription

Reverse transcription of extracted mRNA was performed to synthesise the more stable, single-stranded cDNA, which was then utilised to analyse gene expression.

This analysis was conducted using High-Capacity cDNA Reverse Transcription Kit (ThermoFisher, Paisley, UK). To 350 ng of RNA, 13 µl of a master-mix formed from the kit's components was added (see table 1). This was then made up to a total volume of 20 µl, through the addition of RNAse-free water. The master-mix was then placed in a GeneAmp® PCR System 2700 thermocycler (ThermoFisher, Paisley, UK) to run. For each run, pre-optimised settings were used: for the first 10 minutes, a temperature of 25°C was used, followed by 60 minutes at 37°C for and 48°C for 30 minutes. Following this, the samples were subjected to 95°C for 5 minutes and then left to rest at 4°C until the samples were removed. The cDNA was placed in storage at -20°C until needed for experiments.

Reagent	**Volume (µl) used per single reaction**
10x RT buffer	2
25mM $MgCl_2$	4.4
2.5mM dNTPs	4
Random hexamers	1
RNAse inhibitors	0.4
Reverse transcriptase	1.2

Table 2: Quantity of kit component added per single reaction in the reverse transcription master mix

2.2.3. Real-Time quantitative reverse transcription PCR (qRT-PCR)

qRT-PCR amplifies target genes of interest and quantifies their expression in a specific reaction. To be able to do so, real-time PCR uses a fluorogenic TaqMan probe and specific primers. The TaqMan probe has a reporter fluorochrome at the 5' end and a quencher dye at the 3' end which functions to inhibit the fluorescent signal (see figure 2.1). Briefly, the temperature is raised at the start of PCR process which causes denaturing of the double-stranded cDNA to form a single-stranded

template. During this step, the fluorescence emitted from the reported dye at the 5' end is inhibited by the quencher at the 3' end. The annealing step follows where the probe and primers bind to their specific target sequences. During extension, the Taq DNA polymerase uses the template strand and the primers to synthesize a new DNA strand. Once the polymerase reaches the TaqMan probe, it utilises its 5' exonuclease activity to degrade the probe. This cleavage allows the inhibited fluorescent dye to be released from the quencher, causing an increase in the fluorescence emitted (see figure 2.1). The amount of fluorescent signal detected positively correlates with the level of the gene of interest that is produced. The number of cycles needed for the fluorescence emission to exceed the baseline is called the cycle threshold (CT) value.

For each target gene, a PCR master mix was prepared. This was made up of 3.5 µl RNAse free water, 1µl SensiFAST^{TM} Probe Lo-ROX (Bioline, Nottingham, UK) and 0.5 µl of a specific TaqMan Gene Expression Assay probe (Applied Biosystems, Warrington, UK) per sample. To each well of a microarray optical 96-well reaction plate (MicroAmp®, Applied Biosystems, Warrington, UK), 9 µl of the master mix and 1 µl of cDNA was added. Each reaction was performed in duplicate. For each gene, a negative control which consisted of only the master mix was also added to the plate. An 18S housekeeping gene was used as an internal control for each sample. A film was used to seal the plate. The plate was spun for 1 minute at 1,200 rpm to remove any air bubbles, and then transferred to ABI7500 qPCR machine (Applied Biosystems, Warrington) to run under a set 96-minute cycle. This cycle consisted of a pre-cycle step which lasted 10 minutes at 95°C, followed by 40 cycles at the same temperature for 15 seconds. The cycle was ended by cooling the plate at 60°C for 1 minute.

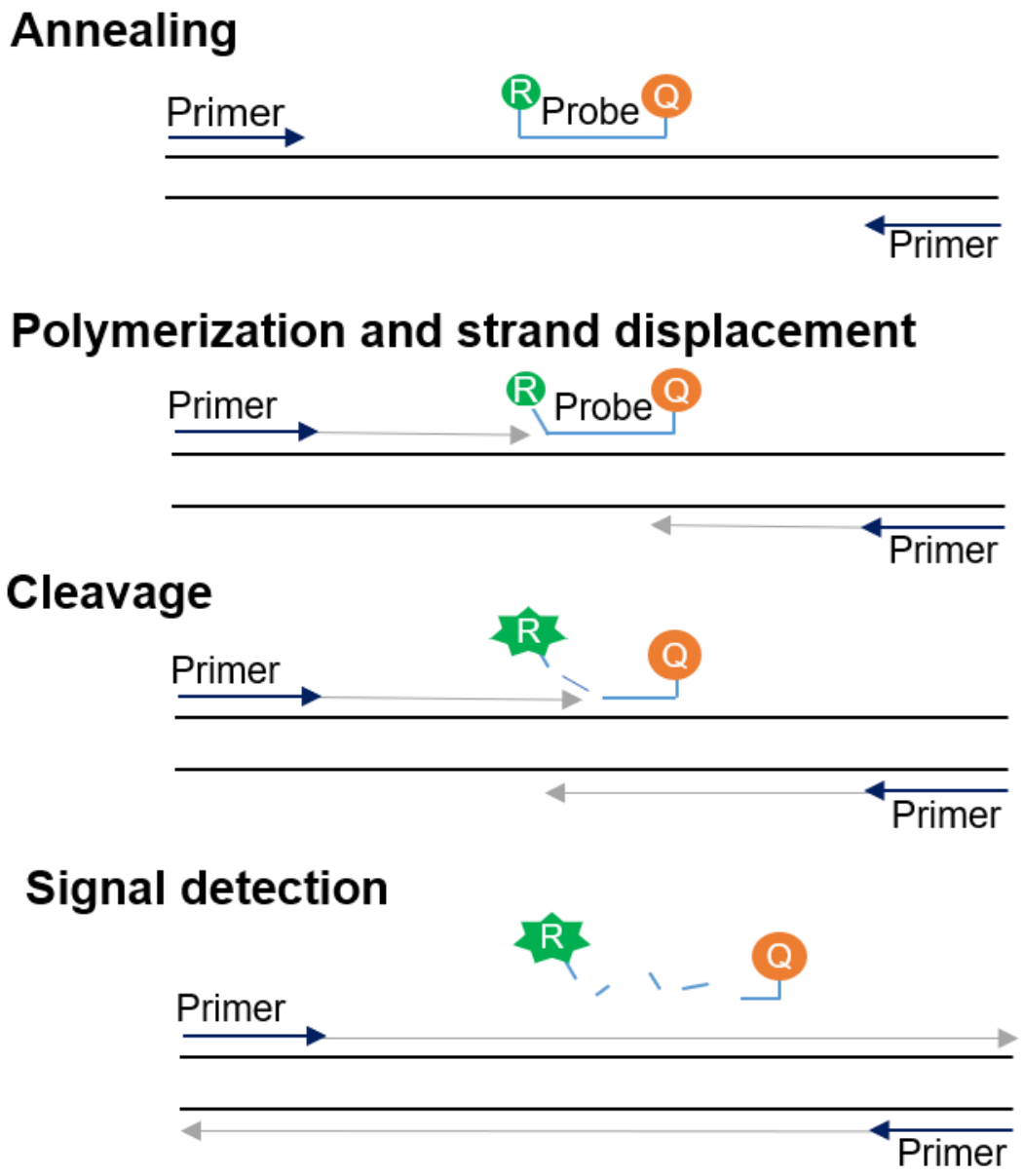

Figure 2.2: TaqMan based qRT-PCR

Real-Time quantitative reverse transcription PCR (qRT-PCR) is carried out in a quantitative thermal cycler. The TaqMan probe is key to qRT-PCR, which harbours two fluorophores: a reporter fluorophore (R) and a quencher fluorophore (Q), which rely on the 5' and 3' nuclease activity of the DNA polymerase respectively. When in close contact, the fluorescent emissions from the reporter fluorophore are inhibited by the quencher. The Taq DNA polymerase possesses a 5' to 3' exonuclease activity, which starts to cleave the nucleotides at the 5' end. As the DNA strand is extended due to the addition of the primers, the polymerase reaches the probe attached to the reporter fluorophore. The R is cleaved and prevents it from being quenched. The fluorescence emitted by the reported is detected and quantified. The fluorescence level is directly related to the level of gene expression present within the sample.

2.2.4. Statistical analysis of qRT-PCR

For each gene, ΔCT value was calculated. This was done by obtaining CT values, averaging the duplicates, and normalising to 18S [CT (gene of interest) – CT (18S housekeeping gene)]. ΔCT values were then presented as fold change, expressed as arbitrary units (AU) which was calculated using the following equation:

$$\text{Arbitrary units (AU)} = 1000 \times (2^{-\Delta CT})$$

Statistical analysis was then conducted using the arbitrary values. To determine statistical significance, GraphPad Prism software (GraphPad, San Diego, USA) was used. Either a one-way ANOVA or two-way ANOVA analysis with a Tukey multiple comparison test were used. N numbers are stated in each figure legend. $P \leq 0.05$ was determined as being statistically significant. * represents $P \leq 0.05$, ** represents $P \leq 0.01$ and *** represents $P \leq 0.001$

2.3. Enzyme linked immunosorbent assays (ELISAs)

ELISAs were used to analyse the presence of proteins in a sample. For samples obtained from experiments, cell culture media from each well was harvested post completion of the treatment period. This media was then stored in an ultra-cold freezer at 80°C prior to use. All standards and samples were measured in duplicate.

2.3.1. Sandwich ELISA – principles and protocol

A sandwich ELISA can be employed to detect and calculate protein levels within a sample. First, the wells of a microtiter assay plate are coated with a capture antibody specific to the target protein. The sample is added to the wells of the microtiter plate, so that the target protein directly binds to the capture antibody and becomes immobilised on the plate. The unbound sample is washed off and a detection

antibody specific to the protein of interest is added. The detection antibody is generally conjugated to biotin or directly to an enzyme, particularly horseradish peroxidase (HRP). Detection antibodies bound to biotin require a separate step where HRP-streptavidin conjugate is added. The HRP-streptavidin conjugate will bind to the biotin. Next, a chromogenic HRP substrate such as tetramethylbenzidine (TMB) is added, which results in the production of a quantifiable coloured product. The amount of coloured product positively correlates to the level of the target protein present within the sample. Finally, an acid is added to stop the assay. Standards containing a known protein concentration are run alongside the samples so that colour intensities can be compared and protein concentrations to be quantified (see figure 2.2).

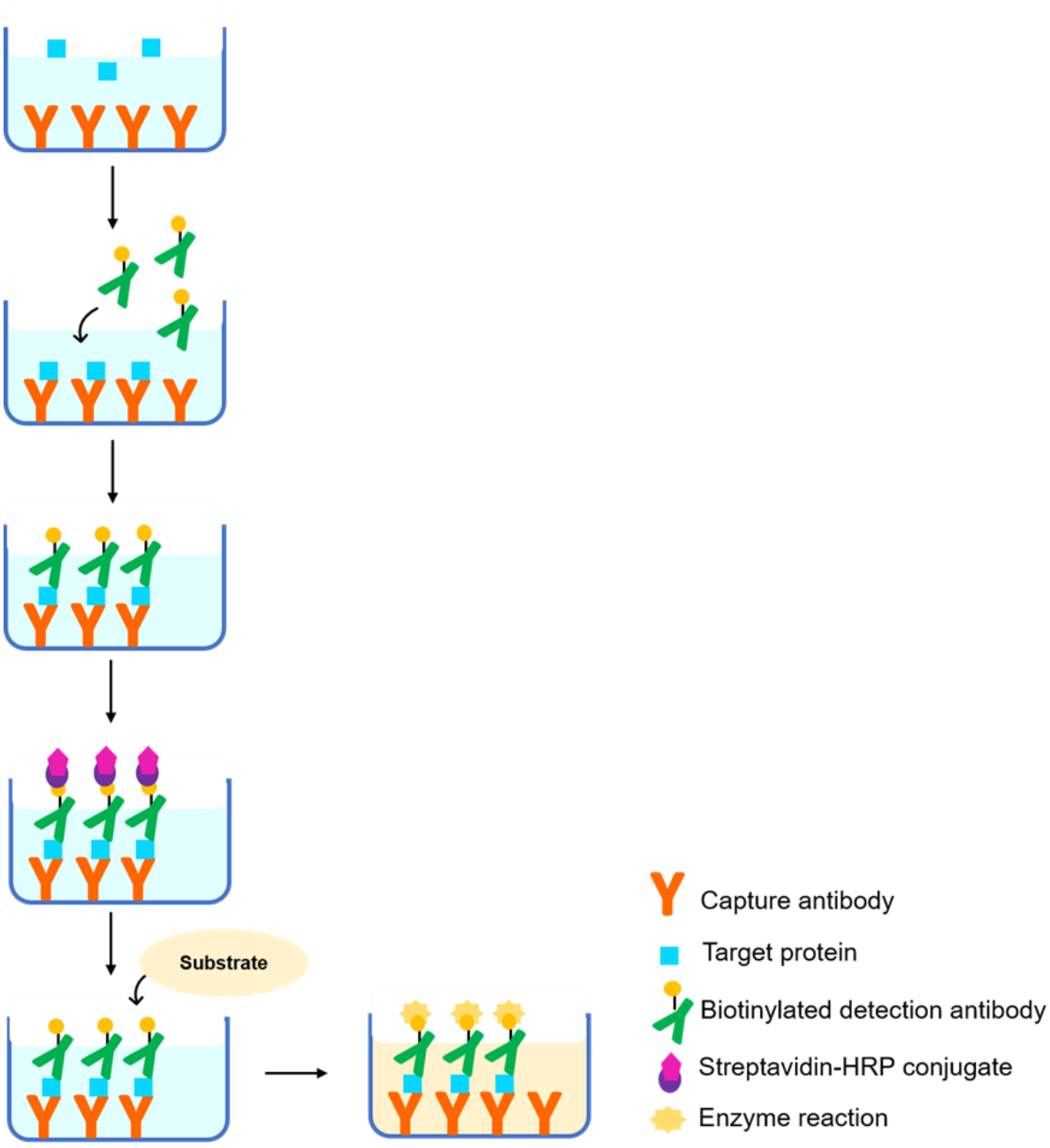

Figure 2.3: Principles of a Sandwich ELISA

The surface of the assay plate is covered with a capture antibody specific to the target protein. The protein of interest binds to the capture antibody. Detection antibody is then added to the well, which tends to be specific to the target protein. This detection antibody is conjugated to biotin or to horseradish peroxidase (HRP). If bound to biotin, streptavidin-HRP conjugate is added. A chromogenic substrate is added, which mediates an enzyme reaction, and this is seen as a colour change.

2.3.2. Human IL-6 ELISA

A commercially available hIL-6 ELISA kit (BD Biosciences, California, USA) was utilised to quantify the levels of the pro-inflammatory cytokine IL-6 in the conditioned media collected from the cell culture experiments. The microtiter plate provided with the kit was first coated with an anti-human monoclonal capture antibody specific to hIL-6. The plate was sealed to prevent evaporation and incubated overnight at 4°C. The subsequent day, the contents of the wells were aspirated. The plate was washed with wash buffer, inverted, and then blotted onto absorbent paper to remove residual buffer. 200 µl of Assay Diluent was added to the plate and incubated for 1 hour at room temperature. Following incubation, the aspiration and washing steps were repeated and 100 µl of standard and sample dilutions in Assay Diluent were added. Extra Assay Diluent was used as a blank control and added to two wells of the microtiter plate. The plate was placed in an incubator with for 2 hours at room temperature. During each incubation period, the plate was sealed using an adhesive strip. After being washed five times, 100 µl of human IL-6 conjugate (monoclonal antibody specific for hIL-6 conjugated with streptavidin-HRP) was pipetted to each well and left to incubate for 1 hour at room temperature. The washing step was repeated seven times, after which 100 µl of a Substrate Solution (composed of 1:1 mixture of TMB and hydrogen peroxide) was added to all wells and left to incubate for half an hour in the dark at room temperature. The reaction between HRP and TMB produced a colorimetric change to yield a blue colour. The reaction was stopped by the addition of 50 µl of a sulfuric acid, which acted as a Stop Solution. The optical density (OD) was then measured within 30 minutes. For this, a VICTOR^3 1420 Multilabel counter (PerkinElmer, Llantrisant, UK) plate reader calibrated to 450 nm was used. The mean absorbance for each duplicate was determined and the

mean zero standard absorbance was deducted from all the averaged readings. Graphs using the values obtained for the standards against their known concentrations (pg/ml) were generated.

From the graph, a line of best fit was used to create an equation which allowed the concentration of the samples to be measured. Where dilution factors were used, samples were multiplied by these factors.

2.3.3. Human Pro-Collagen I α1 (hCOLIA1) ELISA

To measure the collagen levels in the growth media obtained from the conditioned media experiments, a commercially available hCOL1A1 ELISA kit (R&D Systems, Abingdon, UK) was utilised. Firstly, the assay plate was coated with anti-human pro-collagen I α1 capture antibody, sealed, and left to incubate overnight at room temperature. Following the incubation period, the plate was washed three times and blotted to ensure complete removal of the liquid. 300 µl of Reagent Diluent was added to each well to block plates and left to incubate at room temperature for one hour. The aspiration and washing step were repeated, after which samples were added. An undiluted sample was added along with various dilutions of it (in Reagent Diluent) 1 in 10, 1 in 100, 1 in 500 and 1 in 1000). Standards were added alongside the samples and extra reagent diluent was added to two wells in the plate to be used as a negative control. The plate was incubated for 2 hours at room temperature. Wells were washed, 100 µl of the detection antibody was added to each well and left to incubate for 2 hours at room temperature. After being washed three times, 100 µl of streptavidin-HRP was added to each well. After incubating for 20 minutes at room temperature in the dark and being washed, Substrate Solution was added to the plate. The Substrate Solution consisted of equal volumes of TMB

and hydrogen peroxide. Addition of TMB caused a colour change from yellow to blue. The plate was incubated for a further 20 minutes at room temperature in the dark. Finally, the reaction was stopped by the addition of a hydrochloric acid (Stop Solution) and gently tapping the assay plate. The OD was measured immediately using a VICTOR^3 1420 Multilabel counter (PerkinElmer, Llantrisant, UK) plate reader set at two wavelengths: 450 nm and at 540 nm. To adjust for optical imperfections in the plate, OD readings for each well at 540 nm were subtracted from the readings obtained at 450 nm. Once subtracted, results were calculated and plotted in the same way as outlined in section 2.3.2.

2.3.4. Statistical analysis of ELISA

For each biological replicate (individual patient i.e., each bone chip, or cryopreserved vial), experiments on three technical replicates were performed. From the results obtained from the technical replicates, an average value was calculated on which statistical analysis was carried out. GraphPad Prism software (GraphPad, San Diego, USA) was used to calculate statistical significance. Either a one-way ANOVA or two-way ANOVA analysis with a Tukey multiple comparison test were used. N numbers are listed in figure legends. $P \leq 0.05$ was determined as being statistically significant. * represents $P \leq 0.05$, ** represents $P \leq 0.01$ and *** represents $P \leq 0.001$.

2.4. 11β-HSD1 activity assay

The oxoreductase activity of 11β-HSD1 was established by calculating the conversion of radiolabelled ^{3}H-cortisone to ^{3}H-cortisol using thin layer chromatography (TLC). TLC is a chromatographic technique used to separate

compounds in a mixture based on their solubility in two distinct stages: the stationary phase and the mobile phase. The stationary phase consists of the TLC plate being coated with an absorbent material (typically silica gel) while the mobile phase refers to the solvent used in the developing tank to run the TLC plate. For the mobile phase, chloroform and ethanol were the solvents utilised. The compounds in the mixture separate between the two phases, according to their structures and polarities. Those compounds that are most water-soluble travel slower up the plate as they bind strongly to the silica gel (favouring the stationary phase), whilst non-polar compounds move quickly up the plate as they are more soluble in the mobile phase. Radiolabelled steroid substrates and products were measured using a BioScanner, allowing the percentage of GC converted during the assay.

2.4.1. Treatment with steroids

Cells were seeded on a 6-well plate and allowed to reach 100% confluence. Once confluent, culture media was collected, and cells were washed in PBS. The plate was incubated at 37°C for 3 hours in serum-free DMEM which contained ^{3}H-cortisone and 1 µl of cold steroid. This media was then aspirated, transferred to borosilicate glass tubes, and stored in the freezer at -20°C until required.

2.4.2. Thin layer chromatography (TLC)

To measure the rate of GC conversion, frozen media was defrosted and used to perform TLC. The steroid treatments were first extracted by adding 5 ml of dichloromethane into each of the media-containing borosilicate tubes. The samples were vortexed for 10 seconds and then centrifuged for 15 minutes at 1,500 rpm. The centrifugation allowed for the solution to separate into two phases: an aqueous

phase (the media) and an organic phase (steroid-containing dichloromethane). The aqueous phase above the dichloromethane was aspirated off and extra care was given to ensure removal of all the contaminating debris and media. The organic phase containing the steroids was evaporated at 50°C with continuous air flow for 3 hours using a Dri-Block® Heater DB100/3 (Techne, Staffordshire, UK). Steroids were re-suspended in 90 µl of dichloromethane, vortexed and spotted using a glass Pasteur pipette (VWR, Lutterworth, UK) onto a labelled silica-coated TLC plate (Sigma, Gillingham, UK). ^{3}H-steroid controls were also added on the plate as spots, together with the samples. Each spot was separated by 2 cm from the adjacent samples and 2 cm from the bottom side of the plate. Steroids were then separated according to their molecular making by TLC. A tank containing 200 ml of chloroform: ethanol (92:8) was used as the mobile phase, in which the plate was run for 90 minutes. The plate is then transferred onto an AR-2000 bioscanner (Bioscan, Oxford, UK) to assess the radioactivity of the sample. To calculate the percentage (%) conversion, region counts from both active and inactive steroid peaks were used. Enzyme activity was conveyed in picomoles of steroid converted per mg of protein per hour (pmol/mg/hr). Steroid conversion rate was calculated using:

Conversion rate = Percentage conversion x () x ()

in which S = concentration of steroid substrate (pmol), T = time in hours, and P = concentration of protein (mg). Radioactivity of the separated ^{3}H-cortisone and ^{3}H-cortisol was determined using a Bioscan 200 Imaging Scanner (LabLogic, Sheffield, UK) 10 minutes per lane.

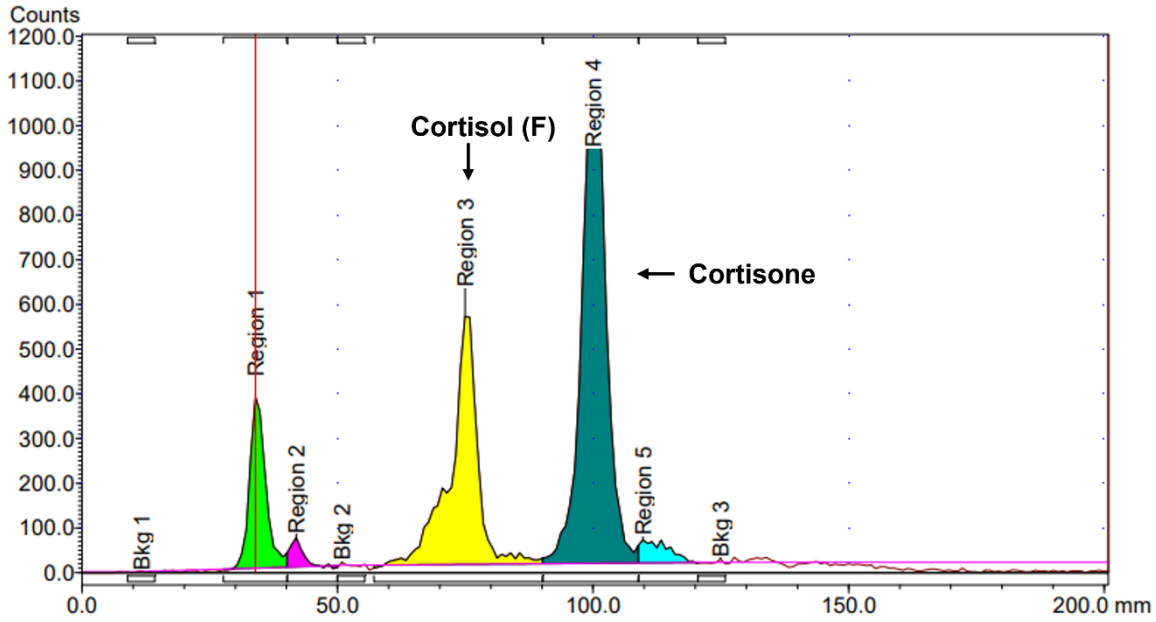

Figure 2.4: Example of a chromatogram from 11β-HSD1 activity assay

Representative image of a chromatogram, where the peaks denote human steroids: Cortisol (F) and its inactive counterpart, cortisone (E)

2.5. Micro-CT analysis

All *in vivo* work was carried out by Dr Chloe Fenton carried out under guidelines outlined by the Animal (Scientific Procedures) Act 1986 in line with the project licence (P51102987). All procedures were approved by the Birmingham Ethical Review Subcommittee (BERSC). All mice were housed in the Biomedical Science Unit in individually ventilated cages at a humidity of 55% and temperature of 21-23°C.

The animal models were used for this thesis: WT, TNF-Tg mesenchymal-specific KO of 11β-HSD1 (Twist2-CRE) and global KO of 11β-HSD1 (11βKO).

2.5.1 Models of polyarthritis

Professor George Kollias (BSRC Fleming, Athens, Greece) kindly provided the TNF-Tg murine model of chronic inflammatory polyarthritis, which was maintained on C57BL/6 background and compared to the WT group (Keffer et al., 1991).

Briefly, from the first onset of measurable polyarthritis, mice received either 100 µg/ml of GC treatment (100 µg/ml corticosterone with 0.66% ethanol) (Sigma Gillingham, UK) in their drinking water for three week or vehicle (0.66 ethanol). The mice were scored as described previously (Hardy et al., 2016; Naylor et al., 2017). At the end of the experiments (7 weeks of age), mice were culled by cervical dislocation and their tibias were collected by dissection following animals being euthanised by a schedule 1 method. One tibia was fixed in 4% formalin and stored in 70% ethanol, whilst the other was homogenised for RNA isolation.

2.5.2 Target deletion of 11β-HSD1

11β-HSD1 KO mice with a global deletion of 11β-HSD1 were crossed with TNF-Tg mice to generate TNF-tg11βKO mice as previously described (Hardy et al., 2018). For mesenchymal specific 11β-HSD1 KOs, flx/flx-HSD11B1 mice were crossed with Twist2-cre mice. Twist 2 is expressed in mesenchymal derived cell populations and its recombinase activity has been shown in osteoblasts. This generated 11βHSD1flx/flx/Twist2cre animals (Twist2-CRE) which were crossed with TNF-tg animals, result of which was TNF-tg11βHSD1flx/flx/Twist2cre (TNF-CRE) (Yu et al., 2003; Semjonous et al., 2011; Li et al., 2013). Cre recombinase activity has been reported to target mesenchymal derived cell populations, which one such population being the osteoblasts.

Using a Skyscanner 1172 (Bruker Micro-CT, Belgium), X-ray images of the tibias and front paws (fixed in the same manner as tibias) were obtained. For these images, the source voltage was set to 60 kV and the current settings were set at 167 µA. At every 0.45° rotation, projections were taken using an exposure of 580 ms. 3D model of the tibias and front paws were then generated using NRecon software (Bruker Micro-CT, Belgium). For each reconstruction, 20% beam hardening and ring artefact correction of 4 were used. A misalignment compensation of ±5 was accepted, but anything outside this range was rejected and the sample was rescanned.

2.5.3 Quantitative micro-CT analysis

Reconstructed tibia models were analysed using the CT-analyser software (CTan, Bruker Micro-CT, Belgium). CTan allowed for cross-sectional slices of the tibias to be visualised. For tibias, 150 slices (1 mm of bone) directly below the growth plate in the metaphysis were selected for evaluation by drawing around the cortical bone using an upper grey threshold of 255 and lower grey threshold of 51. These slices were then de-speckled and 3D analysis was performed for the following parameters: cortical cross-sectional thickness (Crt.Cs.T), cortical cross-sectional area (Crt.Cs.A), endosteal medullary area (Med.A) and periosteal perimeter (Per.P) using the Bruker Bone Analysis (Bouxsein et al., 2010). 3D meshes of the tibias were produced using MeshLab software.

2.5.4. Qualitative micro-CT analysis

Using the CTan software (Bruker Micro-CT, Belgium), reconstructed models of the front paws were generated. For processing, 255 and 100 were utilised as the upper

and lower grey threshold. Each scan was subject to de-speckling and processed to create a .ply file. This file was then transferred onto MeshLab, where it was modified by means of ambient occlusion (to improve depth cues). Each model was scored blindly by three independent people for approximate area affected and erosion. Erosion scores for each region are outlined in table 2.

Approximate area affected	**0**	None
	1	A few, small, localised areas
	2	Multiple small-medium areas
	3	Multiple medium-large areas or extensive
	4	Complete decalcification of joint (appears missing)
Erosion score	**0**	Normal - no signs of erosion
	1	Roughness
	2	Pitting
	3	Full thickness holes

Table 2: Qualitative scoring system of front paws: criteria for approximate area affected and erosion scores.

Final score was a product of the area and erosion scores for each region and obtaining an overall sum. Example of this is shown in table 3.

	Erosion score	**Area affected**	**Total**
Wrist region	2	2	3
Metacarpals	3	1	3
Phalanges	2	3	6
Total			**12**

Table 3: Qualitative scoring system of front paws: Example of how the total erosion scores were calculated.

Chapter 3: Results

Sections of this chapter have been published as part of a research paper (see appendix)

3.1. Establishing primary human osteoblast cultures

To explore the actions of GCs and inflammation on bone forming osteoblasts, bone chips isolated from hip osteoarthritis patients were cultured in osteoblast culture media using the method outlined in section 2.1. This was to enable the release of osteoblasts from the bone chips. Pre-mature osteoblasts were used as a negative control and cultured alongside the bone chips. Following differentiation for three weeks, the media from mature osteoblasts and pre-osteoblast control was collected, and both groups were stained with alizarin red S and assessed for mineralised nodule formation. Whilst mature osteoblasts successfully differentiated and exhibited mineralised nodule formation *in vitro* in the form of positive alizarin red S staining, the pre-osteoblasts control failed to produce any mineralised nodules (see figure 3.1a). Pre-mature osteoblasts are hereafter referred to as pre-osteoblasts.

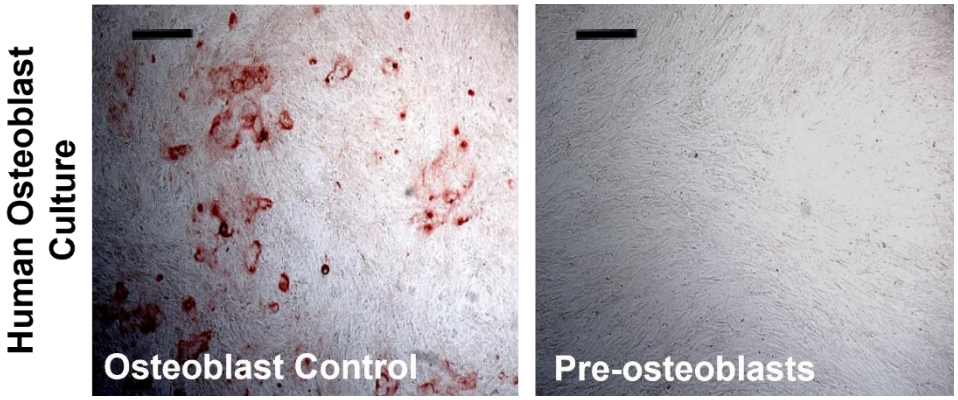

Figure 3.1. *In vitro* mineralised nodule formation
Representative images of mineralised nodules formed *in vitro* in mature osteoblasts (Osteoblast control) and in pre-osteoblasts. Both have been sourced from trabecular bone chips. Both have been stained with alizarin red S. Scale bars: 1000 μM

Subsequently, the media was subjected to mRNA analysis using RT-qPCR. Gene expression of multiple osteoblast differentiation markers was studied. In mature osteoblasts, a significant upregulation of BGLAP (0.0063 AU ± 0.0001, P≤0.001), RANKL (0.1831 AU ± 0.0044, P≤0.01), ALPL (0.00004 AU ± 0.000002, P≤0.01), RUNX2 (0.0045 AU ± 0.0002, P≤0.01) and OPG (0.0074 AU ± 0.0004, P≤0.001)

was observed in mature osteoblasts relative to the pre-osteoblasts which showed little to no expression for the aforementioned markers (see figure 3.2).

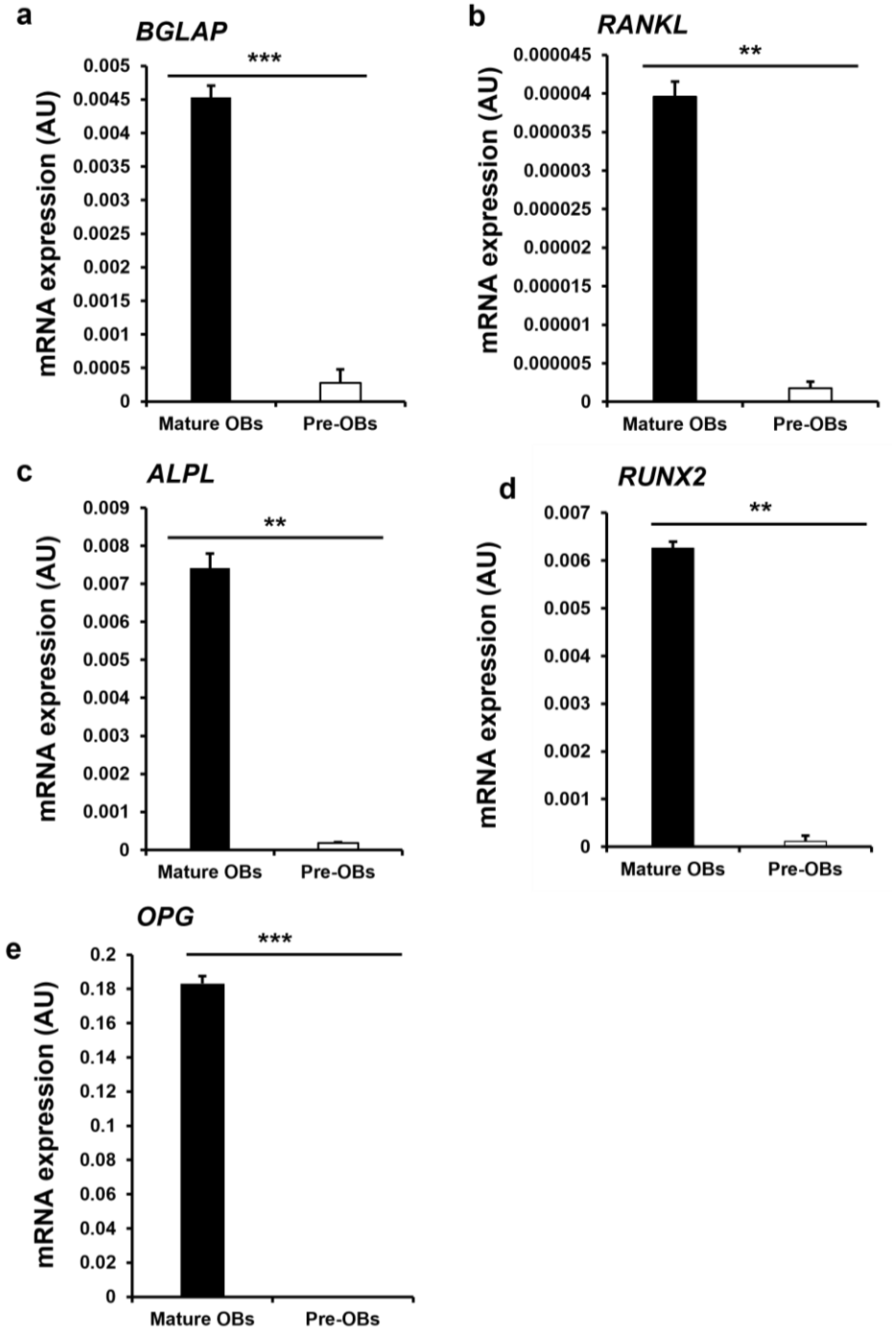

Figure 3.2. Quantification of gene expression

Quantification of mRNA expression (AU) of (**a**) BGLAP (**b**) RANKL (**c**) ALPL (**d**) RUNX2 and (**e**) OPG in mature osteoblasts and pre-mature osteoblast, as determined by RT-qPCR. Housekeeping gene used: 18S. Each dataset is presented as mean ± standard error of the mean (SEM) from the bone chips obtained for 3 independent patients (n=3). Statistical significance was established using two-way ANOVA with Tukey's multiple comparisons test (** represents P≤0.01 and *** represents P≤0.001).

Consequently, type 1 collagen, a systemic marker of bone formation was examined using an ELISA assay. Mature osteoblasts formed significant levels of collagen (0.611 pg/ml ± 0.03, P≤0.01) relative to the pre-osteoblasts which failed to produce any detectable collagen (see figure 3.3).

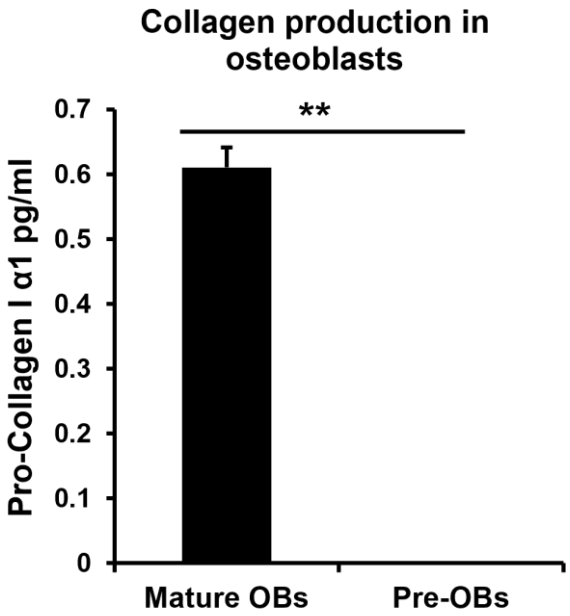

Figure 3.3. Collagen production in osteoblasts
ELISA analysis (pg/ml) of collagen production in the media of mature osteoblasts and pre-osteoblasts using a human pro-collagen I alpha 1 ELISA Kit. The dataset is presented as mean ± standard error of the mean (SEM) from the bone chips obtained for 3 independent patients (n=3). Statistical significance was established using two-way ANOVA with Tukey's multiple comparison test (** represents P≤0.01).

Following validation of bone chips being able to differentiate into mature osteoblasts, upregulate markers of osteogenic differentiation and synthesise collagen, the actions of GCs on osteoblasts was explored.

3.2. Glucocorticoids inhibit markers of mature osteoblasts

To assess the effect of GCs on osteogenic differentiation, mature osteoblasts (n=3) obtained from bone chips as previously outlined, were treated with different concentrations of cortisol (F), the primary GC in humans. These concentrations

modelled both endogenous GCs (F10: 10 ng/ml and F50: 50 ng/ml) and therapeutic GCs (F100: 100 ng/ml, F500: 500 ng/ml, and F1000: 1000 ng/ml). Alongside the treatments, osteoblasts in the absence of any treatments (control group) were grown. The media representing different GCs concentration was collected for ELSA and gene expression analysis. To confirm that mature osteoblasts had responded to the GC treatments, the expression of a GC response gene, GILZ, was assessed. GILZ expression increased with increasing concentration of F (see figure 3.4a). GILZ expression was significant when comparing the control group with: F10 (0.0027 AU ± 0.0009, P≤0.05), F50 (0.004 AU ± 0.002, P≤0.05), F100 (0.006 AU ± 0.003, P≤0.01), F500 (0.012 AU ± 0.007, P≤0.001) and F1000 (0.024 AU ± 0.017, P≤0.001). mRNA expression of markers of osteogenic differentiation were then studied. Gene expression of osteocalcin (encoded by BGLAP gene) was potently suppressed in the presence of GCs (see figure 3.4b). This suppression was statistically significant (P≤0.001) when comparing the control group with: F10 (0.0001 AU ± 0.00008), F50 (0.000007 AU ± 0.0000006, F100 (0.0000057 AU ± 0.0000024), F500 (0000057 AU ± 0.0000046) and F1000 (0.000002840 AU ± 0.0000024). However, GCs stimulated the expression of RANKL, which is a marker of immature osteoblasts (see figure 3.4c). A similar pattern of gene expression upregulation was seen with a marker of osteoblast activity called alkaline phosphate (encoded by ALPL gene) (see figure 3.4d). The expression of RUNX2, a key transcription factor associated with osteogenic differentiation was induced with increasing concentrations of F (see figure 3.4e). The gene expression increases for RANKL, ALPL and RUNX2 were not statistically non-significant. Changes in the expression levels of OPG were observed with varying GC concentrations. GC

concentrations were shown to decrease OPG expression (see figure 3.4f). Tukey's multiple comparisons test reported these changes as non-significant.

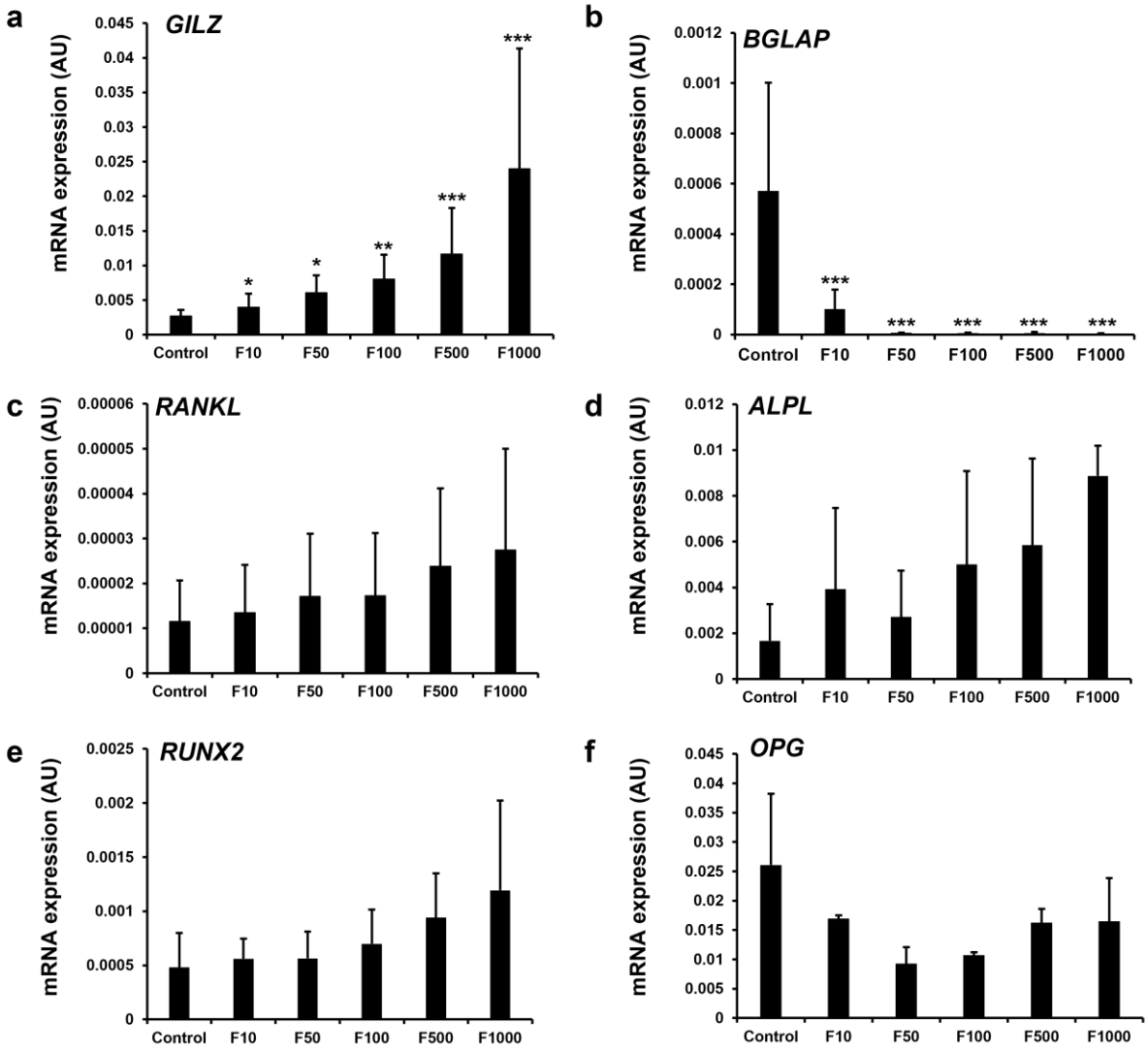

Figure 3.4: Quantification of gene expression for different doses of GC treatment
Quantification of mRNA expression (AU) of (**a**) GILZ (**b**) BGLAP (**c**) RANKL (**d**) ALPL (**e**) RUNX2 and (**f**) OPG in mature osteoblasts (n=3) in the presence of different concentrations of cortisol (F) as determined by RT-qPCR. 18S was used as a housekeeping gene. Each dataset is presented as mean ± standard error of the mean (SEM). The cells were sourced from the bone chips obtained for 3 independent patients (n=3). Statistical significance was established using one-way ANOVA with Tukey's multiple comparisons test (* represents P≤0.05, ** represents P≤0.01 and *** represents P≤0.001). The absence of * signifies the data is statistically insignificant.

3.3. Analysis of collagen production in response to GCs

Collagen production was then evaluated using the treated media collected from cell culture. ELISA analysis of the treated media showed a pattern mirroring the OPG expression – an overall non-significant increase in collagen synthesis was observed when the cells were treated with GCs (see figure 3.5).

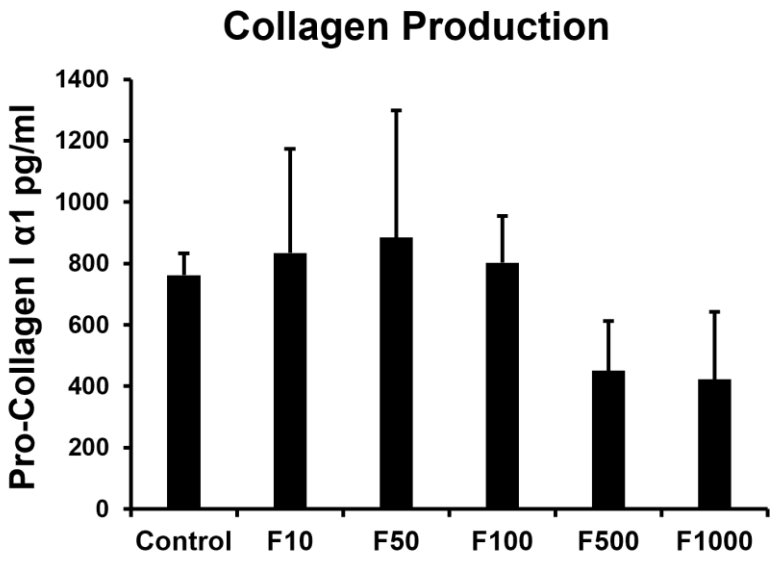

Figure 3.5. Pro-collagen I alpha 1 ELISA analysis at different GC doses
ELISA analysis of collagen production in the media of mature osteoblasts (n=3, obtained from trabecular bone chips) in the presence of different concentrations of cortisol (F) using a human pro-collagen I alpha 1 ELISA Kit. The dataset is presented as mean ± SEM. Statistical significance was established using one-way ANOVA with Tukey's multiple comparison test. (* represents P≤0.05, ** represents P≤0.01 and *** represents P≤0.001). The absence of * signifies the data is statistically insignificant.

3.4. Glucocorticoids inhibit expression of WNT signalling factors

Due to the important role WNT signalling plays in osteoblastic differentiation, several markers of WNT signalling were examined at the mRNA level. Using the treated cells, gene expression of a WNT antagonist: DKK-1 and WNT agonists (10B and 11) encoded by respective WNT 10B and WNT 11 genes were examined. In the presence of increasing concentrations of GCs, DKK-1 expression was

upregulated (see figure 3.6a). However, the expression levels of WNT10B and WNT11 generally decreased with increased F concentrations (see figure 3.6b-c) - a trend which mirrors the pattern seen with expression levels of OSC suggesting the suppression of osteoblast differentiation with increasing GC concentrations.

For WNT 10B, statistical significance ($P \leq 0.05$) was observed for control vs: F10 (0.000056 AU ± 0.00002), F50 (0.000026 AU ± 0.00002), F500 (0.000058 AU ± 0.0000005) and F1000 (0.000058 AU ± 0.000003). However, no statistical significance was observed for DKK-1 and WNT11. Together, these results may indicate an overall decrease in anabolic WNT signalling in response to GCs.

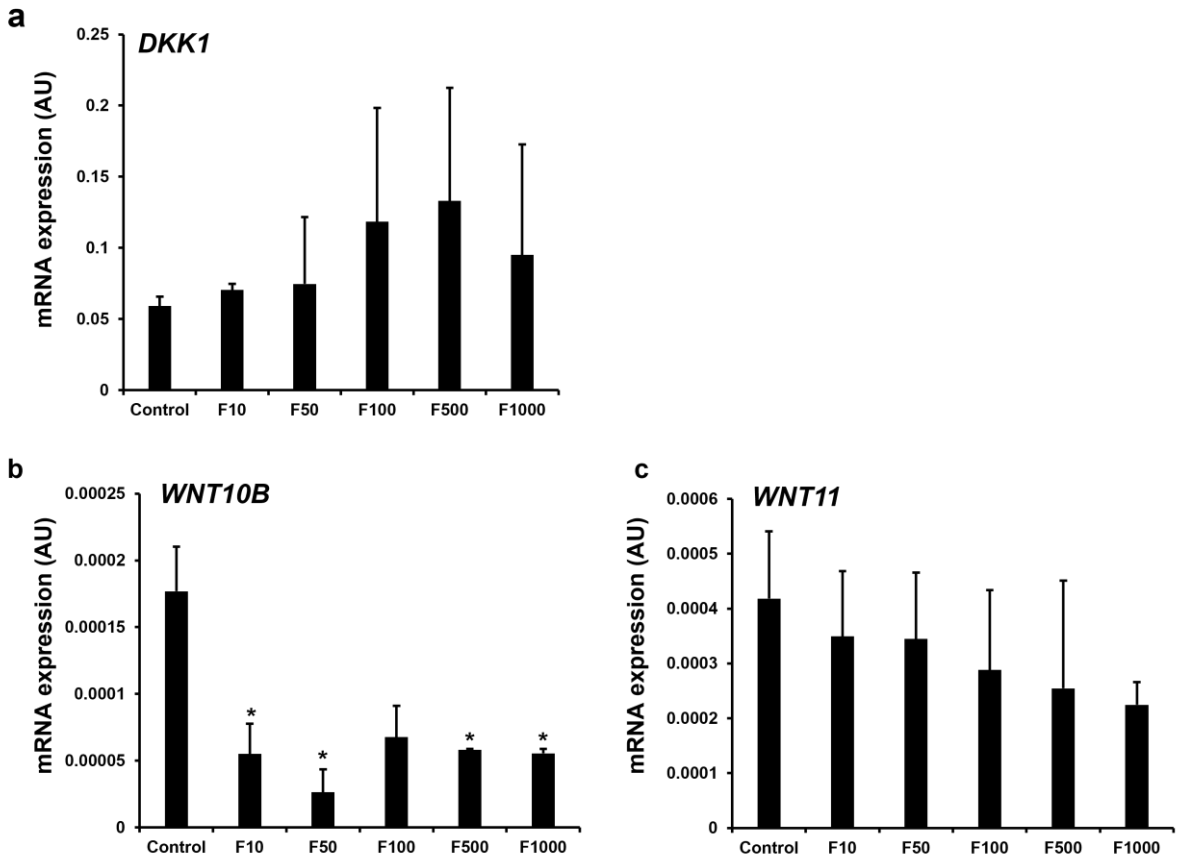

Figure 3.6. Gene expression of WNT signalling factors at different GC doses

Quantification of mRNA expression (AU) of (**a**) DKK-1 (**b**) WNT 10B and (**c**) WNT 11 in mature osteoblasts (grown and differentiated from trabecular bone chips, n=3) in the presence of different concentrations of cortisol (F) as determined by RT-qPCR. For each RT-PCR, 18S was used as a housekeeping gene. Each dataset is presented as mean ± standard error of the mean (SEM). Statistical significance was established using one-way ANOVA with Tukey's multiple comparisons test (* represents P≤0.05). The absence of * signifies the data is statistically insignificant.

3.5. Glucocorticoids suppress the inflammatory mediator IL-6

To examine the effect of GCs in the regulation of basal inflammation when there is no inflammatory stimulus present, the gene expression of pro-inflammatory cytokines, IL1-β and IL-6 (respectively encoded by IL1-β and IL-6 genes) was investigated. As before, gene expression analysis using the treated media was performed. mRNA results for both pro-inflammatory cytokines suggested that compared to control, GCs suppress the expression of IL1-β and IL-6, but with increasing concentrations of F, levels of both pro-inflammatory mediators show a non-significant increase (see figure 3.7a-b). However, an ELISA assay was used to measure pro-inflammatory IL-6, which showed that compared to the control group, GCs potently inhibit IL-6 production. Statistical significance ($P \leq 0.001$) was observed for control vs: F10 (0.660 AU ± 0.178), F50 (0.747 AU ± 0.219), F100 (0.410 AU ± 0.043), F500 (0.577 AU ± 0.101) and F1000 (0.566 AU ± 0.076) (see figure 3.7c).

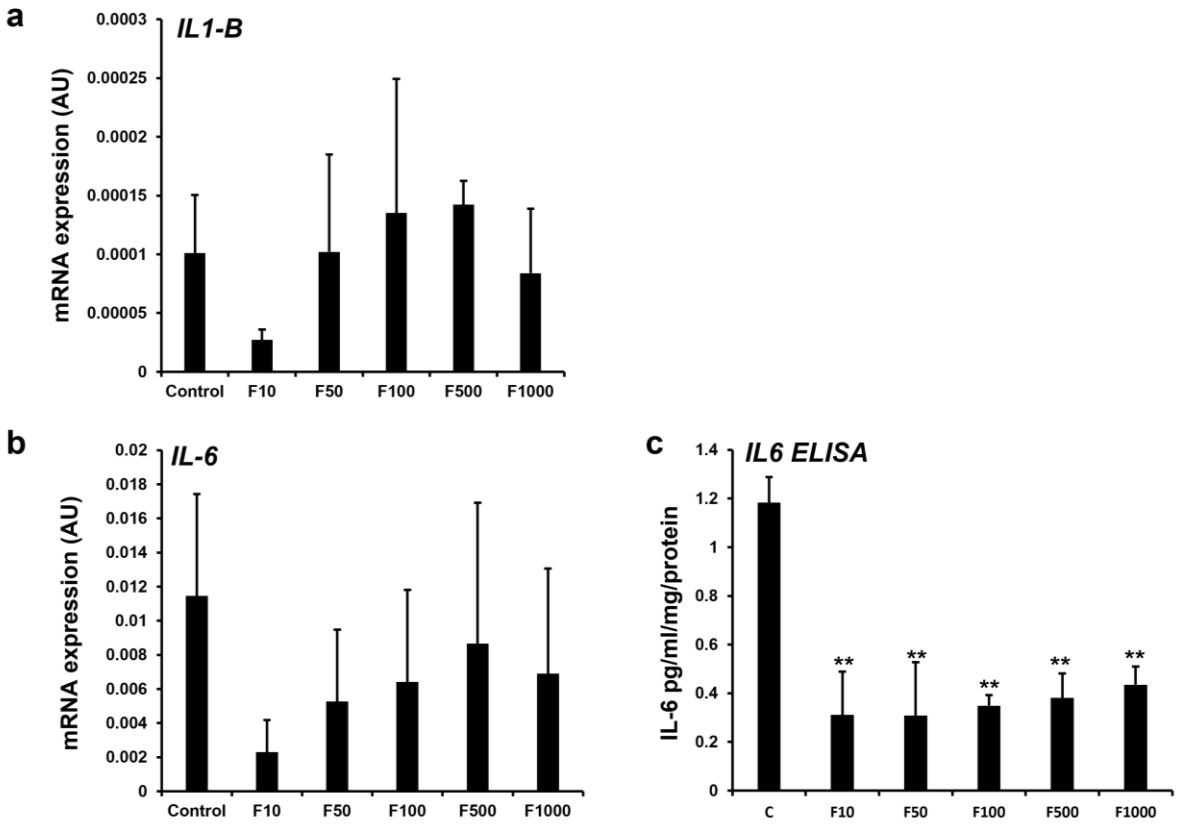

Figure 3.7: Gene expression and ELISA analysis of inflammatory mediators at different GC doses

Quantification of mRNA expression (AU) of (**a**) IL1-β and (**b**) IL-6 in mature osteoblasts (differentiated from trabecular bone chips, n=3) in the presence of different concentrations of cortisol (F) as determined by RT-qPCR (where 18S housekeeping gene acted as an internal control) (**c**) ELISA analysis (pg/ml/mg/protein) of IL-6 in the media of mature osteoblasts treated with different concentrations of cortisol (F). The dataset is presented as mean ± standard error of the mean (SEM). Statistical significance was established using one-way ANOVA with Tukey's multiple comparisons test (** represents P≤0.001). The absence of * signifies the data is statistically insignificant.

3.6. Examination of different markers under inflammatory TNF-α stimulus

To examine the effect of GCs on osteoblasts during inflammation, separate mature (differentiated) osteoblasts (n=3) were grown from bone chips (as previously discussed) and cultured alongside the above-mentioned cell culture experiments. However, to model an inflammatory stimulus, TNF-α (10 ng/ml) was added together with F at the same concentrations (F10, F50, F100, F500, F1000). As before, mRNA expression of the same genes (GILZ, BGLAP, RANKL, ALPL, RUNX2 and OPG)

was analysed. Although, TNF-α was shown to induce GILZ expression at increasing concentrations of GCs, when compared with F only experiments, the overall GILZ response was noted to be suppressed (see figure 3.8a). This may be suggestive of a reduced GC signalling response in the presence of an inflammatory stimulus. In the context of BGLAP, the same pattern was seen in the presence of TNF-α + F as with the F only experiments. TNF-α also potently inhibited osteocalcin (see figure 3.8b) suggesting inhibition of osteoblast differentiation. Gene expression of RANKL in the presence of TNF-α + F showed a general increase with increasing concentrations of GCs, mimicking the F only response for RANKL (see figure 3.8c). Although, mRNA analysis of ALPL and RUNX2 also showed a general increase for TNF-α + F experiments, when compared to the F only experiment, a combination of an inflammatory stimulus and GCs showed a marked decrease in the expression levels of these genes (see figure 3.8d-e). The expression level of OPG showed very little changes of the effect GCs exert on it when TNF-α is present (see figure 3.8d), suggesting inflammation has minimal effect on OPG expression. Statistical analysis comparing F only groups with TNF-α + F groups showed no statistical significance.

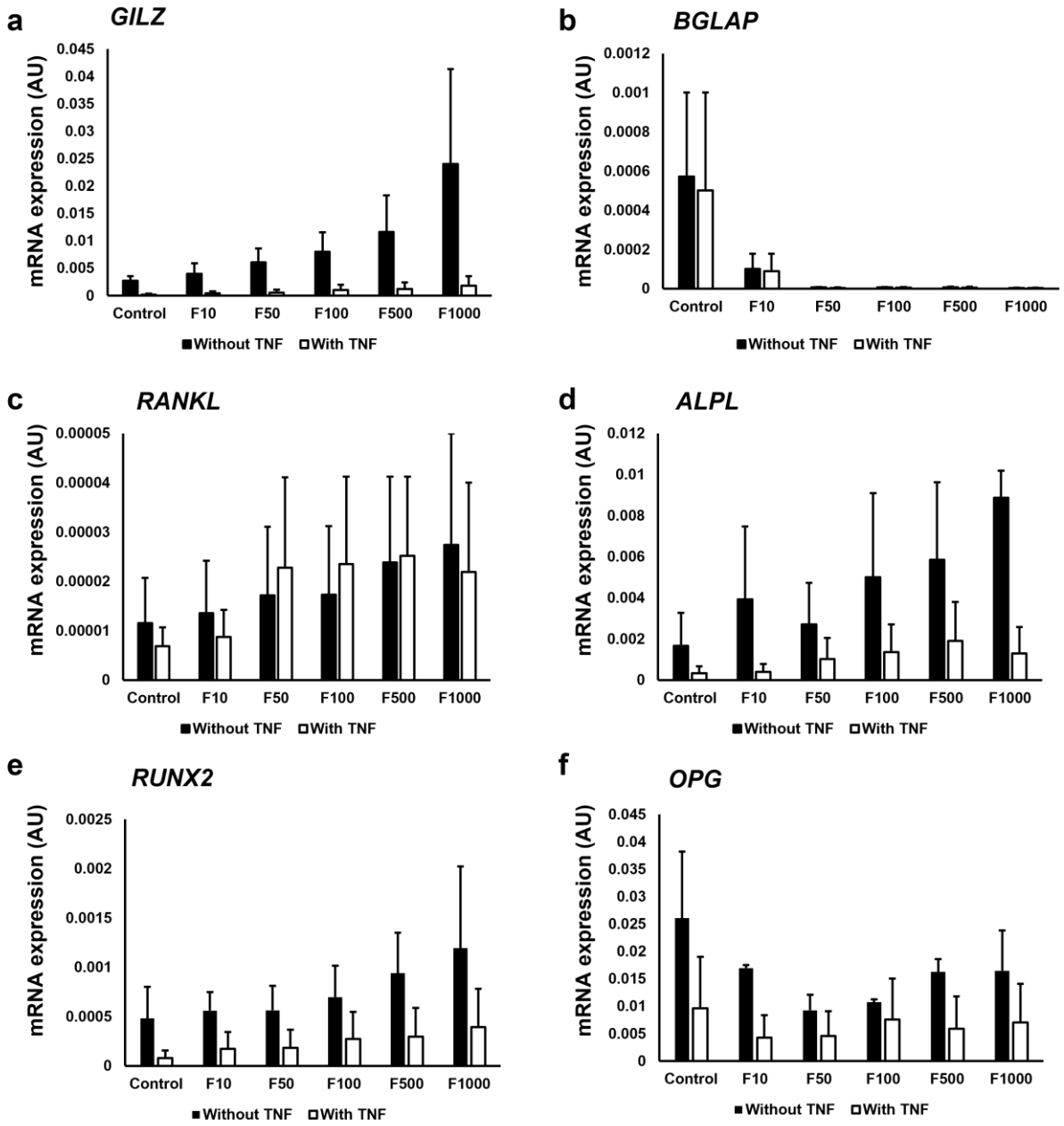

Figure 3.8: Quantification of gene expression in presence and absence of TNF-α
Quantification of mRNA expression (AU) of (**a**) *GILZ* (**b**) *BGLAP* (**c**) *RANKL* (**d**) *ALPL* (**e**) *RUNX2* and (**f**) *OPG* in mature osteoblasts (n=3) in the presence of different concentrations of cortisol (F) only or in the presence of F + TNF as determined by RT-qPCR. An 18S housekeeping gene was used for RT-PCR experiments. The cells were obtained by allowing cells to grow and differentiate from trabecular bone chips. The dataset is presented as mean ± standard error of the mean (SEM). Statistical significance was established using two-way ANOVA with Tukey's multiple comparisons test. The absence of * signifies the data is statistically insignificant.

3.7. TNF-α reduced expression of WNT agonists

To investigate if inflammation has a similar suppressive effect on WNT-mediated osteoblastogenesis, the media treated with TNF-α, and varying GC concentrations was used for mRNA analysis. Although, an overall increase in the expression of DKK-1 was observed with GCs in the presence of an inflammatory stimulus, TNF-α appeared to be downregulating DKK-1 relative to GC only treatments (see figure 3.9a). Furthermore, the addition of TNF-α caused downregulation of both WNT agonists, WNT 10B and WNT 11 at endogenous GCs levels and an increase in the therapeutic GCs concentrations (see figure 3.9b-c). However, these changes are muted and statistically non-significant relative to the F only group.

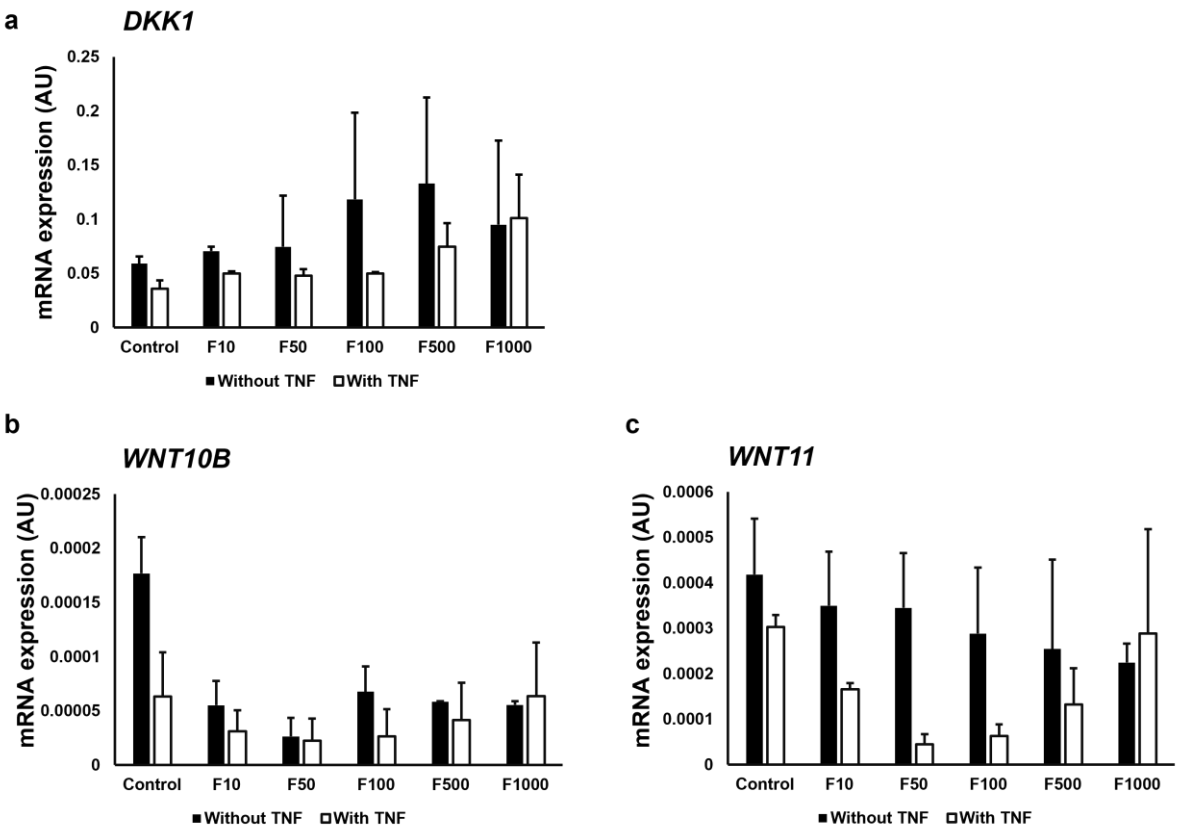

Figure 3.9: Gene expression of WNT signalling factors in presence and absence of TNF-α

Quantification of mRNA expression (AU) of (**a**) DKK-1 (**b**) WNT 10B (**c**) WNT 11 in mature osteoblasts (sourced from trabecular bone chips, n=3) in the presence of different concentrations of cortisol (F) only or in the presence of cortisol (F) and TNF-α as determined by RT-qPCR. An 18S housekeeping gene was used as an internal control. The dataset is presented as mean ± standard error of the mean (SEM). Statistical significance was established using two-way ANOVA with Tukey's multiple comparisons test. The absence of * signifies the data is statistically insignificant.

3.8. TNF-α and glucocorticoids synergistically suppress inflammatory mediators

To assess the impact of GCs on bone forming osteoblasts in the presence of inflammation (TNF-α), the gene expression of inflammatory mediators, IL1-β and IL-6, was studied. Gene expression analysis performed by RT-qPCR revealed that TNF-α and GCs cause suppression of IL1-β and IL-6 expression. The higher the concentration of GCs, the higher the suppression. However, these results were statistically non-significant (see figure 3.10)

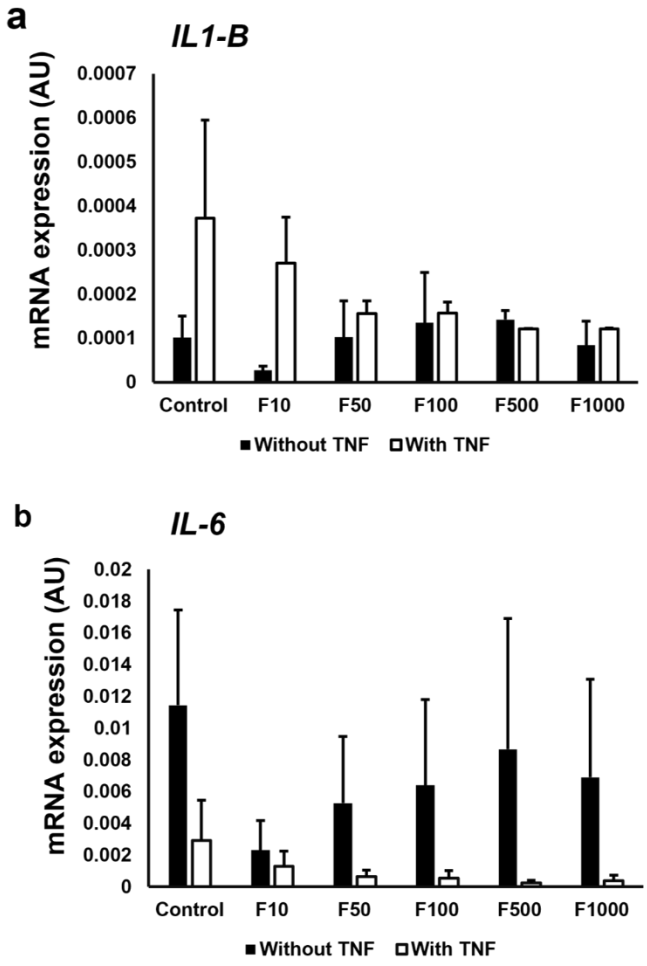

Figure 3.10: Gene expression of inflammatory mediators in presence and absence of TNF-α

Quantification of mRNA expression (AU) of (**a**) *IL1-β* and (**b**) *IL-6* in mature osteoblasts (n=3) in the presence of different concentrations of cortisol (F) only or in the presence of cortisol (F) and TNF-α as determined by RT-qPCR, where 18S was used as a housekeeping gene. The cells were grown and differentiated from bone chips extracted from patients with hip osteoarthritis. The dataset is presented as mean ± standard error of the mean (SEM). Statistical significance was established using two-way ANOVA with Tukey's multiple comparisons test. The absence of * signifies the data is statistically insignificant.

3.9. Glucocorticoids and inflammation synergistically increase 11β-HSD1 expression

Following the preliminary dose dependent experiments investigating the effects of GCs on osteoblasts in the presence and absence of inflammation, optimised experiments with a greater n number were carried out. 100 nmol/L was used as an optimal physiological GCs concentration for the new set of experiments.

Primary human osteoblasts (n=5) were obtained from a cryopreserved vial and plated using the same method as outlined in section 2.1. Once 80% confluent, osteoblasts were transferred into 12-well plate and 96-well plate for the addition of different treatments. These include a negative control (no treatment), TNF (10 ng/ml), F100 (100 nmol/L) and a combination of TNF-α and F at the stated concentrations. After being differentiated for three weeks, the treated media was collected, and the cells were stained with alizarin red S to visualise mineralised nodule formation. Control and F only groups showed relatively the same amounts of nodule formation (see figure 3.11a [A and C] – 3.11b), whilst TNF-α appeared to increase the formation of nodules (See figure 3.11a [B] and 3.11b). TNF-α + F caused a synergistic increase in the production of mineralised nodules (see figure 3.11a [D] and 3.11b). However, the increase in the nodule formation was not statistically significant. The representative images revealed atypical nodule staining as a biofilm was noted which resulted in non-specific staining.

Using the treated media collected from cell culture, mRNA expression of 11β-HSD1 was measured using RT-qPCR (see figure 3.11c). Whilst minimal 11β-HSD1 expression was observed in the control and F only group, TNF-α induced 11β-HSD1 expression. The expression levels were significantly increased ($P \leq 0.05$) in the TNF-α + F group relative to the control and F only group (0.0255 AU ± 0.0089 vs control:

0.00034 AU ± 0.0001, P≤0.05). This suggests that the inflammatory stimulus and GCs had a synergistic effect on 11β-HSD1 expression.

3.10. Glucocorticoids and inflammation synergistically reduce collagen production

Treated media collected from optimised cell culture experiments (n=5) were used for ELISA analysis to assess the impact of GCs and TNF-α on collagen production (see figure 3.11d). Results demonstrated that in relation to the control group (no treatment), TNF-α caused a significant reduction (TNF-α: 50.07 pg/ml ± 50.07 vs control: 524.09 pg/ml ± 72.47, P≤0.01) in the production of collagen. Significant decrease was also seen with F only group (F: 158.53 pg/ml ± 79.12 vs control: 524.09 pg/ml ± 72.47, P≤0.05) and TNF-α and F group (TNF-α and F: 0.57 pg/ml ± 0.45 vs control: 524.09 pg/ml ± 72.47, P≤0.01) when compared with the control. The latter appeared to be synergistically suppressing collagen production.

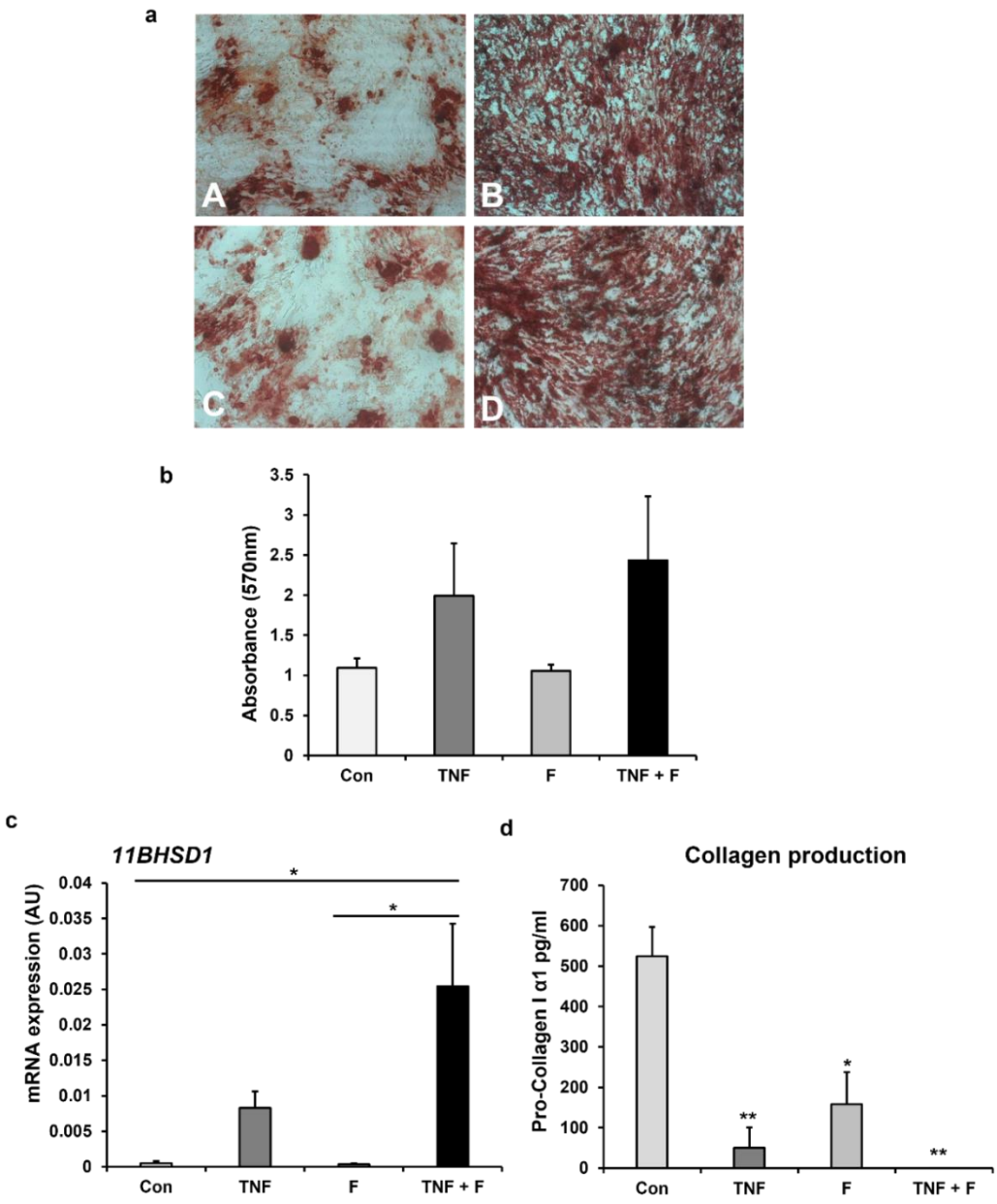

Figure 3.11. Confirmation of bone mineralisation and 11β-HSD1 expression

(**a**) Representative images of Alizarin Red S stained mineralised nodules formed by mature osteoblasts (n=5) in (A) control group and treated with (B) TNF-α at 10 ng/ml (C) Cortisol [F] at 100 nmol/L and (D) TNF-α (10 ng/ml) + F (100 nmol/L) (**b**) Quantification of Alizarin Red S stain in mature osteoblasts (n=5) in the control, F, TNF-α and TNF-α + F groups using a microplate reader (**c**) Quantification of mRNA expression (AU) of 11βHSD1 the media of mature osteoblasts (n=5) in the control group and those treated with F, TNF-α and TNF-α + F groups. The housekeeping gene used was 18S. (**d**) ELISA analysis of collagen production in the media of mature osteoblasts (n=5) in control group and those treated with F, TNF-α, and TNF-α + F group was quantified using a human pro-collagen I alpha 1 ELISA Kit. The dataset is presented as mean ± SEM, where the cells were thawed, grown, and differentiated from cryopreserved vials. Statistical significance was established using one-way ANOVA with Tukey's multiple comparison test (* represents P≤0.05, ** represents P≤0.01 and *** represents P≤0.001). The absence of * signifies the data is statistically insignificant.

3.11. TNF-α inhibits osteoblast differentiation *in vitro*

The actions of inflammation and GCs on mRNA expression of osteoblast differentiation markers was analysed using RT-qPCR.

The expression of BGLAP was reduced in the presence of an inflammatory stimulus but upregulated in the presence of GCs (see figure 3.12a). Consequently, when osteoblasts were treated with TNF-α and F together, TNF-α suppressed the F induced upregulation producing an overall decrease in BGLAP expression relative to the control (see figure 3.12a). These changes were statistically non-significant.

RANKL, an osteoclastogenic cytokine, was upregulated in the presence of TNF-α (see figure 3.12b). However, minimal expression was observed in the control and F only group (see figure 3.12b). In the presence of TNF-α and F, GCs were shown to be antagonising TNF-α induced increase in RANKL expression (see figure 3.12b). This resulted in an overall non-significant decrease.

TNF-α lowered the expression levels of ALPL in relation to the control group, whilst GCs increased ALPL levels. When TNF-α and F were added together (see figure 3.12c), TNF-α suppressed the ALPL increase that was induced by F, causing an overall reduction (see figure 3.12c). Changes seen in the expression of ALPL were statistically non-significant.

RUNX2, a marker used as a measure of differentiation, decreased with TNF-α relative to the control group, but was induced with GCs (see figure 3.12d). When TNF-α and F were added together, RUNX2 expression was increased further (see figure 3.12d). This may be attributable to GCs exerting a stronger stimulatory effect to oppose the suppression induced by TNF-α. Changes in expression levels of RUNX2 were statistically non-significant.

3.12. TNF-α upregulates pro-inflammatory cytokine expression *in vitro*

Gene expression of inflammatory mediators, IL1-β and IL-6, was heightened in the presence of TNF-α (see figure 3.12e-f). This induction was statistically significant for both cytokines (IL1-β: 0.0014 AU ± 0.0005, P≤0.05 and IL-6: 0. 08 AU ± 0.02, P≤0.01). The addition of F only treatment caused a non-significant reduction in the levels of both IL1-β and IL-6 relative to the control. However, F-induced decrease were statistically significant relative to the TNF-α treated osteoblasts for both IL1-β (F: 0.000015 AU ± 0.000012 vs TNF-α: 0.001416 AU ± 0.000446, P≤0.05) and IL-6 (F: 0.002271 AU ± 0.000662 vs TNF-α: 0.078 AU ± 0.021932, ≤0.01). When present together, F was shown to cause a non-significant reduction in the TNF-α mediated increase in the IL1-β and IL-6 expression level (see figure 3.12e-f). For IL-6, the results shown for TNF-α + F treatment were statistically significant relative to the F only treatment (TNF-α + F: 0.023175 AU ± 0.003238 vs F: 0.002271 AU ± 0.000662, P≤0.05).

Together, these results suggest that GCs suppress the expression of inflammatory mediators, whilst in the context of inflammation, IL1-β and IL-6 expression is increased.

3.13. Exploring the role of 11βHSD1 in osteoblast during inflammation *in vitro*

To study the effect of 11βHSD1 in osteoblasts, it was important to ascertain if osteoblasts possessed any 11βHSD1 responsiveness. To investigate this, mRNA expression of 11βHSD1 in the treated media was analysed using RT-qPCR (see figure 3.13a). 11βHSD1 expression was muted in the control and GC only group. The expression of 11βHSD1 appeared to be upregulated with TNF-α. Further synergistic increase in the 11βHSD1 levels were seen in the TNF-α + F group, which was statistically significant compared to the control (no treatment) (TNF-α + F: 0.0255 AU ± 0.0089 vs control: 0.0005 AU ± 0.0003, $P \leq 0.05$) and F only group (TNF-α + F: 0.0255 AU ± 0.0089 vs F: 0.000343005 AU ± 0.000139754, $P \leq 0.05$).

Following validation of 11βHSD1 expression in osteoblasts, an 11βHSD1 activity assay was done on new set of mature osteoblasts (n=5) treated with TNF-α, cortisone (E) and TNF-α + E. Other treatments used were 11βHSD1 inhibitor, glycyrrhetinic acid (GE), TNF-α + E + GE. A negative control (no treatment) was used alongside the treatments. For this set of experiments, E was used instead of F, because being a bi-directional enzyme, 11βHSD1 mainly activates GCs (F to E). This would enable the activation of F to be monitored and quantified. The 11βHSD1 activity assay was run as per the method outlined in section 2.4. In the presence and absence of GE. Results showed that inflammation upregulates the 11βHSD1 activity compared to the control and E only groups, whilst TNF + E synergistically increase 11βHSD1 activity (see figure 3.13b). In the presence of GE, 11βHSD1 activity is still present which may indicate that GE is causing partial inhibition of enzyme activity. These results are statistically non-significant.

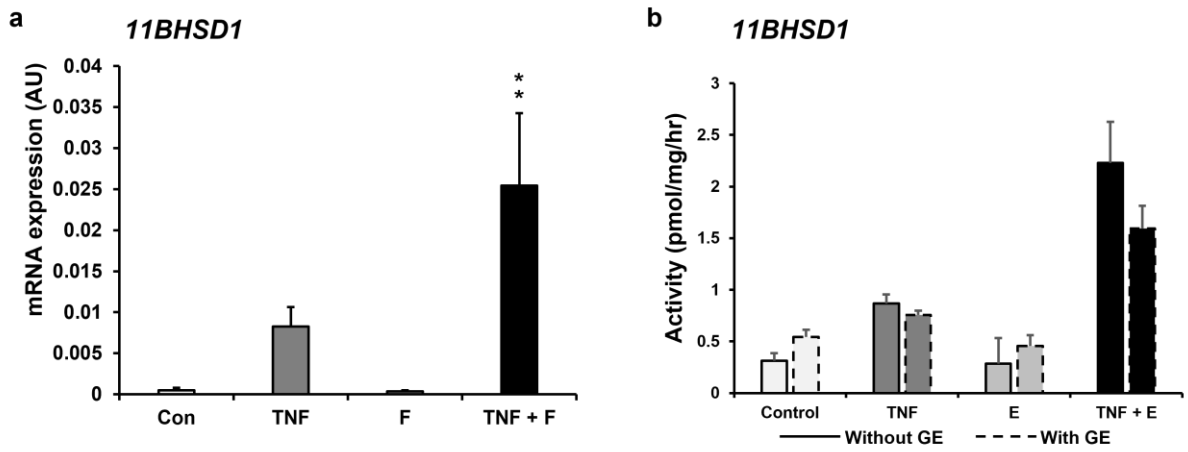

Figure 3.13: Validation of 11β-HSD1 expression and activity

Quantification of mRNA expression (AU) of (a) 11β-HSD1 present in the media of mature osteoblasts (grown and differentiated from frozen vials, n=5) in the control, TNF-α, F and TNF-α + F groups. Housekeeping gene used: 18S (b) Quantification of 11β-HSD1 activity in mature osteoblast (n=5) in the presence of a 11β-HSD1 inhibitor, glycyrrhetinic acid (GE) (solid black line border) and in the absence of a GE (dashed black line border) in the control, TNF-α, F and TNF-α +F groups. Each dataset is presented as mean ± standard error of the mean (SEM). Statistical significance was established using one-way ANOVA with Tukey's multiple comparisons test (* represents P≤0.05). The absence of * signifies the data is statistically insignificant.

3.14. TNF-α and GE inhibit osteoblastogenesis and increase inflammatory mediators

mRNA expression of selective osteoblast differentiation markers and inflammatory mediators was quantified using mRNA analysis. This was to explore the impact of GE on osteoblastogenesis in the presence of inflammation.

TNF-α suppresses BGLAP expression, which appears to be induced with TNF-α + E relative to the control group (see figure 3.14a). In the presence of TNF-α + E, an increase in the expression of BGLAP is observed which may be due to E exerting a stronger stimulatory effect on BGLAP relative to TNF-α (see figure 3.14a). The addition of GE results in the suppression of BGLAP. When TNF-α + E + GE are present together, the stimulatory effect of E is being suppressed by GE which results

in the decreased activity compared with TNF-α + E (see figure 3.14a). Statistical analysis reveals these results as non-significant.

Inflammation strongly induces RANKL expression, which is suppressed in the control, E only and GE only groups (see figure 3.14b). The stimulatory effect of TNF-α was suppressed in TNF-α + E group, which may have been attributable to E being converted to F, and F suppressing the inflammatory effect of TNF-α (see figure 3.14b). Treatments in which TNF-α, E and GE are present together, an induction of RANKL expression is seen (see figure 3.14b). However, these results are not statistically significant.

In the presence of TNF-α, ALPL expression is reduced whereas, E is shown to increase ALPL levels (see figure 3.14c). When added together as a treatment, the suppressive activity of TNF-α decreases E-induced ALPL expression. GE has a similar stimulatory effect on ALPL, with levels increased in the GE group relative to control (see figure 3.14c). TNF-α exerts its suppressive activity in the TNF-α + E + GE group causing the levels of ALPL expression to be decreased (see figure 3.14c).

TNF-α decreases the activity of RUNX2 in comparison to the control group, whilst E positively influences RUNX2 (see figure 3.14d). TNF-α + E treatment results in a significant increase in ALPL expression relative to TNF-α only group (TNF-α + E: 0.0011 AU ± 0.00017 vs TNF-α: 0.0002 AU ± 0.0002, $P \leq 0.05$). The expression level of RUNX2 with GE was like the control only group. However, in the TNF-α + E + GE group, the expression levels showed significant increase compared to the TNF-α group (TNF-α + E + GE: 0.0011 AU ± 0.00017 vs TNF-α: 0.0002 AU ± 0.0002, $P \leq 0.05$).

In the presence of TNF-α, expression of both inflammatory mediators (see figure 3.14e-f), IL-1β and IL-6 is significantly increased (IL-1β: 0.00142 AU ± 0.00045, P≤0.05 and IL-6: 0.067 AU ± 0.019, P≤0.01) compared to the control. E is shown to significantly inhibit IL-1β and IL-6 synthesis (IL-1β: 0.00002 AU ± 0.00001, P≤0.05 and IL-6: 0.00180 AU ± 0.00057, P≤0.001). Whilst TNF-α + E cause an increase in both, IL-1β and IL-6 (relative to the control), the increase is only significant in IL6 expression (IL6: 0.207 AU ± 0.0028, P≤0.05) relative to TNF-α only treatment. This may be due to E suppressing the TNF's inhibitory effect. The expression of both inflammatory mediators is significantly inhibited by GE compared to TNF-α only treatment (IL-1β: 0.00003 AU ± 0.00002 and IL-6: 0.0066 AU ± 0.0047, P≤0.05). TNF-α + E + GE increased both, IL-1β and IL-6, although statistical significance was only noted for IL-6 expression (IL-6: 0.0468 AU ± 0.0093, P≤0.05).

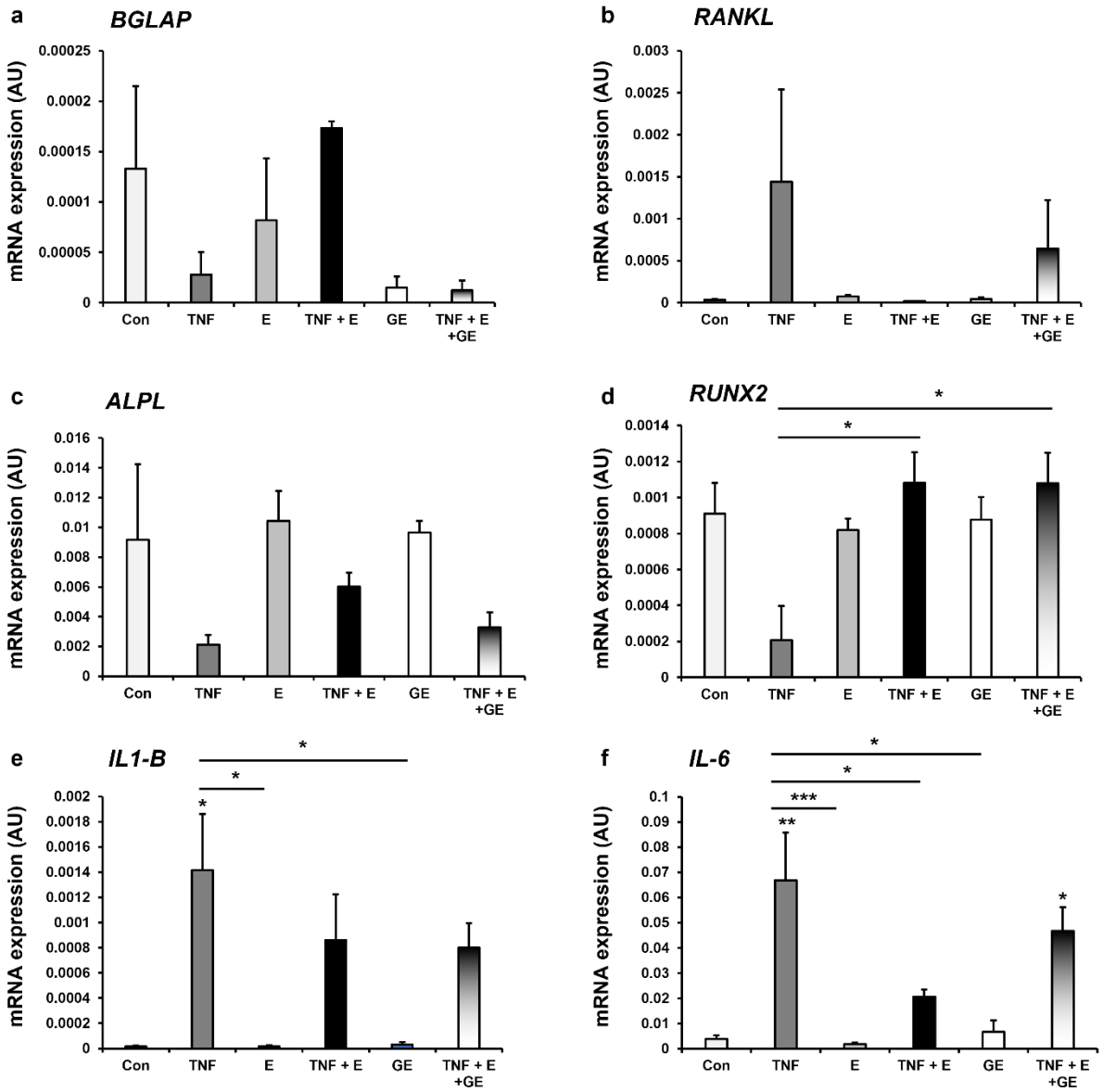

Figure 3.14: Gene expression of osteoblast markers with cortisone and 11β-HSD1 inhibitor

Quantification of mRNA expression (AU) of (**a**) BGLAP (**b**) RANKL (**c**) ALPL (**d**) RUNX2 (**e**) IL1-β and (**f**) IL6 present in the media of mature osteoblasts (n=5) in the control, TNF-α, cortisone [E], TNF-α + E, glycyrrhetinic acid (GE) and TNF-α + E + GE groups.18S was used as a housekeeping gene for RT-PCR. Each dataset is presented as mean ± standard error of the mean (SEM). Statistical significance was established using one-way ANOVA with Tukey's multiple comparisons test (* represents P≤0.05, ** represents P≤0.01 and *** represents P≤0.001). The black lines above the graphs represent the groups which are statistically significant. The absence of * signifies the data is statistically insignificant. Source of cells – cryopreserved osteoblasts, which were thawed, grown, and differentiated into mature osteoblasts.

3.15. Exploring the role of 11β-HSD1 in osteoblast during inflammation *in vivo*

Following investigation of 11β-HSD1 function in osteoblasts *in vitro*, murine models were used to explore the activity of 11β-HSD1 on bone *in vivo.* To study this, 3 mouse models were used: wildtype (WT), TWIST-2-CRE (CRE) mice in which mesenchymal 11βHSD1 was knocked out and the global 11β-HSD1 KO mice. To validate the abrogation of 11β-HSD1 in these mouse models, 11β-HSD1 activity assay was done to assess F activation. WT's ability to activate F was significantly increased relative to CRE and 11β-HSD1KO (WT: 2.88 pg/mg protein/ hr ± 0.33 vs CRE: 0.63 pg/mg protein/ hr ± 0.15 and 11β-HSD1KO: 0.21 pg/mg protein/ hr ± 0.02 respectively. p≤0.001), whist the ability of CRE to activate cortisol showed a non-signifcant increase in comparison to the 11β-HSD1 KO mice.

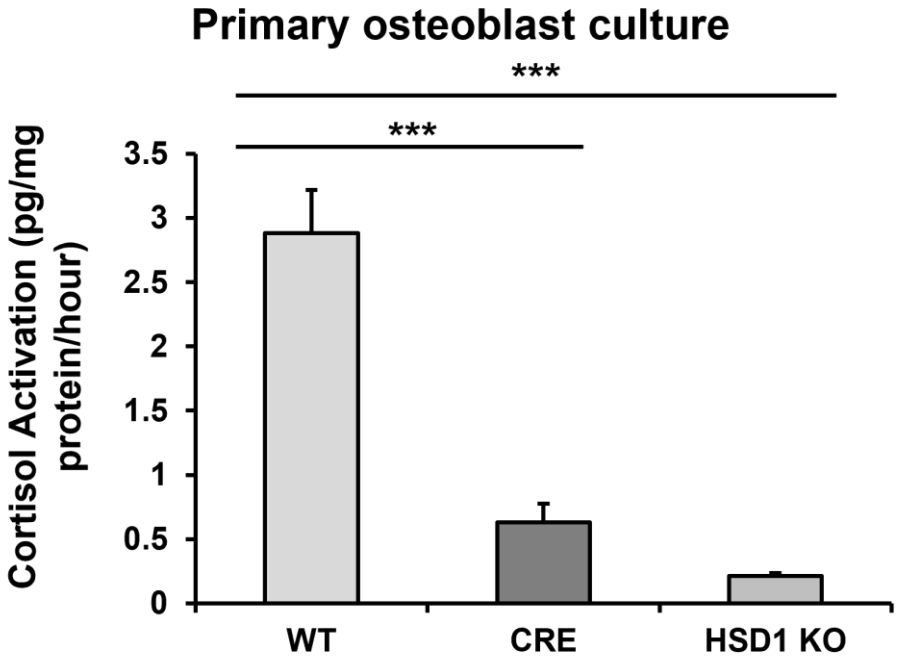

Figure 3.15. Validating the CRE and 11β-HSD1 KO mouse model
Cortisol activation in tibia ex vivo biopsies obtained from wildtype (WT), CRE and 11βHSD1 knock out (11βHSD1KO) mice was analysed using scanning thin-layer chromatography. The dataset is presented as mean ± standard error of the mean (SEM). Statistical significance was established using two-way ANOVA with Tukey's multiple comparisons test (** represents P≤0.01 and *** represents p≤0.001). The black lines above the graphs represent the groups which are statistically significant.

3.16. Glucocorticoid treatment induces systemic bone loss (i.e., bone erosions)

Following confirmation of 11βHSD1 abrogation in the CRE and 11βHSD1 KO (11βKO) mice and the analysis of cortisol activation in these murine models alongside the WT mice, all murine models were given corticosterone (cort, 100 mg/L) in their drinking water for 3 weeks. Cort is the main glucocorticoid in mice. Alongside the corticosterone treatment, mice without any treatments were maintained as controls. The following mouse groups were used to carry out quantitative analysis for the purpose of this thesis: WT, WT cort, WT-Twist-2 CRE (WT CRE), WT-Twist-2 CRE cort (WT CRE cort), TNF-Tg, TNF-Tg cort, TNF-Twist-2 CRE (TNF CRE) and TNF-Twist-2 CRE cort (TNF CRE cort),

To study the action of GCs and an inflammatory stimulus (TNF-α) on joints, excised front paws were subject to micro-CT analysis. This enabled the degree of bone erosions to be investigated. Micro-CT analysis showed that both the untreated WT and WT CRE mice had relatively the same degree of joint erosions. However, the addition of cort to the WT group substantially increased the degree of bone erosion. Although WT CRE mice receiving cort also demonstrated increased bone erosion, this increase was not observed in the WT cort group (see figure 3.16a). The degree of change between WT and WT cort was statistically significant (5.42 AU ± 0.99 vs TNF: 13.58 AU ± 0.99, $p \leq 0.001$). The increased bone erosions are observable in images of reconstructed front paws and cross-sectional bone (see figure 3.16b-c).

Cortical bone parameters of tibias from WT and WT CRE mice receiving cort was analysed. Change in cortical bone area was statistically significant for WT mice receiving cort (22.46 AU ± 0.3097 vs 24.59564 AU ± 0.309767, $p \leq 0.001$) (see figure 3.16d) and for the same group, in periosteal perimeter (421.36 AU ± 4.60 vs 468.77

AU ± 19.22, p≤0.001) (see figure 3.16g). However, for the remaining parameters, muted changes and no statistical significance was observed.

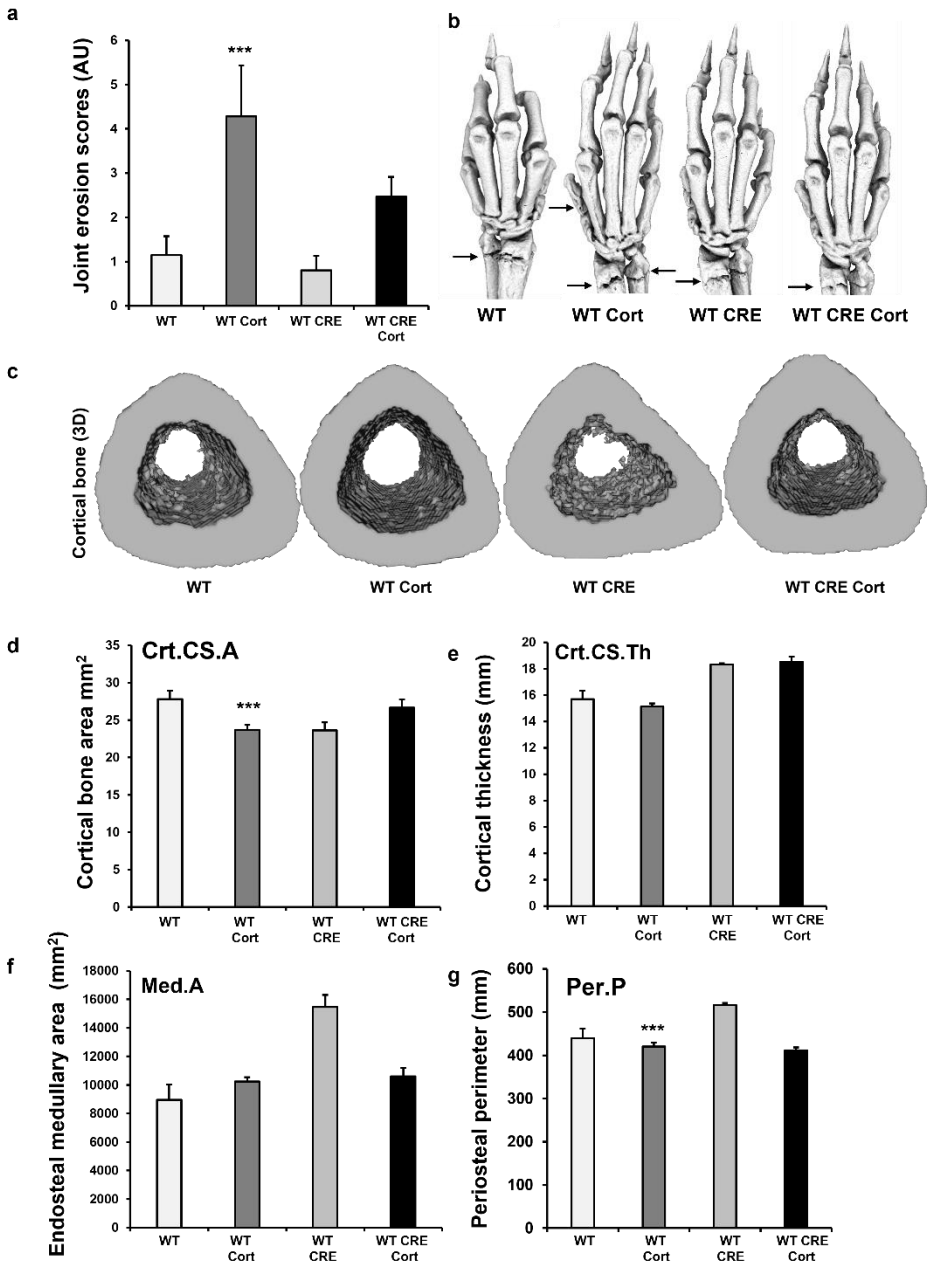

Figure 3.16. Bone erosion scores and cortical parameters in WT and WT-Twist-2-CRE (WT CRE) mice with and without cort, with reconstructed images

(**a**) Quantification of bone erosions (AU) in WT (n=8) and WT CRE (n=6) mice receiving either vehicle control, or corticosterone (cort; 100 µg/ml): WT CRE cort (n=5) and WT Cort (n=6) mice (**b-c**) Representative images of reconstructed front paws and cross-sectional cortical bone by micro-CT scans. Bone erosions are highlighted by arrows (**d**) Representative images of 3D reconstructions of tibia cortical bone using micro-CT from WT and WT CRE mice receiving either vehicle control or corticosterone (100 µg/ml): WT CRE cort and WT cort. Micro-CT analysis of (**d**) cortical cross-sectional thickness (Crt.Cs.T), (**e**) cortical cross-sectional area (Crt.Cs.A) (**f**) endosteal medullary area (Med.A) and (**g**) periosteal perimeter (Per.P) achieved by using Meshlab software in WT and WT CRE mice receiving either vehicle control or corticosterone (100 µg/ml). Each dataset is presented as mean ±

SEM and statistical significance was determined using two-way ANOVA with Tukey's multiple comparisons test (*** represents p≤0.001)

3.17. Glucocorticoids have a protective effect on JXA bone erosions during inflammation

Micro-CT analysis showed an increase in bone erosions in the untreated TNF-Tg mice relative to the TNF-Twist2-CRE (TNF CRE) mice, which may be indicative of inflammatory bone loss being mediated by 11β-HSD1. Following GC treatment, TNF-Tg and TNF CRE mice both showed a decrease in bone erosions in comparison to their untreated controls (see figure 3.17). Whilst the decrease in bone erosion in TNF-Tg mice receiving cort was statistically significant compared to their untreated counterpart (5.42 AU ± 0.99 vs TNF: 13.58 AU ± 0.99, p≤0.001), no statistical significance was reported for TNF CRE mice on cort.

Assessment of cortical bone parameters revealed that generally GC treatment causes a reduction in the cortical thickness, medullary area, and periosteal perimeter in TNF-Tg mice relative to their untreated group. Similar effect was seen for TNF CRE mice on cort with reductions being observed in cortical area and thickness. The addition of GC treatment had little effect on medullary area and periosteal perimeter in WT CRE mice on cort compared to their untreated counterparts. Statistical analysis revealed these results as non-significant. Once again, suggesting cortical bone to be a poor responder of GC treatment.

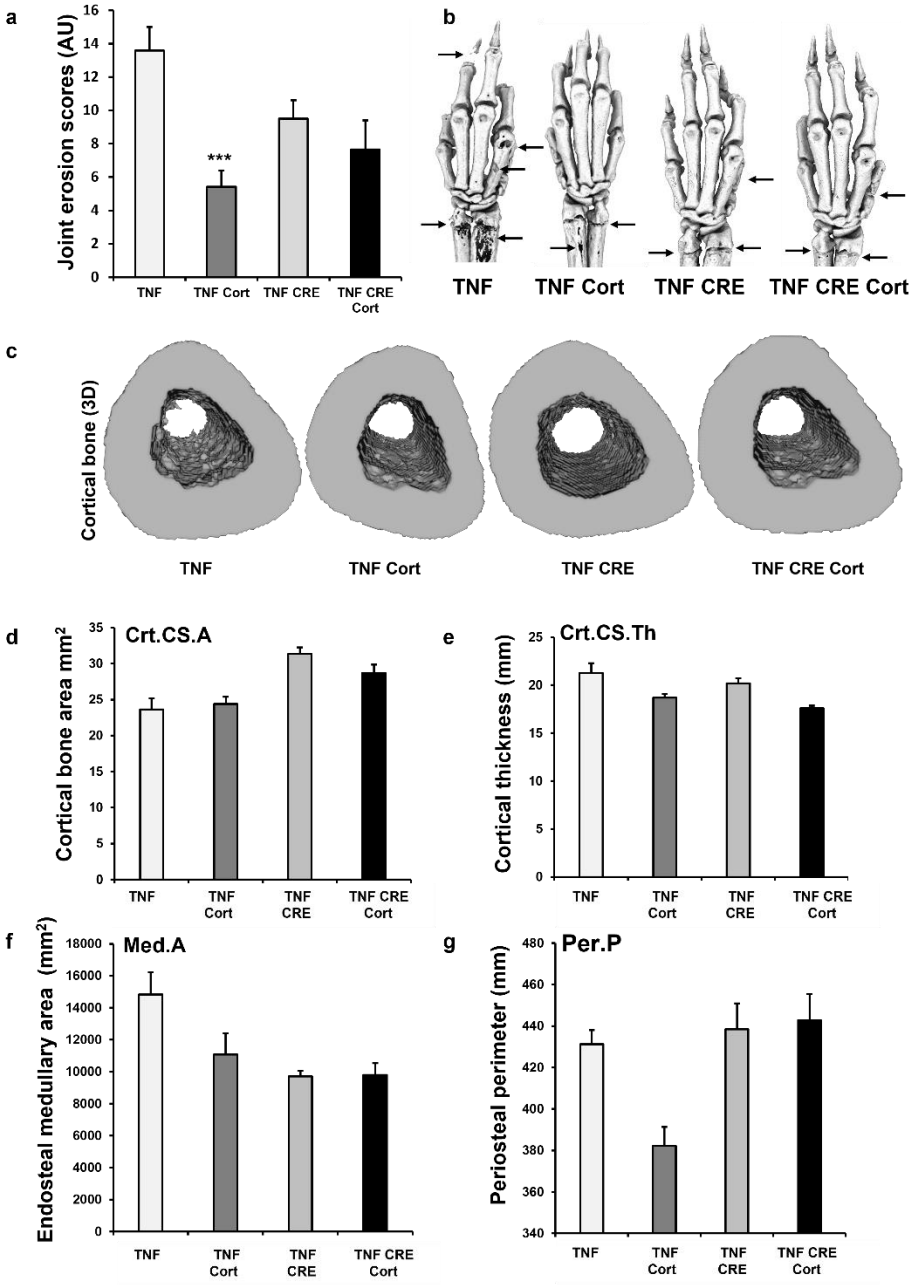

Figure 3.17. Bone erosion scores and cortical parameters in TNF-tg and Twist-2-CRE mice with and without cort

(**a**) Quantification of bone erosions (AU) in TNF (n=6) and TNF CRE (n=6) mice receiving either vehicle control or corticosterone (cort; 100 µg/ml): TNF cort (n=7) and TNF CRE cort (n=5) mice (**b**) Representative images of reconstructed front paws and cross-sectional cortical bone by micro-CT scans. Bone erosions are highlighted by arrows (**c**) Representative images of 3D reconstructions of tibia cortical bone using micro-CT from TNF and TNF CRE mice receiving either vehicle control or corticosterone (100 µg/ml): TNF cort and TNF Cre cort. Micro-CT analysis of (**d**) cortical cross-sectional thickness (Crt.Cs.T), (**e**) cortical cross-sectional area (Crt.Cs.A) (**f**) endosteal medullary area (Med.A) and (**g**) periosteal perimeter (Per.P) achieved by using Meshlab software in TNF and TNF CRE mice receiving either vehicle control or corticosterone (100 µg/ml). Each dataset is presented as mean ± SEM and statistical significance was determined using two-way ANOVA with Tukey's multiple comparisons test.

3.18. Glucocorticoid treatment increase bone erosion in global 11βKO mice

To assess the role of 11β-HSD1 in mediating systemic bone loss, bone erosion was quantified in the global 11β-HSD1 KO mice receiving cort and compared with WT mice on GCs.

Bone erosion was significantly increased in WT mice receiving GCs relative to its untreated group (5.42 AU ± 0.99 vs TNF: 13.58 AU ± 0.99, p≤0.001) (see figure 3.18a). Conflicting results were identified when comparing the WT on cort and 11βKO on cort groups which revealed lower joint erosion scores for the 11βKO group receiving cort (and subsequently, higher joint erosion scores for WT on cort). This may suggest a protective role of 11β-HSD1.

Analysis of cortical bone parameters showed little change in the context of cortical area for 11βKO on and off cort but statistical significance was reported for WT cort vs WT control group (22.46 AU ± 0.3097 vs 24.59564 AU ± 0.309767, p≤0.001) (see figure 3.18d). For periosteal perimeter, statistical significance was noted for WT cort vs WT control group (421.36 AU ± 4.60 vs 468.77 AU ± 19.22, p≤0.001) (see figure 3.18g), however this was not significant for 11βKO. The remaining parameters showed muted changes and were statistically non-significant. 11β-HSD1 has a role in protecting cortical bone against GC-mediated bone loss. However, these results contradict the observation noted from the joint erosion scores where 11βKO appears protective.

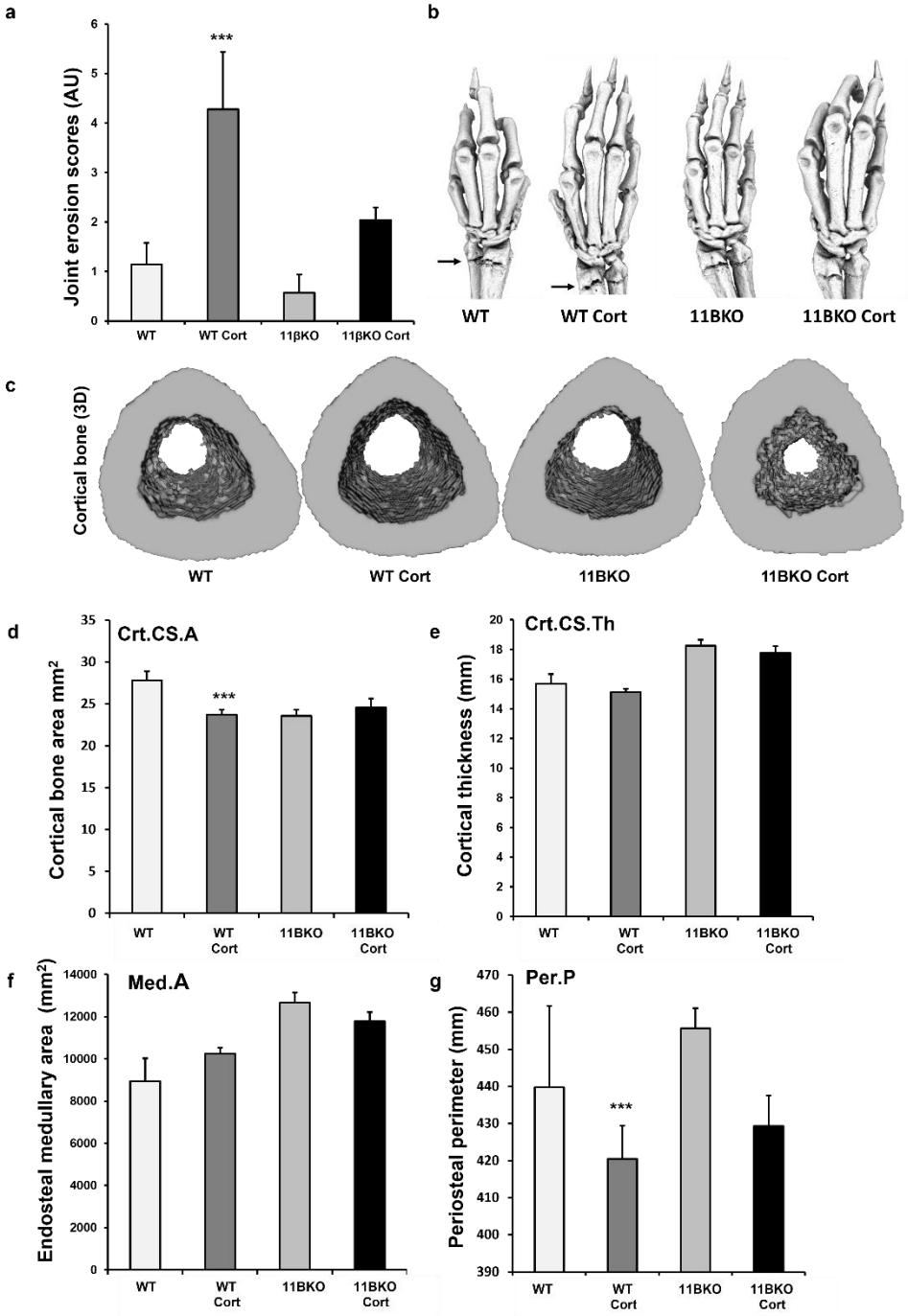

Figure 3.18. Bone erosion scores and cortical parameters in WT and 11βKO mice with and without cort

(**a**) Quantification of bone erosions (AU) in WT (n=8) and WT CRE (n=6) mice receiving either vehicle control, or corticosterone (cort; 100 µg/ml): WT CRE cort (n=5) and WT Cort (n=6) mice (**b**) Representative images of reconstructed front paws by micro-CT scans. Bone erosions are highlighted by arrows (**c**) Representative images of 3D reconstructions of tibia cortical bone using micro-CT from WT and WT CRE mice receiving either vehicle control or corticosterone (100 µg/ml): WT CRE cort and WT Cort. Micro-CT analysis of (**d**) cortical cross-sectional area (Crt.Cs.A) (**e**) cortical cross-sectional thickness (Crt.Cs.T), (**f**) endosteal medullary area (Med.A) and (**a**) periosteal perimeter (Per.P) achieved by using Meshlab software in WT and WT CRE mice receiving either vehicle control or corticosterone (100 µg/ml). Each dataset is presented as mean ± SEM and statistical significance was determined using two-way ANOVA with Tukey's multiple comparisons test.

Chapter 4: Discussion

Chronic inflammatory polyarthritis refers to conditions characterised by systemic inflammation, joint deformity, multiple extra-articular features, which when combined with the complications of therapy, can result in significant morbidity (Turesson, 2013; Verheul et al., 2015; Zabotti et al., 2016). Due to their potently anti-inflammatory activity and their disease modifying effects, glucocorticoids (GCs) are a clinical mainstay for the management of inflammatory disorders (Straub and Cutolo, 2016). However, their long-term use as therapeutics is limited due to the occurrence of unfavourable side effects (van Staa et al., 2002; Curtis et al., 2006). An example of such adverse effect is systemic bone loss. The principal objective of this thesis was to explore the effect of local GC activation and metabolism in bone forming cells, called osteoblasts, during chronic inflammation. This was done by establishing primary cultures of human osteoblasts and characterising the inflammatory suppression of their differentiation and function. The role of steroid metabolism in this process in response to endogenously derived steroids in combination with selective inhibitors of steroid metabolism was then assessed. These findings were then examined *in vivo* using mouse models of chronic inflammation with osteoblast targeted disruption of steroid metabolism, where the bone phenotype was studied by micro-CT.

To investigate the actions of GCs on osteoblasts in the context of chronic inflammatory polyarthritis, primary human osteoblast cultures were established from either bone chips isolated from hip osteoarthritis patients (for preliminary experiments, n=3) or cryopreserved vials (optimised experiments, n=5). Alongside these osteoblasts, undifferentiated mesenchymal cells were grown. Once differentiated, both cell cultures were stained with Alizarin Red S stain to detect the presence of mineralised nodules, which provided an informative index to evaluate

function of mature osteoblast and culture status. Previous literature has reported that ECM deposition is a maker of osteoblast differentiation, which in *in vitro* cultures is seen to accumulate after 7-days and its mineralisation, which accounts for the final phase of the osteoblast phenotypic developments is seen after 14 days of cultures (Quarles et al., 1992). Whilst mature osteoblasts successfully formed nodules, no signs of mineralisation were detected in the negative control. Osteoblast differentiation can be also characterised by the progressive expression of distinctive osteoblast makers. The most commonly utilised markers of osteoblastogenesis and mature osteoblasts include osteocalcin, RANKL, ALPL, and type 1 collagen (Col1a1) (Huang et al., 2007). Alongside these, OPG, an inhibitor of osteoclast formation, was also quantified using mRNA analysis. Mature osteoblasts were observed to successfully upregulate the production of the aforementioned markers, thereby suggesting their ability to differentiate. This confirmed that cells being used from bone chips and cryopreserved vials were able to successfully release bone-forming osteoblasts, which consequently had the capability to differentiate into mature osteoblasts (as observed by alizarin red staining and quantified using mRNA expression of different osteoblastogenesis markers), thus validating their use for *in vitro* experiments examining effect of different GC treatments.

Consequently, a series of dose dependent experiments modelling the effect of endogenous and therapeutic GCs on osteoblasts in the absence and presence of inflammation were performed. Existing literature states that different doses of GCs have different effects on osteoblasts. Whilst high GC doses cause osteocyte apoptosis, low doses of GCs are pro-osteoblast differentiation (Weinstein et al., 1998; Swanson et al., 2006). Using a range of GC concentrations (endogenous and

therapeutic), we were able to identify the concentration at which GCs suppress inflammation in OBs. Quantification of a sensitive GC-responsive molecule, GILZ, was performed as a control. Previously it has been reported that GCs induce GILZ expression, which increases with increasing GCs concentrations. Alongside GILZ, GR is also activated by GCs, hence GILZ can be utilised as a surrogate of GR and its GC-induced expression suggests that GR signalling is taking place. Once activated, GR signalling can negatively impact bone directly or indirectly by either inhibiting OSC expression or suppressing ERK activation respectively (Sevilla et al., 2021). To validate this, future experiments using GR antagonist RU-486 can be performed, which would suppress GR signalling pathways and consequently, promote osteogenic activity (Lewis-Tuffin et al., 2007).

OSC, encoded by the BGLAP gene was significantly inhibited by GCs in the absence of inflammation and strongly suppressed in the presence of the TNF-α inflammatory stimulus. This suggests that following GC administration, the development of the osteoblast phenotype and expression of OSC is suppressed. As per existing literature, this may be due to the inhibitory effect GCs exert on the transcription regulatory factor, Krox20 (also known as early growth response protein 2 [EGR2]) and its co-activator, HCF-1 (Leclerc et al., 2005). Although best studied in the nervous system, Krox20 is also expressed in osteoblasts where WNT signalling pathway strongly inhibits Krox20 expression in response to GC treatment. This repression of Krox20 consequently impacts the growth and differentiation of osteoblasts, as well as contributing to the development of systemic bone loss, for instance in GC-induced osteoporosis (Westendorf et al., 2004; Glass and Karsenty, 2006).

In the context of other differentiation markers, a dose dependent induction of RANKL was seen both by GCs alone, and in the presence of inflammation, whilst a general decline was observed for its decoy receptor, OPG - a finding that has been well documented previously (Rubin et al., 1998; Hofbauer et al., 1999). This may be attributable to GCs' role in stimulating osteoclastogenesis through increases in RANKL expression, which stimulates osteoclast activity, resulting in bone loss and weakened bone architecture (Riggs et al., 1998). Alternatively, it can be due to TNF-α exerting a stimulatory effect on the differentiation of osteoclast progenitors through increases in osteoclastogenic cytokines, such as RANKL, resulting in bone resorption (Xiong et al., 2014; Yy et al., 2014). A recent study has reported that TNF-α upregulates NFATc1 and an inflammatory kinase, Ikkα, which contributes to the activation of the NF-κB pathway – a signalling pathway which is critical in osteoclastogenesis (Razani et al., 2011; Luo et al., 2018). The induction in RANKL by GCs may also be attributable to GCs causing indirect inhibition of IFN-γ, which is an antagonist of osteoclast differentiation (Takuma et al., 2003). Hence, IFN-γ inhibition stimulates osteoclastogenesis. GCs may exert direct effects by upregulating RANK signalling or by increasing RANKL synthesis, which together with GCs inhibiting OPG in osteoblasts, favours an osteoclastogenic environment (Hofbauer et al., 1999). The net result of which is GC-induced bone loss (Weinstein, 2001). The production of GR ligands which possess anti-inflammatory effects but do not supress OPG expression and/or do not increase RANKL synthesis may prove useful as they could prevent adverse effects on bone associated with GC therapy. An extension of this may be to identify co-regulators which are recruited by GR ligands so that they can be regulated in a manner where OPG is not inhibited and RANKL will not be stimulated, thereby preventing bone resorption.

Previously, it has been reported that GCs increase alkaline phosphatase activity, thus GCs play an important role in promoting the development of a more differentiated OB phenotype (Perizzolo et al., 2001; Sugawara et al., 2002; Eijken et al., 2006; Wong et al., 2009). Concordant results were seen with the cell cultures, as a marked increase in ALPL expression was observed following GC treatment. This was in line with the general increase in collagen production observed post addition of endogenous concentrations of GCs but contradictory to the suppression noted at therapeutic concentrations . In an inflammatory setting, ALPL levels were also increased with dose-dependent GC treatment which may be due to TNF-α stimulating tissue non-specific ALPL expression. For future experiments, to see if TNF-α also stimulates mineralisation synergistically with GCs, the gene expression of peroxisome proliferator-activated receptor-γ (PPAR-γ) in osteoblasts can be quantified. This is because TNF-α has been shown to induce bone mineralisation by suppressing osteoblastic PPAR-γ (Lencel et al., 2012). Additionally, this can be supplemented by performing a collagen ELISA on the cell culture media collected from TNF-α and GCs treated osteoblasts to confirm bone mineralisation.

Similarly, RUNX2 expression demonstrated a dose-dependent increase to GC treatments, which may be representative of cell commitment to osteoblastic lineage or the proliferation of osteoblast progenitor. To fully elucidate the effect of RUNX2 on osteoblastogenesis, future experiments examining the expression of Hox genes, particularly Hox11 are required. This is because osteoblasts need Hox proteins to mature, and in their absence, failed OB maturation and abnormal mineralisation is observed (Song et al., 2020). In the presence of inflammation, GC treatments induced a smaller dose-dependent increase in RUNX2 which may be attributable to TNF-α increasing Smurf1 and Smurf2 gene expression which negatively regulates

RUNX2 levels through proteosomal degradation (Kaneki et al., 2006). To validate this, gene expression studies looking at the expression levels of Smurf1 and Smurf2 using the treated media from cell culture can be performed in the future.

We further examined markers of WNT signalling which shown an increase in the level of WNT antagonist, DKK-1, and a decline in WNT agonists, WNT 10. The increase in DKK-1 and decrease in WNT 10 may explain the suppression of OB differentiation we see with GC treatments, a finding which has previously been documented by existing literature (Ohnaka et al., 2005; Butler et al., 2010). These studies suggest GCs inhibit osteoblast synthesis by inhibiting the WNT signalling pathway. Contrastingly, very little effect was observed on WNT agonist by GCs treatment in the presence of an inflammatory stimulus. Whereas TNF-α and GCs were seen to have a synergistic inhibitory effect on DKK-1 expression, which has been reported by existing literature (Diarra et al., 2007; Li et al., 2015). This suggests that GCs, through inhibition of WNT agonist and upregulation of DKK-1 inhibit bone formation and cause reduction in OPG level resulting in increased osteoclastogenesis and suppression of anabolic effects of osteoblasts, mirroring the findings of an existing study (Diarra et al., 2007). Repeating experiments with a higher sample size (n number), studying the expression of other WNT agonists (such as WNT 3a and 7b) and WNT antagonist (sclerostin) may provide a better insight into the effect of GCs on WNT signalling in the absence and presence of inflammation.

The effect of GCs on pro-inflammatory mediators was investigated which revealed that when acting alone, GCs have little effect on expression of IL1-β and IL-6. However, in the presence of an inflammatory stimulus, GCs exert a strong anti-inflammatory effect on pro-inflammatory mediators, thereby decreasing their

expression. This may be due to the downregulation of the pro-inflammatory cytokine's promoter activity or via the suppression of the transcription factor, AP-1 (Ray et al., 1990; Waage et al., 1990; Patil et al., 2018). However, to confirm these findings and investigate if there is a dose-dependent difference in how GCs regulate inflammatory cytokine expression in osteoblasts, experiments with greater n numbers are required.

Together, these dose-dependent experiments reported GCs negatively regulate OSC, thus suggesting GCs inhibit OB differentiation. GCs stimulate RANKL expression and suppress OPG expression, pointing towards the formation of a pro-osteoclastogenic signal and bone resorption. This was supplemented with the experiments involving WNT signalling which also suggests the role of GCs in increasing osteoclastogenesis in the absence and presence of inflammation. We decided to perform further optimised experiments to confirm these findings and overcome the variability in results variability in results, which may be attributable to differences in cell viability in each replicate, different degrees of osteoarthritis in patients from whom the bone chips were obtained from and/or variation in the technique used to extract the bone chips. The optimisation involved choosing an optimal physiological GC dose (100 nmol/L) and increasing the n number (n=5). Due to a lack of bone chips from hip osteoarthritis patient to satisfy an increased n number (n=5), it was decided to use cryopreserved osteoblasts for the optimised experiments.

Optimised experiments showed that TNF may cause a mitogenic increase in number of osteoblast cells resulting an increase in Alizarin Red S staining relative to the control group as highlighted by increased absorbance. However, this needs further validation as the Alizarin Red Staining reveals the hyperproliferation of the

cell population which may be contributing to the increased absorbance results through aberrant overproduction of nodules. This pattern of staining is inconsistent with osteoblast cell culture, collagen ELISA results and existing literature.

Based on the more subjective analysis of collagen ELISA, a clear reduction is noted in the production of collagen by GCs only group. This effect is additive when both, GCs and an inflammatory stimulus (i.e., TNF-α) are present. This finding correlates with results of existing literature which state that GCs suppress osteoblast differentiation and promote osteoblast apoptosis at therapeutic doses (Mak et al., 2009; Chen et al., 2014). To overcome this for future experiments, it may be useful to quantify the number of viable cells using a hemacytometer and trypan blue to investigate if collagen content is a measure of number of cells or representation of the regulation of expression. Quantifying protein content may also help validate the collagen content.

Before quantifying the expression of osteoblast markers, transcriptional regulation of 11β-HSD1 by GCs in the presence and absence of inflammation was measured. GCs inhibited the expression of 11β-HSD1 when present alone. However, when present in conjunction with TNF-α, a strong stimulatory effect was observed. This may be due to the upregulation of 11β-HSD1 reductase activity by TNF-α, which increases the F/E shuttle (Escher et al., 1997). Alternatively, this synergism may be due to effect on p38-MAPK, MAPK phosphate or by increase the stability of 11β-HSD1 mRNA. A promoter-reporter assay can used to analyse the contribution of the proximal promoter in mediating this synergistic increase.

To further assess which mechanism causes this synergistic increase, western blotting utilising extracts from the mature osteoblast can be done. This will help

confirm if this rise in 11β-HSD expression is due to increased 11β-HSD1 protein expression (Kaur et al., 2009). Combined GC and pro-inflammatory cytokine treatment have also been reported as an endogenous mechanism to lessen synovitis by synergistically induce expression of 11β-HSD1.

Analysis of collagen ELISA and mRNA expression of the previously mentioned osteoblast markers revealed similar findings. In the presence of TNF-α, GCs osteoblast formation and differentiation were inhibited. This was highlighted by the potent suppression of OSC and alkaline phosphatase. This suppression may be due to pro-inflammatory cytokines (such as TNF-α) inducing the expression of inducible form of nitric oxide synthase (iNOS). iNOS stimulates the production of nitric oxide (NO) which activates the cyclooxygenase (COX) pathway. COX produces prostaglandin E2 (PGE2) which in turn inhibits activity and expression of alkaline phosphatase (Kanematsu et al., 1997). Furthermore, it has previously been reported that NO stimulated by TNF-α can impact the viability of osteoblasts due to induction of apoptosis (Damoulis and Hauschka, 1997). To investigate if the decrease in alkaline phosphatase activity and decrease in bone mineralisation is due a down-regulated response of viable osteoblast cells, the viability of the osteoblasts can be investigated using trypan blue exclusion. As reported for existing literature, the decrease in ALP activity may be due to NO may have a stimulatory effect on COX in osteoclasts. The activation of COX will release PGE2, which would function to inhibit the function of osteoblast whist stimulating osteoclast function i.e., bone resorption (Raisz et al., 1991). To identify if NOS and COX contribute to the inhibition of bone formation, NOS and COX inhibitor can be used which would ultimately show an increase in bone mineralisation and ALP activity. Similar mechanism of bone resorption by other inflammatory mediators (namely, IL-1β and

IL-6) have been reported (Kanematsu et al., 1997). This supports the already reported finding that inflammation drives bone away from formation and towards a resorptive state. Alongside the NOS and COX pathway, inflammatory mediators act synergistically with TNF-α to directly upregulate RANKL production, which induces osteoclastogenesis (Wei et al., 2005).

To explore the contribution of 11β-HSD1 in mediating the effects of GCs, an activity assay was done alongside qRT-PCR which studied gene expression of 11β-HSD1. The activity assay involved the use of 18α- glycyrrhetinic acid (GE). GE, derived from the natural product glycyrrhizin, is a selective inhibitor of 11β-HSD1 (Classen-Houben et al., 2009). Using *in vivo* models, GE has been demonstrated to inhibit 11β-HSD1, thereby producing pro-inflammatory effects. This inhibition was also reported to induce GC metabolism (Teelucksingh et al., 1990). As per the results of the 11β-HSD1 assay, an inhibition with GE was seen although it was not a potent suppression. Generating new GE with a higher concentration may help to better visualise its activity for future experiments. 11β-HSD1 mediate the inhibitory effect GCs exert on anabolic bone formation. To explore this effect, cell cultures using E, TNF-α, GE and a combination of these treatments was used. For cell culture experiments in which GE was used, E was used in place of cortisol. This is due to 11β-HSD1 activating cortisone to produce F. TNF-α was seen to downregulate OSC and ALP, markers of mature osteoblasts and increased the RANKL effect, suggesting that inflammation favours bone resorption. Whereas E is seen to induce OSC, ALP and inhibit RANKL, suggesting GC's role in bone formation. When added in combination with TNF-α, E protects against a reduction in osteoblast differentiation, which reinforces that GCs have anti-inflammatory effects. Similarly,

effects are seen when examining the expression of inflammatory mediators, IL1-β and IL-6.

Although, *in vitro* experiments showed potent effects on OSC and ALP, conflicting and statistically non-significant results were obtained when quantifying the gene expression of other osteoblast markers. This may suggest that although osteoblast numbers may be subject to a change, differentiation is not being greatly affected. This may be due to *in vitro* work not being able to fully model the processes taking place *in vivo*. For instance, *in vitro* cell cultures are unable to consider other secreted factors, including TGF-β, other components of WNT signalling and bone morphogenic cells, which may be involved in the regulation and survival of osteoblasts. The same applies to other factors releases from bone lining cells, bone marrow cells, osteocytes, and endothelium. For future *in vitro* experiments, using co-cultures to look interaction between different factors and luciferase reported assays to study the role of proteins on the activation status of target genes may be useful. Using online bone transcriptomic resources and performing analysis of *ex vivo* biopsies may prove useful.

Conflicting results were reported for the preliminary and optimised *in vitro* experiments. These differences may be attributable to the source of cells. Fresh cells from bone chips had to be manually extracted, which may have resulted in a potential genetic drift. Fresh cells produced a higher yield of low passage cells and may have been more resistant to stress and manipulation during the process of cell culture – a property which the frozen cells lack. Whilst the cells obtained from trabecular bone cells are a good reflection of patient variability, there could have been an unusual outlier patient with abnormal osteoblasts or higher metabolic rate that may have impacted the reproducibility of other patients. For fresh cells, the

differentiation also needed to be validated each time by direct observation, which may not have been correctly interpreted. Whilst cryopreserved osteoblasts helped reproducibility of results, and once validated were stored as aliquots to be used across experiments, they did require outgrowth to establish required numbers (which may have resulted in senescence). The process of cryopreservation may have caused cells to undergo phenotypical changes, which could have impacted our results. For the frozen vials, cells did not need to be isolated from tissues, reducing any possibility of genetic drift. It may have been possible that cells were lost or damage during the thawing process, where the damage may have affected the phenotype (as with the cryopreservation process).

Statistical analysis for RT-PCR was performed using the fold values (AU) (i.e., relative quantification), rather than the ΔCT value, which could have adversely impacted the statistical outcome. For future experiments, it would be beneficial to use the ΔCT values as AU assumes that each gene has the same amplification efficiency, which may not be the case. In the case that fold change is used, the average, upper and lower limits of the confidence interval need to be exponentiated before they can be used for a more reliable statistical analysis.

Having looked at the effect GCs exert on osteoblasts *in vitro*, the role of GCs on the bone in the presence of an inflammatory stimulus was explored *in vivo*. This was done by adding corticosterone (principal glucocorticoid in mice) in the drinking water of WT, Twist2-CRE (mesenchymal-specific KO of 11β-HSD1) and global KO of 11β-HSD1 (11βKO) were used. As stated earlier, high GC concentration suppress differentiation of osteoblast and induce apoptosis (Mak et al., 2009; Chen et al., 2014). However, GCs exert an inhibitory effect on inflammation. If inflammation is left untreated, GCs can activate osteoclast differentiation and suppress the

differentiation of osteoblasts, resulting in inflammatory bone loss (Palmqvist et al., 2002; Abbas et al., 2003; Wei et al., 2005; Yoshitake et al., 2008). Thus, through the murine models, we aimed to investigate the balance between the negative anti-anabolic effects of GCs and anti-inflammatory actions of GCs on bone. Firstly, it was necessary to validate the Twist2-CRE and the 11βKO models, which was done using thin layer chromatography. Results showed that whilst WT (with no disruption of 11β-HSD) had the greatest F activation, CRE and 11βKO showed significantly less activity. This was due to the absence of 11β-HSD1 in mesenchymal tissue and globally, which was needed to activate the F.

Following validation, each mouse model received oral GC treatment (corticosterone). The results showed that TNF-Tg mice and TNF CRE on corticosterone were protected against inflammatory bone loss/ joint erosions. However, whether this corresponded with a suppression in the level of proinflammatory mediators was not investigated. Investigating the levels of osteoclastogenic cytokines in future experiments may be valuable. Such cytokines include IL-1, IL-6 and TNF-α, each of which have been reported to increase osteoclastogenesis (Ragab et al., 2002). As outlined above, TNF-α is a potent activator of osteoclastogenesis, which it can stimulate independently of RANKL signalling. To explore this, measuring the ratio of RANKL to OPG, in addition to quantifying the number and activity of bone resorbing osteoclasts may be beneficial (Kudo et al., 2002; Kim et al., 2005). Other recruiters of osteoclast progenitors, such as the chemokine, CCL2, produced by osteoblasts. Studies have reported that CCL2 has an important role in osteoclast recruitment during inflammation and can promote osteoclastogenesis (Rahimi et al., 1995; Kim et al., 2005). Hence, decreasing the expression levels of inflammatory mediators and such chemokines

can prevent the recruitment and release of osteoclast progenitors, whilst suppressing these factors may prevent bone resorption by inhibiting osteoclastogenesis. Generating a TNF-Tg mouse with a targeted deletion of RANKL/ OPG can be used to investigate if TNF-α is responsible for mediating GC actions or if RANKL/ OPG contribute to regulating GC effects. The effect of GC treatment on markers of osteoblasts function and maturation (OSC, ALP, collagen production) needs to be investigated to assess the full impact of GCs on the mice model. Whilst changes in bone erosions were observed, muted changes in the cortical parameters were observed. These were statistically non-significant.

Majority of the work that was conducted for this thesis was using *in vitro* models, which heavily restricted the number of aspects and conditions of *in vivo* studies the thesis was able to model. Although, *in vivo* models were briefly used, they had several limitations. It is unclear how much of the work that was conducted on mouse models is translatable to humans as none of the work for this project was carried out on human subjects. Male mice were used for the animal studies, although RA is a disease which is more common in female – for this reason, it may be beneficial to repeat the studies using female mice. Additionally, it may be worthwhile extending the timeframes of the treatments used in mouse models as it was noted that 3 weeks were not enough to induce and/or observe macroscopic changes. At 7 weeks, the process of bone formation is not complete, and it may be susceptible to GCs and inflammatory mediators, so using mature animals may be beneficial to validate our findings. Sample size was another drawback for our studies, which can be overcome by increasing the number of mice per group and the number of groups. Each mouse model received oral GC treatment which was mixed with water, but

there may have been variation in the dose of GCs ingested so dose variation was another limitation encountered.

In summary, we have explored the effect of GC metabolism in osteoblasts during inflammation *in vitro* and *in vivo* settings. The *in vitro* models showed an inhibitory effect of GCs on collagen formation and osteoblast differentiation, as well as some suppression of pro-inflammatory mediators. However, a large variation in the results highlights the need for further experiments to fully validate these findings. *In vivo*, we examined cortical bone parameters, which showed little changes as cortical bone is known to be a poor responder of GC treatment. To fully understand the effect of GCs on bone, analysis of trabecular bone and other bone parameters (aside from the joint) with a longer timeframe are required to fully understand the role of therapeutic GCs.

References

1. Abbas, S., Zhang, Y. and Clohisy, J. et al. (2003) Tumor necrosis factor-α inhibits pre-osteoblast differentiation through its type-1 receptor. Cytokine, 22 (1-2): 33-41

2. Agerbæk, M., Eriksen, E. and Kragstrup, J. et al. (1991) A reconstruction of the remodelling cycle in normal human cortical iliac bone. Bone and Mineral, 12 (2): 101-112

3. Aguilera, G. (1994) Regulation of Pituitary ACTH Secretion during Chronic Stress. Frontiers in Neuroendocrinology, 15 (4): 321-350

4. Ahasan, M., Hardy, R. and Jones, C. et al. (2012) Inflammatory regulation of glucocorticoid metabolism in mesenchymal stromal cells. Arthritis & Rheumatism, 64 (7): 2404-2413

5. Al-Dujaili, S., Lau, E. and Al-Dujaili, H. et al. (2011) Apoptotic osteocytes regulate osteoclast precursor recruitment and differentiation in vitro. Journal of Cellular Biochemistry, 112 (9): 2412-2423

6. Allen, M., Hock, J. and Burr, D. (2004) Periosteum: biology, regulation, and response to osteoporosis therapies. Bone, 35 (5): 1003-1012

7. Anderson, P. (2010) Post-transcriptional regulons coordinate the initiation and resolution of inflammation. Nature Reviews Immunology, 10 (1): 24-35

8. Andrews, R., Rooyackers, O. and Walker, B. (2003) Effects of the 11β-Hydroxysteroid Dehydrogenase Inhibitor Carbenoxolone on Insulin Sensitivity in Men with Type 2 Diabetes. The Journal of Clinical Endocrinology & Metabolism, 88 (1): 285-291

9. Arlt, W. and Allolio, B. (2003) Adrenal insufficiency. The Lancet, 361 (9372): 1881-1893

10. Arlt, W. and Stewart, P. (2005) Adrenal Corticosteroid Biosynthesis, Metabolism, and Action. Endocrinology and Metabolism Clinics of North America, 34 (2): 293-313

11. Asquith, D., Miller, A. and McInnes, I. et al. (2009) Animal models of rheumatoid arthritis. European Journal of Immunology, 39 (8): 2040-2044

12. Atanasov, A., Nashev, L. and Schweizer, R. et al. (2004) Hexose-6-phosphate dehydrogenase determines the reaction direction of 11β-hydroxysteroid dehydrogenase type 1 as an oxoreductase. FEBS Letters, 571 (1-3): 129-133

13. Atkins, G. and Findlay, D. (2012) Osteocyte regulation of bone mineral: a little give and take. Osteoporosis International, 23 (8): 2067-2079

14. Atkins, G., Kostakis, P. and Vincent, C. et al. (2006) RANK Expression as a Cell Surface Marker of Human Osteoclast Precursors in Peripheral Blood, Bone Marrow, and Giant Cell Tumors of Bone. Journal of Bone and Mineral Research, 21 (9): 1339-1349

15. Auphan, N., DiDonato, J. and Rosette, C. et al. (1995) Immunosuppression by Glucocorticoids: Inhibition of NF-kappaB Activity Through Induction of IkappaB Synthesis. Science, 270 (5234): 286-290

16. Ayroldi, E., Cannarile, L. and Migliorati, G. et al. (2012) Mechanisms of the anti-inflammatory effects of glucocorticoids: genomic and nongenomic interference with MAPK signaling pathways. The FASEB Journal, 26 (12): 4805-4820

17. Bafico, A., Liu, G. and Yaniv, A. et al. (2001) Novel mechanism of Wnt signalling inhibition mediated by Dickkopf-1 interaction with LRP6/Arrow. Nature Cell Biology, 3 (7): 683-686

18. Bamberger, C., Bamberger, A. and de Castro, M. et al. (1995) Glucocorticoid receptor beta, a potential endogenous inhibitor of glucocorticoid action in humans. Journal of Clinical Investigation, 95 (6): 2435-2441

19. Barney, M., Call, G. and McIlmoil, C. et al. (2000) Stimulation by Interleukin-6 and Inhibition by Tumor Necrosis Factor of Cortisol Release from Bovine Adrenal Zona Fasciculata Cells Through Their Receptors. Endocrine, 13 (3): 369-377

20. Beato, M. (1989) Gene regulation by steroid hormones. Cell, 56 (3): 335-344

21. Beaulieu, E. and Morand, E. (2011) Role of GILZ in immune regulation, glucocorticoid actions and rheumatoid arthritis. Nature Reviews Rheumatology, 7 (6): 340-348

22. Beck, I., De Bosscher, K. and Haegeman, G. (2011) Glucocorticoid receptor mutants: man-made tools for functional research. Trends in Endocrinology & Metabolism, 22 (8): 295-310

23. Bentolila, V., Boyce, T. and Fyhrie, D. et al. (1998) Intracortical remodeling in adult rat long bones after fatigue loading. Bone, 23 (3): 275-281

24. Berkenbosch, F., van Oers, J. and del Rey, A. et al. (1987) Corticotropin-releasing factor-producing neurons in the rat activated by interleukin-1. Science, 238 (4826): 524-526

25. Bernardini, R., Kamilaris, T. and Calogero, A. et al. (1990) Interactions between Tumor Necrosis Factor-α, Hypothalamic Corticotropin-Releasing Hormone, and Adrenocorticotropin Secretion in the Rat*. Endocrinology, 126 (6): 2876-2881

26. Bhandi, S., Alkahtani, A. and Reda, R. et al. (2021) Parathyroid Hormone Secretion and Receptor Expression Determine the Age-Related Degree of Osteogenic Differentiation in Dental Pulp Stem Cells. Journal of Personalized Medicine, 11 (5): 349

27. Bledsoe, R., Montana, V. and Stanley, T. et al. (2002) Crystal Structure of the Glucocorticoid Receptor Ligand Binding Domain Reveals a Novel Mode of Receptor Dimerization and Coactivator Recognition. Cell, 110 (1): 93-105

28. Bonewald, L. (2011) The amazing osteocyte. Journal of Bone and Mineral Research, 26 (2): 229-238

29. Bonewald, L. and Johnson, M. (2008) Osteocytes, mechanosensing and Wnt signaling. Bone, 42 (4): 606-615

30. Bornstein, S., Allolio, B. and Arlt, W. et al. (2016) Diagnosis and Treatment of Primary Adrenal Insufficiency: An Endocrine Society Clinical Practice Guideline. The Journal of Clinical Endocrinology & Metabolism, 101 (2): 364-389

31. Bouxsein, M.L., Boyd, S.K., Christiansen, B.A., et al. (2010) Guidelines for assessment of bone microstructure in rodents using micro-computed tomography. Journal of Bone and Mineral Research, 25 (7): 1468–1486

32. Brem, A., Bina, R. and King, T. et al. (1995) Bidirectional activity of 11β-hydroxysteroid dehydrogenase in vascular smooth muscle cells. Steroids, 60 (5): 406-410

33. Brown, E., Gamba, G. and Riccardi, D. et al. (1993) Cloning and characterization of an extracellular Ca2+-sensing receptor from bovine parathyroid. Nature, 366 (6455): 575-580

34. Brown, S., Smith, L. and Blalock, J. (1987) Interleukin 1 and interleukin 2 enhance proopiomelanocortin gene expression in pituitary cells. J Immunol, 139 (10): 3181-3

35. Bucay, N., Sarosi, I. and Dunstan, C. et al. (1998) osteoprotegerin-deficient mice develop early onset osteoporosis and arterial calcification. Genes & Development, 12 (9): 1260-1268

36. Bujalska, I., Draper, N. and Michailidou, Z. et al. (2005) Hexose-6-phosphate dehydrogenase confers oxo-reductase activity upon 11β-hydroxysteroid dehydrogenase type 1. Journal of Molecular Endocrinology, 34 (3): 675-684

37. Bujalska, I., Kumar, S. and Stewart, P. (1997) Does central obesity reflect “Cushing's disease of the omentum”?. The Lancet, 349 (9060): 1210-1213

38. Busillo, J. and Cidlowski, J. (2013) The five Rs of glucocorticoid action during inflammation: ready, reinforce, repress, resolve, and restore. Trends in Endocrinology & Metabolism, 24 (3): 109-119

39. Butler, J., Queally, J. and Devitt, B. et al. (2010) Silencing Dkk1 expression rescues dexamethasone-induced suppression of primary human osteoblast differentiation. BMC Musculoskeletal Disorders, 11 (1)

40. Campbell, I., Hamilton, J. and Wicks, I. (2000) Collagen-induced arthritis in C57BL/6 (H-2b) mice: new insights into an important disease model of rheumatoid arthritis. European Journal of Immunology, 30 (6): 1568-1575

41. Canalis, E., Centrella, M. and Burch, W. et al. (1989) Insulin-like growth factor I mediates selective anabolic effects of parathyroid hormone in bone cultures. Journal of Clinical Investigation, 83 (1): 60-65

42. Carballo, E. (1998) Feedback Inhibition of Macrophage Tumor Necrosis Factor- Production by Tristetraprolin. Science, 281 (5379): 1001-1005

43. Carlberg, C., Bendik, I. and Wyss, A. et al. (1993) Two nuclear signalling pathways for vitamin D. Nature, 361 (6413): 657-660

44. Carrick, D., Lai, W. and Blackshear, P. (2004) The tandem CCCH zinc finger protein tristetraprolin and its relevance to cytokine mRNA turnover and arthritis. Arthritis Research & Therapy, 6 (6): 248

45. Cevc, G. and Blume, G. (2004) Hydrocortisone and dexamethasone in very deformable drug carriers have increased biological potency, prolonged effect, and reduced therapeutic dosage. Biochimica et Biophysica Acta (BBA) - Biomembranes, 1663 (1-2): 61-73

46. Chapman, K., Coutinho, A. and Gray, M. et al. (2009) The role and regulation of 11β-hydroxysteroid dehydrogenase type 1 in the inflammatory response. Molecular and Cellular Endocrinology, 301 (1-2): 123-131

47. Charmandari, E., Tsigos, C. and Chrousos, G. (2005) Endocrinology of the stress response. Annual Review of Physiology, 67 (1): 259-284

48. Chen, F., Zhang, L. and OuYang, Y. et al. (2014) Glucocorticoid Induced Osteoblast Apoptosis by Increasing E4BP4 Expression via Up-regulation of Bim. Calcified Tissue International, 94 (6): 640-647

49. Chen, H., Senda, T. and Kubo, K. (2015) The osteocyte plays multiple roles in bone remodeling and mineral homeostasis. Medical Molecular Morphology, 48 (2): 61-68

50. Chen, X., Murakami, T. and Oppenheim, J. et al. (2004) Differential response of murine CD4+CD25+and CD4+CD25-T cells to dexamethasone-induced cell death. European Journal of Immunology, 34 (3): 859-869

51. Chen, Y., Bai, B. and Zhang, S. et al. (2014) Effects of Parathyroid Hormone on Calcium Ions in Rat Bone Marrow Mesenchymal Stem Cells. BioMed Research International, 2014: 1-6

52. Cheng, J., Liu, J. and Shi, Z. et al. (2011) Interleukin-4 inhibits RANKL-induced NFATc1 expression via STAT6: A novel mechanism mediating its blockade of osteoclastogenesis. Journal of Cellular Biochemistry, 112 (11): 3385-3392

53. Cheung, J. and Smith, D. (2000) Molecular Chaperone Interactions with Steroid Receptors: an Update. Molecular Endocrinology, 14 (7): 939-946

54. Clarke, B. (2008) Normal Bone Anatomy and Physiology. Clinical Journal of the American Society of Nephrology, 3 (Supplement 3): S131-S139

55. Cole, T., Blendy, J. and Monaghan, A. et al. (1995) Targeted disruption of the glucocorticoid receptor gene blocks adrenergic chromaffin cell development and severely retards lung maturation. Genes & Development, 9 (13): 1608-1621

56. Colnot, C. (2009) Skeletal Cell Fate Decisions Within Periosteum and Bone Marrow During Bone Regeneration. Journal of Bone and Mineral Research, 24 (2): 274-282

57. Cooper, M., Walker, E. and Bland, R. et al. (2000) Expression and functional consequences of 11β-hydroxysteroid dehydrogenase activity in human bone. Bone, 27 (3): 375-381

58. Cowles, E., DeRome, M. and Pastizzo, G. et al. (1998) Mineralization and the Expression of Matrix Proteins During In Vivo Bone Development. Calcified Tissue International, 62 (1): 74-82

59. Cronstein, B., Kimmel, S. and Levin, R. et al. (1992) A mechanism for the antiinflammatory effects of corticosteroids: the glucocorticoid receptor regulates leukocyte adhesion to endothelial cells and expression of endothelial-leukocyte adhesion molecule 1 and intercellular adhesion molecule 1. Proceedings of the National Academy of Sciences, 89 (21): 9991-9995

60. Curtis, J., Westfall, A. and Allison, J. et al. (2006) Population-based assessment of adverse events associated with long-term glucocorticoid use. Arthritis & Rheumatism, 55 (3): 420-426

61. Dallas, S., Prideaux, M. and Bonewald, L. (2013) The Osteocyte: An Endocrine Cell … and More. Endocrine Reviews, 34 (5): 658-690

62. Damoulis, P. and Hauschka, P. (1997) Nitric Oxide Acts in Conjunction with Proinflammatory Cytokines to Promote Cell Death in Osteoblasts. Journal of Bone and Mineral Research, 12 (3): 412-422

63. Dao-Phan, H., Formstecher, P. and Lefebvre, P. (1997) Disruption of the Glucocorticoid Receptor Assembly with Heat Shock Protein 90 by a Peptidic Antiglucocorticoid. Molecular Endocrinology, 11 (7): 962-972

64. Datta, H., Ng, W. and Walker, J. et al. (2008) The cell biology of bone metabolism. Journal of Clinical Pathology, 61 (5): 577-587

65. Datta, N., Pettway, G. and Chen, C. et al. (2007) Cyclin D1 as a Target for the Proliferative Effects of PTH and PTHrP in Early Osteoblastic Cells. Journal of Bone and Mineral Research, 22 (7): 951-964

66. Day, T., Guo, X. and Garrett-Beal, L. et al. (2005) Wnt/β-Catenin Signaling in Mesenchymal Progenitors Controls Osteoblast and Chondrocyte Differentiation during Vertebrate Skeletogenesis. Developmental Cell, 8 (5): 739-750

67. De Bosscher, K. and Haegeman, G. (2009) Minireview: Latest Perspectives on Antiinflammatory Actions of Glucocorticoids. Molecular Endocrinology, 23 (3): 281-291

68. de Castro, M., Elliot, S. and Kino, T. et al. (1996) The Non-Ligand Binding β-Isoform of the Human Glucocorticoid Receptor (hGRβ): Tissue Levels, Mechanism of Action, and Potential Physiologic Role. Molecular Medicine, 2 (5): 597-607

69. Di Dalmazi, G., Pagotto, U. and Pasquali, R. et al. (2012) Glucocorticoids and Type 2 Diabetes: From Physiology to Pathology. Journal of Nutrition and Metabolism, 2012: 1-9

70. Diarra, D., Stolina, M. and Polzer, K. et al. (2007) Dickkopf-1 is a master regulator of joint remodeling. Nature Medicine, 13 (2): 156-163

71. Diederich, S., Eigendorff, E. and Burkhardt, P. et al. (2002) 11β-Hydroxysteroid Dehydrogenase Types 1 and 2: An Important Pharmacokinetic Determinant for the Activity of Synthetic Mineralo- and Glucocorticoids. The Journal of Clinical Endocrinology & Metabolism, 87 (12): 5695-5701

72. Diederich, S., Hanke, B. and Bähr, V. et al. (1996) The metabolism of 9α-fluorinated steroids in the human kidney. Endocrine Research, 22 (4): 803-810

73. Diederich, S., Hanke, B. and Oelkers, W. et al. (1997) Metabolism of Dexamethasone in the Human Kidney: Nicotinamide Adenine Dinucleotide-Dependent 11β-Reduction. The Journal of Clinical Endocrinology & Metabolism, 82 (5): 1598-1602

74. Dieken, E. and Miesfeld, R. (1992) Transcriptional transactivation functions localized to the glucocorticoid receptor N terminus are necessary for steroid

induction of lymphocyte apoptosis. Molecular and Cellular Biology, 12 (2): 589-597

75. Douni, E., Akassoglou, K. and Alexopoulou, L. et al. (1995) Transgenic and knockout analyses of the role of TNF in immune regulation and disease pathogenesis. J Inflamm, 47 (12): 27-38

76. Dreyfuss, G., Kim, V. and Kataoka, N. (2002) Messenger-RNA-binding proteins and the messages they carry. Nature Reviews Molecular Cell Biology, 3 (3): 195-205

77. Drouin, J., Yu Lin, S. and Nemer, M. (1989) Glucocorticoid repression of pro-opiomelanocortin gene transcription. Journal of Steroid Biochemistry, 34 (1-6): 63-69

78. Dunn, J., Nisula, B. and Robdard, D. (1981) Transport of Steroid Hormones: Binding of 21 Endogenous Steroids to Both Testosterone-Binding Globulin and Corticosteroid-Binding Globulin in Human Plasma. The Journal of Clinical Endocrinology & Metabolism, 53 (1): 58-68

79. Dzyakanchuk, A., Balázs, Z. and Nashev, L. et al. (2009) 11β-Hydroxysteroid dehydrogenase 1 reductase activity is dependent on a high ratio of NADPH/NADP+ and is stimulated by extracellular glucose. Molecular and Cellular Endocrinology, 301 (1-2): 137-141

80. Eijken, M., Koedam, M. and van Driel, M. et al. (2006) The essential role of glucocorticoids for proper human osteoblast differentiation and matrix mineralization. Molecular and Cellular Endocrinology, 248 (1-2): 87-93

81. Eriksen, E., Hodgson, S. and Eastell, R. et al. (1990) Cancellous bone remodeling in type i (postmenopausal) osteoporosis: Quantitative assessment of rates of formation, resorption, and bone loss at tissue and cellular levels. Journal of Bone and Mineral Research, 5 (4): 311-319

82. Erkut, Z., Pool, C. and Swaab, D. (1998) Glucocorticoids Suppress Corticotropin-Releasing Hormone and Vasopressin Expression in Human Hypothalamic Neurons1. The Journal of Clinical Endocrinology & Metabolism, 83 (6): 2066-2073

83. Escher, G., Galli, I. and Vishwanath, B. et al. (1997) Tumor Necrosis Factor α and Interleukin 1β Enhance the Cortisone/Cortisol Shuttle. Journal of Experimental Medicine, 186 (2): 189-198

84. Evans, R. (1988) The steroid and thyroid hormone receptor superfamily. Science, 240 (4854): 889-895

85. Evanson, N., Tasker, J. and Hill, M. et al. (2010) Fast Feedback Inhibition of the HPA Axis by Glucocorticoids Is Mediated by Endocannabinoid Signaling. Endocrinology, 151 (10): 4811-4819

86. Exton, J. (1979) Regulation of Gluconeogenesis by Glucocorticoids. Glucocorticoid Hormone Action, pp. 535-546

87. Faccio, R., Novack, D. and Zallone, A. et al. (2003) Dynamic changes in the osteoclast cytoskeleton in response to growth factors and cell attachment are controlled by β3 integrin. Journal of Cell Biology, 162 (3): 499-509

88. Fardet, L., Flahault, A. and Kettaneh, A. et al. (2007) Corticosteroid-induced clinical adverse events: frequency, risk factors and patient?s opinion. British Journal of Dermatology, 157 (1): 142-148

89. Feig, P., Shah, S. and Hermanowski-Vosatka, A. et al. (2011) Effects of an 11β-hydroxysteroid dehydrogenase type 1 inhibitor, MK-0916, in patients with type 2 diabetes mellitus and metabolic syndrome. Diabetes, Obesity and Metabolism, 13 (6): 498-504

90. Fenton, C., Webster, J. and Martin, C. et al. (2019) Therapeutic glucocorticoids prevent bone loss but drive muscle wasting when administered in chronic polyarthritis. Arthritis Research & Therapy, 21 (1): 182

91. Fretz, J., Zella, L. and Kim, S. et al. (2007) 1,25-Dihydroxyvitamin D3 induces expression of the Wnt signaling co-regulator LRP5 via regulatory elements located significantly downstream of the gene's transcriptional start site. The Journal of Steroid Biochemistry and Molecular Biology, 103 (3-5): 440-445

92. Frost, H. (1990) Skeletal structural adaptations to mechanical usage (SATMU): 2. Redefining Wolff's Law: The remodeling problem. The Anatomical Record, 226 (4): 414-422

93. Fukata, J., Usui, T. and Naitoh, Y. et al. (1989) Effects of recombinant human interleukin-1α, -1β, 2 and 6 on ACTH synthesis and release in the mouse pituitary tumour cell line AtT-20. Journal of Endocrinology, 122 (1): 33-39

94. Garnero, P., Borel, O. and Byrjalsen, I. et al. (1998) The Collagenolytic Activity of Cathepsin K Is Unique among Mammalian Proteinases. Journal of Biological Chemistry, 273 (48): 32347-32352

95. Gaur, T., Lengner, C. and Hovhannisyan, H. et al. (2005) Canonical WNT Signaling Promotes Osteogenesis by Directly Stimulating Runx2 Gene Expression. Journal of Biological Chemistry, 280 (39): 33132-33140

96. Ge, C., Xiao, G. and Jiang, D. et al. (2009) Identification and Functional Characterization of ERK/MAPK Phosphorylation Sites in the Runx2 Transcription Factor. Journal of Biological Chemistry, 284 (47): 32533-32543

97. Giles, K., Ross, K. and Rossi, A. et al. (2001) Glucocorticoid Augmentation of Macrophage Capacity for Phagocytosis of Apoptotic Cells Is Associated

with Reduced p130Cas Expression, Loss of Paxillin/pyk2 Phosphorylation, and High Levels of Active Rac. The Journal of Immunology, 167 (2): 976-986

98. Gilmour, J., Coutinho, A. and Cailhier, J. et al. (2006) Local Amplification of Glucocorticoids by 11β-Hydroxysteroid Dehydrogenase Type 1 Promotes Macrophage Phagocytosis of Apoptotic Leukocytes. The Journal of Immunology, 176 (12): 7605-7611

99. Giraldi, F., Moro, M. and Cavagnini, F. (2003) Gender-Related Differences in the Presentation and Course of Cushing's Disease. The Journal of Clinical Endocrinology & Metabolism, 88 (4): 1554-1558

100. Glass, D. and Karsenty, G. (2006) Molecular Bases of the Regulation of Bone Remodeling by the Canonical Wnt Signaling Pathway. Current Topics in Developmental Biology, 73: 43-84. Available from:

101. Govindan, M. (2010) Recruitment of cAMP-response Element-binding Protein and Histone Deacetylase Has Opposite Effects on Glucocorticoid Receptor Gene Transcription. Journal of Biological Chemistry, 285 (7): 4489-4510

102. Guerrini, M., Sobacchi, C. and Cassani, B. et al. (2008) Human Osteoclast-Poor Osteopetrosis with Hypogammaglobulinemia due to TNFRSF11A (RANK) Mutations. The American Journal of Human Genetics, 83 (1): 64-76

103. Gullick, N. and Scott, D. (2011) Co-morbidities in established rheumatoid arthritis. Best Practice & Research Clinical Rheumatology, 25 (4): 469-483

104. Gutierrez, S., Javed, A. and Tennant, D. et al. (2002) CCAAT/Enhancer-binding Proteins (C/EBP) β and δ Activate Osteocalcin Gene Transcription and Synergize with Runx2 at the C/EBP Element to Regulate Bone-specific Expression. Journal of Biological Chemistry, 277 (2): 1316-1323

105. Hadley, M. and Haskell-Luevano, C. (2006) The Proopiomelanocortin System. Annals of the New York Academy of Sciences, 885 (1): 1-21

106. Hafez, E., Mansour, H. and Hamza, S. et al. (2011) Bone Mineral Density Changes in Patients with Recent-Onset Rheumatoid Arthritis. Clinical Medicine Insights: Arthritis and Musculoskeletal Disorders, 4: CMAMD.S7773

107. Hakeda, Y., Kobayashi, Y. and Yamaguchi, K. et al. (1998) Osteoclastogenesis Inhibitory Factor (OCIF) Directly Inhibits Bone-Resorbing Activity of Isolated Mature Osteoclasts. Biochemical and Biophysical Research Communications, 251 (3): 796-801

108. Halleen, J., Räisänen, S. and Salo, J. et al. (1999) Intracellular Fragmentation of Bone Resorption Products by Reactive Oxygen Species

Generated by Osteoclastic Tartrate-resistant Acid Phosphatase. Journal of Biological Chemistry, 274 (33): 22907-22910

109. Hammond, G. (2016) Plasma steroid-binding proteins: primary gatekeepers of steroid hormone action. Journal of Endocrinology, 230 (1): R13-R25

110. Han, J., Brown, T. and Beutler, B. (1990) Endotoxin-responsive sequences control cachectin/tumor necrosis factor biosynthesis at the translational level. Journal of Experimental Medicine, 171 (2): 465-475

111. Hard, T., Kellenbach, E. and Boelens, R. et al. (1990) Solution structure of the glucocorticoid receptor DNA-binding domain. Science, 249 (4965): 157-160

112. Hardy, R. and Cooper, M. (2009) Bone loss in inflammatory disorders. Journal of Endocrinology, 201 (3): 309-320

113. Hardy, R., Doig, C. and Hussain, Z. et al. (2016) 11β-Hydroxysteroid dehydrogenase type 1 within muscle protects against the adverse effects of local inflammation. The Journal of Pathology, 240 (4): 472-483

114. Hardy, R., Fenton, C. and Croft, A. et al. (2018) 11 Beta-hydroxysteroid dehydrogenase type 1 regulates synovitis, joint destruction, and systemic bone loss in chronic polyarthritis. Journal of Autoimmunity, 92: 104-113

115. Hardy, R., Filer, A. and Cooper, M. et al. (2006) Differential expression, function and response to inflammatory stimuli of 11β-hydroxysteroid dehydrogenase type 1 in human fibroblasts: a mechanism for tissue-specific regulation of inflammation. Arthritis Research & Therapy, 8 (4): R108

116. Hardy, R., Rabbitt, E. and Filer, A. et al. (2007) Local and systemic glucocorticoid metabolism in inflammatory arthritis. Annals of the Rheumatic Diseases, 67 (9): 1204-1210

117. Hardy, R., Raza, K. and Cooper, M. (2014) Glucocorticoid metabolism in rheumatoid arthritis. Annals of the New York Academy of Sciences, 1318 (1): 18-26

118. Hardy, R.S., Doig, C.L., Hussain, Z., et al. (2016) 11β-hydroxysteroid dehydrogenase type 1 within muscle protects against the adverse effects of local inflammation. The Journal of Pathology, 240 (4): 472–483

119. Hardy, R.S., Fenton, C., Croft, A.P., et al. (2018) 11 beta-hydroxysteroid dehydrogenase type 1 regulates synovitis, joint destruction, and systemic bone loss in chronic polyarthritis. Journal of Autoimmunity, 92: 104–113

120. Harke, N., Leers, J. and Kietz, S. et al. (2008) Glucocorticoids regulate the human occludin gene through a single imperfect palindromic glucocorticoid response element. Molecular and Cellular Endocrinology, 295 (1-2): 39-47

121. Hasegawa, T., Yamamoto, T. and Tsuchiya, E. et al. (2017) Ultrastructural and biochemical aspects of matrix vesicle-mediated mineralization. Japanese Dental Science Review, 53 (2): 34-45

122. Hauge, E., Qvesel, D. and Eriksen, E. et al. (2001) Cancellous Bone Remodeling Occurs in Specialized Compartments Lined by Cells Expressing Osteoblastic Markers. Journal of Bone and Mineral Research, 16 (9): 1575-1582

123. Haussler, M., Haussler, C. and Whitfield, G. et al. (2010) The nuclear vitamin D receptor controls the expression of genes encoding factors which feed the “Fountain of Youth” to mediate healthful aging. The Journal of Steroid Biochemistry and Molecular Biology, 121 (1-2): 88-97

124. Heitzer, M., Wolf, I. and Sanchez, E. et al. (2007) Glucocorticoid receptor physiology. Reviews in Endocrine and Metabolic Disorders, 8 (4): 321-330

125. Hench, P., Kendall, E. and Slocumb, C. et al. (1949) Adrenocortical Hormone in Arthritis : Preliminary Report. Annals of the Rheumatic Diseases, 8 (2): 97-104

126. Hill, P., Tumber, A. and Meikle, M. (1997) Multiple Extracellular Signals Promote Osteoblast Survival and Apoptosis1. Endocrinology, 138 (9): 3849-3858

127. Hofbauer, L., Gori, F. and Riggs, B. et al. (1999) Stimulation of Osteoprotegerin Ligand and Inhibition of Osteoprotegerin Production by Glucocorticoids in Human Osteoblastic Lineage Cells: Potential Paracrine Mechanisms of Glucocorticoid-Induced Osteoporosis1. Endocrinology, 140 (10): 4382-4389

128. Hollberg, K., Nordahl, J. and Hultenby, K. et al. (2005) Polarization and secretion of cathepsin K precede tartrate-resistant acid phosphatase secretion to the ruffled border area during the activation of matrix-resorbing clasts. Journal of Bone and Mineral Metabolism, 23 (6): 441-449

129. Hollenberg, S., Weinberger, C. and Ong, E. et al. (1985) Primary structure and expression of a functional human glucocorticoid receptor cDNA. Nature, 318 (6047): 635-641

130. Holmdahl, R., Jansson, L. and Larsson, E. et al. (1986) Homologous type II collagen induces chronic and progressive arthritis in mice. Arthritis & Rheumatism, 29 (1): 106-113

131. Homma, M., Oka, K. and Niitsuma, T. et al. (1994) A Novel 11β-Hydroxysteroid Dehydrogenase Inhibitor Contained in Saiboku-To, a Herbal Remedy for Steroid-dependent Bronchial Asthma. Journal of Pharmacy and Pharmacology, 46 (4): 305-309

132. Hoppstädter, J. and Ammit, A. (2019) Role of Dual-Specificity Phosphatase 1 in Glucocorticoid-Driven Anti-inflammatory Responses. Frontiers in Immunology, 10

133. Huang, J., Sakata, T. and Pfleger, L. et al. (2003) PTH Differentially Regulates Expression of RANKL and OPG. Journal of Bone and Mineral Research, 19 (2): 235-244

134. Huang, P., Chandra, V. and Rastinejad, F. (2010) Structural Overview of the Nuclear Receptor Superfamily: Insights into Physiology and Therapeutics. Annual Review of Physiology, 72 (1): 247-272

135. Huang, W., Yang, S. and Shao, J. et al. (2007) Signaling and transcriptional regulation in osteoblast commitment and differentiation. Frontiers in Bioscience, 12 (8-12): 3068

136. Humphrey, E., Williams, J. and Davie, M. et al. (2006) Effects of dissociated glucocorticoids on OPG and RANKL in osteoblastic cells. Bone, 38 (5): 652-661

137. Inglis, J., Šimelyte, E. and McCann, F. et al. (2008) Protocol for the induction of arthritis in C57BL/6 mice. Nature Protocols, 3 (4): 612-618

138. Ishida, Y. and Heersche, J. (1998) Glucocorticoid-Induced Osteoporosis: Both In Vivo and In Vitro Concentrations of Glucocorticoids Higher Than Physiological Levels Attenuate Osteoblast Differentiation. Journal of Bone and Mineral Research, 13 (12): 1822-1826

139. Ito, K., Barnes, P. and Adcock, I. (2000) Glucocorticoid Receptor Recruitment of Histone Deacetylase 2 Inhibits Interleukin-1β-Induced Histone H4 Acetylation on Lysines 8 and 12. Molecular and Cellular Biology, 20 (18): 6891-6903

140. Itoh, S., Udagawa, N. and Takahashi, N. et al. (2006) A critical role for interleukin-6 family-mediated Stat3 activation in osteoblast differentiation and bone formation. Bone, 39 (3): 505-512

141. Itzstein, C., Coxon, F. and Rogers, M. (2011) The regulation of osteoclast function and bone resorption by small GTPases. Small GTPases, 2 (3): 117-130

142. Jenkins, J. and Sampson, P. (1967) Conversion of cortisone to cortisol and prednisone to prednisolone. BMJ, 2 (5546): 205-207

143. Jia, D., O'Brien, C. and Stewart, S. et al. (2006) Glucocorticoids Act Directly on Osteoclasts to Increase Their Life Span and Reduce Bone Density. Endocrinology, 147 (12): 5592-5599

144. Jilka, R., Weinstein, R. and Bellido, T. et al. (1998) Osteoblast Programmed Cell Death (Apoptosis): Modulation by Growth Factors and Cytokines. Journal of Bone and Mineral Research, 13 (5): 793-802

145. Joe, B., Griffiths, M. and Remmers, E. et al. (1999) Animal models of rheumatoid arthritis and related inflammation. Current Rheumatology Reports, 1 (2): 139-148

146. Joseph, R., Hunter, A. and Ray, D. et al. (2016) Systemic glucocorticoid therapy and adrenal insufficiency in adults: A systematic review. Seminars in Arthritis and Rheumatism, 46 (1): 133-141

147. Kafienah, W., Bromme, D. and Buttle, D. et al. (1998) Human cathepsin K cleaves native type I and II collagens at the N-terminal end of the triple helix. Biochemical Journal, 331 (3): 727-732

148. Kaneki, H., Guo, R. and Chen, D. et al. (2006) Tumor Necrosis Factor Promotes Runx2 Degradation through Up-regulation of Smurf1 and Smurf2 in Osteoblasts. Journal of Biological Chemistry, 281 (7): 4326-4333

149. Kanematsu, M., Ikeda, K. and Yamada, Y. (1997) Interaction Between Nitric Oxide Synthase and Cyclooxygenase Pathways in Osteoblastic MC3T3-E1 Cells. Journal of Bone and Mineral Research, 12 (11): 1789-1796

150. Kannan, K., Ortmann, R. and Kimpel, D. (2005) Animal models of rheumatoid arthritis and their relevance to human disease. Pathophysiology, 12 (3): 167-181

151. Karsenty, G., Kronenberg, H. and Settembre, C. (2009) Genetic Control of Bone Formation. Annual Review of Cell and Developmental Biology, 25 (1): 629-648

152. Karssen, A. and de Kloet, E. (2007) Synthetic Glucocorticoids. Encyclopedia of Stress, pp. 704-708

153. Katahira, M., Iwasaki, Y. and Aoki, Y. et al. (1998) Cytokine Regulation of the Rat Proopiomelanocortin Gene Expression in AtT-20 Cells. Endocrinology, 139 (5): 2414-2422

154. Kaur, K., Hardy, R. and Ahasan, M. et al. (2009) Synergistic induction of local glucocorticoid generation by inflammatory cytokines and glucocorticoids: implications for inflammation associated bone loss. Annals of the Rheumatic Diseases, 69 (6): 1185-1190

155. Kawai, T., Matsuyama, T. and Hosokawa, Y. et al. (2006) B and T Lymphocytes Are the Primary Sources of RANKL in the Bone Resorptive Lesion of Periodontal Disease. The American Journal of Pathology, 169 (3): 987-998

156. Keffer, J., Probert, L. and Cazlaris, H. et al. (1991) Transgenic mice expressing human tumour necrosis factor: a predictive genetic model of arthritis. The EMBO Journal, 10 (13): 4025-4031

157. Kenkre, J. and Bassett, J. (2018) The bone remodelling cycle. Annals of Clinical Biochemistry: International Journal of Laboratory Medicine, 55 (3): 308-327

158. Kim, H. (2006) Glucocorticoids suppress bone formation via the osteoclast. Journal of Clinical Investigation, 116 (8): 2152-2160

159. Kim, J. and Kim, N. (2014) Regulation of NFATc1 in Osteoclast Differentiation. Journal of Bone Metabolism, 21 (4): 233

160. Kim, N., Kadono, Y. and Takami, M. et al. (2005) Osteoclast differentiation independent of the TRANCE–RANK–TRAF6 axis. Journal of Experimental Medicine, 202 (5): 589-595

161. Kirwan, J., Hällgren, R. and Mielants, H. et al. (2004) A randomised placebo controlled 12 week trial of budesonide and prednisolone in rheumatoid arthritis. Annals of the Rheumatic Diseases, 63 (6): 688-695

162. Kizaki, T., Ookawara, T. and Oh-Ishi, S. et al. (1998) An increase in basal glucocorticoid concentration with age induces suppressor macrophages with high-density FcγRII/III. Immunology, 93 (3): 409-414

163. Klint, E., Grundtman, C. and Engström, M. et al. (2005) Intraarticular glucocorticoid treatment reduces inflammation in synovial cell infiltrations more efficiently than in synovial blood vessels. Arthritis & Rheumatism, 52 (12): 3880-3889

164. Kong, Y., Yoshida, H. and Sarosi, I. et al. (1999) OPGL is a key regulator of osteoclastogenesis, lymphocyte development and lymph-node organogenesis. Nature, 397 (6717): 315-323

165. Kotake, S., Udagawa, N. and Takahashi, N. et al. (1999) IL-17 in synovial fluids from patients with rheumatoid arthritis is a potent stimulator of osteoclastogenesis. Journal of Clinical Investigation, 103 (9): 1345-1352

166. Kouskoff, V., Korganow, A. and Duchatelle, V. et al. (1996) Organ-Specific Disease Provoked by Systemic Autoimmunity. Cell, 87 (5): 811-822

167. Kowenz-Leutz, E. and Leutz, A. (1999) A C/EBPβ Isoform Recruits the SWI/SNF Complex to Activate Myeloid Genes. Molecular Cell, 4 (5): 735-743

168. Kraus-Friedmann, N. (1984) Hormonal regulation of hepatic gluconeogenesis. Physiological Reviews, 64 (1): 170-259

169. Kudo, O., Fujikawa, Y. and Itonaga, I. et al. (2002) Proinflammatory cytokine (TNF?/IL-1?) induction of human osteoclast formation. The Journal of Pathology, 198 (2): 220-227

170. Kulkarni, N., Halladay, D. and Miles, R. et al. (2005) Effects of parathyroid hormone on Wnt signaling pathway in bone. Journal of Cellular Biochemistry, 95 (6): 1178-1190

171. Kumar, R. and Thompson, E. (2003) Transactivation Functions of the N-Terminal Domains of Nuclear Hormone Receptors: Protein Folding and Coactivator Interactions. Molecular Endocrinology, 17 (1): 1-10

172. Kuo, T., Harris, C. and Wang, J. (2013) Metabolic functions of glucocorticoid receptor in skeletal muscle. Molecular and Cellular Endocrinology, 380 (1-2): 79-88

173. Lam, J., Takeshita, S. and Barker, J. et al. (2000) TNF-α induces osteoclastogenesis by direct stimulation of macrophages exposed to permissive levels of RANK ligand. Journal of Clinical Investigation, 106 (12): 1481-1488

174. Laugesen, K., Jørgensen, J. and Petersen, I. et al. (2019) Fifteen-year nationwide trends in systemic glucocorticoid drug use in Denmark. European Journal of Endocrinology, 181 (3): 267-273

175. Lavery, G., Walker, E. and Draper, N. et al. (2006) Hexose-6-phosphate Dehydrogenase Knock-out Mice Lack 11β-Hydroxysteroid Dehydrogenase Type 1-mediated Glucocorticoid Generation. Journal of Biological Chemistry, 281 (10): 6546-6551

176. Leclerc, N., Noh, T. and Khokhar, A. et al. (2005) Glucocorticoids inhibit osteocalcin transcription in osteoblasts by suppressing Egr2/Krox20-binding enhancer. Arthritis & Rheumatism, 52 (3): 929-939

177. Lekva, T., Bollerslev, J. and Kristo, C. et al. (2010) The Glucocorticoid-Induced Leucine Zipper Gene (GILZ) Expression Decreases after Successful Treatment of Patients with Endogenous Cushing's Syndrome and May Play a Role in Glucocorticoid-Induced Osteoporosis. The Journal of Clinical Endocrinology & Metabolism, 95 (1): 246-255

178. Lencel, P., Ayeb, L. and Briolay, A. et al. (2012) TNF-alpha stimulates alkaline phosphatase and mineralization through canonical and non-canonical WNT signals in human osteoblast progenitors. Bone, 50: S72

179. Lewis, J., Bagley, C. and Elder, P. et al. (2005) Plasma free cortisol fraction reflects levels of functioning corticosteroid-binding globulin. Clinica Chimica Acta, 359 (1-2): 189-194

180. Lewis-Tuffin, L., Jewell, C. and Bienstock, R. et al. (2007) Human Glucocorticoid Receptor β Binds RU-486 and Is TranscriptionallyActive. Molecular and Cellular Biology, 27 (6): 2266-2282

181. Li, A., Hardy, R., Stoner, S., et al. (2013) Deletion of mesenchymal glucocorticoid receptor attenuates embryonic lung development and abdominal wall closure. PLoS ONE, 8 (5)

182. Li, C., Zhang, P. and Gu, J. (2015) miR-29a modulates tumor necrosis factor-α-induced osteogenic inhibition by targeting Wnt antagonists. Development, Growth & Differentiation, 57 (3): 264-273

183. Li, W., Gao, L. and Wang, Y. et al. (2006) Enhancement of Cortisol-Induced 11β-Hydroxysteroid dehydrogenase Type 1 Expression by Interleukin 1β in Cultured Human Chorionic Trophoblast Cells. Endocrinology, 147 (5): 2490-2495

184. Li, Y., Ge, C. and Franceschi, R. (2009) Differentiation-dependent association of phosphorylated extracellular signal-regulated kinase with the chromatin of osteoblast-related genes. Journal of Bone and Mineral Research, 25 (1): 154-163

185. Littlejohn, E. and Monrad, S. (2018) Early Diagnosis and Treatment of Rheumatoid Arthritis. Primary Care: Clinics in Office Practice, 45 (2): 237-255

186. Liu, D., Ahmet, A. and Ward, L. et al. (2013) A practical guide to the monitoring and management of the complications of systemic corticosteroid therapy. Allergy, Asthma & Clinical Immunology, 9 (1): 30

187. Liu, Y., Cousin, J. and Hughes, J. et al. (1999) Glucocorticoids promote nonphlogistic phagocytosis of apoptotic leukocytes. J Immunol, 162 (6): 3639-46

188. Ljusberg, J., Wang, Y. and Lång, P. et al. (2005) Proteolytic Excision of a Repressive Loop Domain in Tartrate-resistant Acid Phosphatase by Cathepsin K in Osteoclasts. Journal of Biological Chemistry, 280 (31): 28370-28381

189. Lomaga, M., Yeh, W. and Sarosi, I. et al. (1999) TRAF6 deficiency results in osteopetrosis and defective interleukin-1, CD40, and LPS signaling. Genes & Development, 13 (8): 1015-1024

190. Lu, N. and Cidlowski, J. (2005) Translational Regulatory Mechanisms Generate N-Terminal Glucocorticoid Receptor Isoforms with Unique Transcriptional Target Genes. Molecular Cell, 18 (3): 331-342

191. Luo, G., Li, F. and Li, X. et al. (2018) TNF-α and RANKL promote osteoclastogenesis by upregulating RANK via the NF-κB pathway. Molecular Medicine Reports, 17 (5): 6605–6611

192. Luxenburg, C., Geblinger, D. and Klein, E. et al. (2007) The Architecture of the Adhesive Apparatus of Cultured Osteoclasts: From Podosome Formation to Sealing Zone Assembly. PLoS ONE, 2 (1): e179

193. Mak, W., Shao, X. and Dunstan, C. et al. (2009) Biphasic Glucocorticoid-Dependent Regulation of Wnt Expression and Its Inhibitors in Mature Osteoblastic Cells. Calcified Tissue International, 85 (6): 538-545

194. Malfait, A., Williams, R. and Malik, A. et al. (2001) Chronic relapsing homologous collagen-induced arthritis in DBA/1 mice as a model for testing disease-modifying and remission-inducing therapies. Arthritis & Rheumatism, 44 (5): 1215-122

195. Manolagas, S. (2000) Birth and Death of Bone Cells: Basic Regulatory Mechanisms and Implications for the Pathogenesis and Treatment of Osteoporosis. Endocrine Reviews, 21 (2): 115-137

196. Mark, M., Butler, W. and Prince, C. et al. (1988) Developmental expression of 44-kDa bone phosphoprotein (osteopontin) and bone γ-carboxyglutamic acid (Gla)-containing protein (osteocalcin) in calcifying tissues of rat. Differentiation, 37 (2): 123-136

197. Martinez, F., Gordon, S. and Locati, M. et al. (2006) Transcriptional Profiling of the Human Monocyte-to-Macrophage Differentiation and Polarization: New Molecules and Patterns of Gene Expression. The Journal of Immunology, 177 (10): 7303-7311

198. Matyszak, M., Citterio, S. and Rescigno, M. et al. (2000) Differential effects of corticosteroids during different stages of dendritic cell maturation. European Journal of Immunology, 30 (4): 1233-1242

199. McCutcheon, S., Majeska, R. and Spray, D. et al. (2020) Apoptotic Osteocytes Induce RANKL Production in Bystanders via Purinergic Signaling and Activation of Pannexin Channels. Journal of Bone and Mineral Research, 35 (5): 966-977

200. Miller, A., Webb, M. and Copik, A. et al. (2005) p38 Mitogen-Activated Protein Kinase (MAPK) Is a Key Mediator in Glucocorticoid-Induced Apoptosis of Lymphoid Cells: Correlation between p38 MAPK Activation and Site-Specific Phosphorylation of the Human Glucocorticoid Receptor at Serine 211. Molecular Endocrinology, 19 (6): 1569-1583

201. Mirenda, V. (2004) Modified Dendritic Cells Coexpressing Self and Allogeneic Major Histocompatability Complex Molecules: An Efficient Way to

Induce Indirect Pathway Regulation. Journal of the American Society of Nephrology, 15 (4): 987-997

202. Miyamoto, T. (2011) Regulators of Osteoclast Differentiation and Cell-Cell Fusion. The Keio Journal of Medicine, 60 (4): 101-105

203. Mizuno, A., Kanno, T. and Hoshi, M. et al. (2002) Transgenic mice overexpressing soluble osteoclast differentiation factor (sODF) exhibit severe osteoporosis. Journal of Bone and Mineral Metabolism, 20 (6): 337-344

204. Moore, S. and Dawson, K. (1990) Red and yellow marrow in the femur: age-related changes in appearance at MR imaging. Radiology, 175 (1): 219-223

205. Morgan, S., McCabe, E. and Gathercole, L. et al. (2014) 11 -HSD1 is the major regulator of the tissue-specific effects of circulating glucocorticoid excess. Proceedings of the National Academy of Sciences, 111 (24): E2482-E2491

206. Mori, S. and Burr, D. (1993) Increased intracortical remodeling following fatigue damage. Bone, 14 (2): 103-109

207. Moriishi, T., Fukuyama, R. and Ito, M. et al. (2012) Osteocyte Network; a Negative Regulatory System for Bone Mass Augmented by the Induction of Rankl in Osteoblasts and Sost in Osteocytes at Unloading. PLoS ONE, 7 (6): e40143

208. Moser, M., De Smedt, T. and Sornasse, T. et al. (1995) Glucocorticoids down-regulate dendritic cell functionin vitro andin vivo. European Journal of Immunology, 25 (10): 2818-2824

209. Mueller, J., Gilligan, L. and Idkowiak, J. et al. (2015) The Regulation of Steroid Action by Sulfation and Desulfation. Endocrine Reviews, 36 (5): 526-563

210. Nader, N., Chrousos, G. and Kino, T. (2010) Interactions of the circadian CLOCK system and the HPA axis. Trends in Endocrinology & Metabolism, 21 (5): 277-286

211. Nahoum, V., Gangloff, A. and Legrand, P. et al. (2001) Structure of the Human 3α-Hydroxysteroid Dehydrogenase Type 3 in Complex with Testosterone and NADP at 1.25-Å Resolution. Journal of Biological Chemistry, 276 (45): 42091-42098

212. Naito, A., Azuma, S. and Tanaka, S. et al. (1999) Severe osteopetrosis, defective interleukin-1 signalling and lymph node organogenesis inTRAF6-deficient mice. Genes to Cells, 4 (6): 353-362

213. Nakai, Y., Usui, T. and Tsukada, T. et al. (1991) Molecular mechanisms of glucocorticoid inhibition of human proopiomelanocortin gene transcription. The Journal of Steroid Biochemistry and Molecular Biology, 40 (1-3): 301-306

214. Nakamura, Y., Arai, F. and Iwasaki, H. et al. (2010) Isolation and characterization of endosteal niche cell populations that regulate hematopoietic stem cells. Blood, 116 (9): 1422-1432

215. Nakashima, T., Hayashi, M. and Fukunaga, T. et al. (2011) Evidence for osteocyte regulation of bone homeostasis through RANKL expression. Nature Medicine, 17 (10): 1231-1234

216. Nandakumar, K., Bäcklund, J. and Vestberg, M. et al. (2004) Collagen type II (CII)-specific antibodies induce arthritis in the absence of T or B cells but the arthritis progression is enhanced by CII-reactive T cells. Arthritis Research & Therapy, 6 (6): R544-50

217. Navarra, P., Tsagarakis, S. and Faria, M. et al. (1991) Interleukins-1 and -6 Stimulate the Release of Corticotropin-Releasing Hormone-41 from Rat Hypothalamusin Vitrovia the Eicosanoid Cyclooxygenase Pathway*. Endocrinology, 128 (1): 37-44

218. Naylor, A.J., Desanti, G., Saghir, A.N., et al. (2017) TNFA depleting therapy improves fertility and animal welfare in TNFA-driven transgenic models of polyarthritis when administered in their routine breeding. Laboratory Animals, 52 (1): 59–68

219. Nelson, G., Wilde, G. and Spiller, D. et al. (2003) NF-κB signalling is inhibited by glucocorticoid receptor and STAT6 via distinct mechanisms. Journal of Cell Science, 116 (12): 2495-2503

220. Newell-Price, J., Bertagna, X. and Grossman, A. et al. (2006) Cushing's syndrome. The Lancet, 367 (9522): 1605-1617

221. Nicolaides, N., Kyratzi, E. and Lamprokostopoulou, A. et al. (2015) Stress, the Stress System and the Role of Glucocorticoids. Neuroimmunomodulation, 22 (1-2): 6-19

222. Nishida, S., Yamaguchi, A. and Tanizawa, T. et al. (1994) Increased bone formation by intermittent parathyroid hormone administration is due to the stimulation of proliferation and differentiation of osteoprogenitor cells in bone marrow. Bone, 15 (6): 717-723

223. O'Brien, C., Jia, D. and Plotkin, L. et al. (2004) Glucocorticoids Act Directly on Osteoblasts and Osteocytes to Induce Their Apoptosis and Reduce Bone Formation and Strength. Endocrinology, 145 (4): 1835-1841

224. Oakley, R. and Cidlowski, J. (2013) The biology of the glucocorticoid receptor: New signaling mechanisms in health and disease. Journal of Allergy and Clinical Immunology, 132 (5): 1033-1044

225. Oakley, R. and Cidlowski, J. (2015) Glucocorticoid signaling in the heart: A cardiomyocyte perspective. The Journal of Steroid Biochemistry and Molecular Biology, 153: 27-34

226. Obeyesekere, V., Li, K. and Ferrari, P. et al. (1997) Truncation of the N- and C-terminal regions of the human 11β-hydroxysteroid dehydrogenase type 2 enzyme and effects on solubility and bidirectional enzyme activity. Molecular and Cellular Endocrinology, 131 (2): 173-182

227. O'Brien, C., Plotkin, L. and Galli, C. et al. (2008) Control of Bone Mass and Remodeling by PTH Receptor Signaling in Osteocytes. PLoS ONE, 3 (8): e2942

228. O'Connell, N., Kumar, A. and Chatzipanteli, K. et al. (1994) Interleukin-1 regulates corticosterone secretion from the rat adrenal gland through a catecholamine-dependent and prostaglandin E2-independent mechanism. Endocrinology, 135 (1): 460-467

229. Ohnaka, K., Tanabe, M. and Kawate, H. et al. (2005) Glucocorticoid suppresses the canonical Wnt signal in cultured human osteoblasts. Biochemical and Biophysical Research Communications, 329 (1): 177-181

230. O'Malley, B. (1990) MINIREVIEW: The Steroid Receptor Superfamily: More Excitement Predicted for the Future. Molecular Endocrinology, 4 (3): 363-369

231. Oprea, A., Bonnet, N. and Pollé, O. et al. (2019) Novel insights into glucocorticoid replacement therapy for pediatric and adult adrenal insufficiency. Therapeutic Advances in Endocrinology and Metabolism, 10: 204201881882129

232. Orimo, H. (2010) The Mechanism of Mineralization and the Role of Alkaline Phosphatase in Health and Disease. Journal of Nippon Medical School, 77 (1): 4-12

233. Overman, R., Yeh, J. and Deal, C. (2013) Prevalence of oral glucocorticoid usage in the United States: A general population perspective. Arthritis Care & Research, 65 (2): 294-298

234. Page, G. and Miossec, P. (2005) RANK and RANKL expression as markers of dendritic cell-t cell interactions in paired samples of rheumatoid synovium and lymph nodes. Arthritis & Rheumatism, 52 (8): 2307-2312

235. Palmowski, Y., Buttgereit, T. and Dejaco, C. et al. (2017) “Official View” on Glucocorticoids in Rheumatoid Arthritis: A Systematic Review of International

Guidelines and Consensus Statements. Arthritis Care & Research, 69 (8): 1134-1141

236. Palmqvist, P., Persson, E. and Conaway, H. et al. (2002) IL-6, Leukemia Inhibitory Factor, and Oncostatin M Stimulate Bone Resorption and Regulate the Expression of Receptor Activator of NF-κB Ligand, Osteoprotegerin, and Receptor Activator of NF-κB in Mouse Calvariae. The Journal of Immunology, 169 (6): 3353-3362

237. Palmqvist, P., Persson, E. and Conaway, H. et al. (2002) IL-6, Leukemia Inhibitory Factor, and Oncostatin M Stimulate Bone Resorption and Regulate the Expression of Receptor Activator of NF-κB Ligand, Osteoprotegerin, and Receptor Activator of NF-κB in Mouse Calvariae. The Journal of Immunology, 169 (6): 3353-3362

238. Pan, J., Ju, D. and Wang, Q. et al. (2001) Dexamethasone inhibits the antigen presentation of dendritic cells in MHC class II pathway. Immunology Letters, 76 (3): 153-161

239. Pan, M., Kang, I. and Craft, J. et al. (2004) Resistance to Development of Collagen-Induced Arthritis in C57BL/6 Mice Is Due to a Defect in Secondary, but Not in Primary, Immune Response. Journal of Clinical Immunology, 24 (5): 481-491

240. Paredes, R., Arriagada, G. and Cruzat, F. et al. (2004) The Runx2 transcription factor plays a key role in the 1α,25-dihydroxy Vitamin D3-dependent upregulation of the rat osteocalcin (OC) gene expression in osteoblastic cells. The Journal of Steroid Biochemistry and Molecular Biology, 89-90: 269-271

241. Parvin, R., Saito-Hakoda, A. and Shimada, H. et al. (2017) Role of NeuroD1 on the negative regulation of Pomc expression by glucocorticoid. PLOS ONE, 12 (4): e0175435

242. Patil, R., Naveen Kumar, M. and Kiran Kumar, K. et al. (2018) Dexamethasone inhibits inflammatory response via down regulation of AP-1 transcription factor in human lung epithelial cells. Gene, 645: 85-94

243. Pauli, U. (1994) Control of Tumor Necrosis Factor Gene Expression. Critical Reviews™in Eukaryotic Gene Expression, 4 (2-3): 323-344

244. Penning, T., Chen, M. and Jin, Y. (2015) Promiscuity and diversity in 3-ketosteroid reductases. The Journal of Steroid Biochemistry and Molecular Biology, 151: 93-101

245. Perizzolo, D., Lacefield, W. and Brunette, D. (2001) Interaction between topography and coating in the formation of bone nodules in culture for

hydroxyapatite- and titanium-coated micromachined surfaces. Journal of Biomedical Materials Research, 56 (4): 494-503

246. Picard, D., Salser, S. and Yamamoto, K. (1988) A movable and regulable inactivation function within the steroid binding domain of the glucocorticoid receptor. Cell, 54 (7): 1073-1080

247. Piemonti, L., Monti, P. and Allavena, P. et al. (1999) Glucocorticoids affect human dendritic cell differentiation and maturation. J Immunol, 162 (11): 6473-81

248. Pivonello, R., Simeoli, C. and De Martino, M. et al. (2015) Neuropsychiatric disorders in Cushing's syndrome. Frontiers in Neuroscience, 9 (129): 1-6

249. Poole, K., Van Bezooijen, R. and Loveridge, N. et al. (2005) Sclerostin is a delayed secreted product of osteocytes that inhibits bone formation. The FASEB Journal, 19 (13): 1842-1844

250. Pratt, W. and Toft, D. (1997) Steroid Receptor Interactions with Heat Shock Protein and Immunophilin Chaperones*. Endocrine Reviews, 18 (3): 306-360

251. Prenek, L., Litvai, T. and Balázs, N. et al. (2020) Regulatory T cells are less sensitive to glucocorticoid hormone induced apoptosis than CD4+ T cells. Apoptosis, 25 (9-10): 715-729

252. Pujols, L., Mullol, J. and Roca-Ferrer, J. et al. (2002) Expression of glucocorticoid receptor α- and β-isoforms in human cells and tissues. American Journal of Physiology-Cell Physiology, 283 (4): C1324-C1331

253. Quarles, L., Yohay, D. and Lever, L. et al. (1992) Distinct proliferative and differentiated stages of murine MC3T3-E1 cells in culture: An in vitro model of osteoblast development. Journal of Bone and Mineral Research, 7 (6): 683-692

254. Rae, M., Niven, D. and Critchley, H. et al. (2004) Antiinflammatory Steroid Action in Human Ovarian Surface Epithelial Cells. The Journal of Clinical Endocrinology & Metabolism, 89 (9): 4538-4544

255. Rafacho, A., Gonçalves-Neto, L. and Santos-Silva, J. et al. (2014) Pancreatic Alpha-Cell Dysfunction Contributes to the Disruption of Glucose Homeostasis and Compensatory Insulin Hypersecretion in Glucocorticoid-Treated Rats. PLoS ONE, 9 (4): e93531

256. Ragab, A., Nalepka, J. and Bi, Y. et al. (2002) Cytokines synergistically induce osteoclast differentiation: support by immortalized or normal calvarial cells. American Journal of Physiology-Cell Physiology, 283 (3): C679-C687

257. Raisz, L., Pilbeam, C. and Klein-Nulend, J. et al. (1991) Effects and regulation of prostaglandins in bone: Possible implications for the

pathogenesis of osteoporosis. Journal of Bone and Mineral Metabolism, 9 (2): 39-44

258. Ray, A., LaForge, K. and Sehgal, P. (1990) On the mechanism for efficient repression of the interleukin-6 promoter by glucocorticoids: enhancer, TATA box, and RNA start site (Inr motif) occlusion. Molecular and Cellular Biology, 10 (11): 5736-5746

259. Ray, D., Donn, R. and Berry, A. (2006) Glucocorticoid sensitivity: pathology, mutations and clinical implications. Expert Review of Endocrinology & Metabolism, 1 (3): 403-412

260. Razani, B., Reichardt, A. and Cheng, G. (2011) Non-canonical NF-κB signaling activation and regulation: principles and perspectives. Immunological Reviews, 244 (1): 44-54

261. Redlich, K., Görtz, B. and Hayer, S. et al. (2004) Repair of Local Bone Erosions and Reversal of Systemic Bone Loss Upon Therapy with Anti-Tumor Necrosis Factor in Combination with Osteoprotegerin or Parathyroid Hormone in Tumor Necrosis Factor-Mediated Arthritis. The American Journal of Pathology, 164 (2): 543-555

262. Reinholt, F., Widholm, S. and Ek-Rylander, B. et al. (2009) Ultrastructural localization of a tartrate-resistant acid ATPase in bone. Journal of Bone and Mineral Research, 5 (10): 1055-1061

263. Rhen, T. and Cidlowski, J. (2005) Antiinflammatory Action of Glucocorticoids — New Mechanisms for Old Drugs. New England Journal of Medicine, 353 (16): 1711-1723

264. Riggs, B., Khosla, S. and Melton, L. (1998) A Unitary Model for Involutional Osteoporosis: Estrogen Deficiency Causes Both Type I and Type II Osteoporosis in Postmenopausal Women and Contributes to Bone Loss in Aging Men. Journal of Bone and Mineral Research, 13 (5): 763-773

265. Rivers, C., Levy, A. and Hancock, J. et al. (1999) Insertion of an Amino Acid in the DNA-Binding Domain of the Glucocorticoid Receptor as a Result of Alternative Splicing. The Journal of Clinical Endocrinology & Metabolism, 84 (11): 4283-4286

266. Roberts, D., Brown, J. and Medley, N. et al. (2017) Antenatal corticosteroids for accelerating fetal lung maturation for women at risk of preterm birth. Cochrane Database of Systematic Reviews

267. Robling, A., Castillo, A. and Turner, C. (2006) Biomechanical and molecular regulation of bone remodeling. Annual Review of Biomedical Engineering, 8 (1): 455-498

268. Roca, H., Phimphilai, M. and Gopalakrishnan, R. et al. (2005) Cooperative Interactions between RUNX2 and Homeodomain Protein-binding Sites Are Critical for the Osteoblast-specific Expression of the Bone Sialoprotein Gene. Journal of Biological Chemistry, 280 (35): 30845-30855

269. Rog-Zielinska, E., Thomson, A. and Kenyon, C. et al. (2013) Glucocorticoid receptor is required for foetal heart maturation. Human Molecular Genetics, 22 (16): 3269-3282

270. Roland, B. and Funder, J. (1996) Localization of 11beta-hydroxysteroid dehydrogenase type 2 in rat tissues: in situ studies. Endocrinology, 137 (3): 1123-1128

271. Rosenstock, J., Banarer, S. and Fonseca, V. et al. (2010) The 11-β-Hydroxysteroid Dehydrogenase Type 1 Inhibitor INCB13739 Improves Hyperglycemia in Patients With Type 2 Diabetes Inadequately Controlled by Metformin Monotherapy. Diabetes Care, 33 (7): 1516-1522

272. Roy, M. and Roux, S. (2018) Rab GTPases in Osteoclastic Endomembrane Systems. BioMed Research International, 2018: 1-15

273. Rozkova, D., Horvath, R. and Bartunkova, J. et al. (2006) Glucocorticoids severely impair differentiation and antigen presenting function of dendritic cells despite upregulation of Toll-like receptors. Clinical Immunology, 120 (3): 260-271

274. Rubin, J., Biskobing, D. and Jadhav, L. et al. (1998) Dexamethasone Promotes Expression of Membrane-Bound Macrophage Colony-Stimulating Factor in Murine Osteoblast-Like Cells1. Endocrinology, 139 (3): 1006-1012

275. Ruzzin, J., Wagman, A. and Jensen, J. (2005) Glucocorticoid-induced insulin resistance in skeletal muscles: defects in insulin signalling and the effects of a selective glycogen synthase kinase-3 inhibitor. Diabetologia, 48 (10): 2119-2130

276. Sacedón, R., Vicente, A. and Varas, A. et al. (1999) Glucocorticoid-mediated regulation of thymic dendritic cell function. International Immunology, 11 (8): 1217-1224

277. Sagmeister, M., Taylor, A. and Fenton, A. et al. (2018) Glucocorticoid activation by 11β-hydroxysteroid dehydrogenase enzymes in relation to inflammation and glycaemic control in chronic kidney disease: A cross-sectional study. Clinical Endocrinology, 90 (1): 241-249

278. Sakai, D., Helms, S. and Carlstedt-Duke, J. et al. (1988) Hormone-mediated repression: a negative glucocorticoid response element from the bovine prolactin gene. Genes & Development, 2 (9): 1144-1154

279. Salas, M., Evans, S. and Levell, M. et al. (2008) Interleukin-6 and ACTH act synergistically to stimulate the release of corticosterone from adrenal gland cells. Clinical & Experimental Immunology, 79 (3): 470-473

280. Sato, A., Peacock, M. and Bellido, T. (2018) Glucocorticoid Excess in Bone and Muscle. Clinical Reviews in Bone and Mineral Metabolism, 16 (1): 33-47

281. Sato, K., Suematsu, A. and Okamoto, K. et al. (2006) Th17 functions as an osteoclastogenic helper T cell subset that links T cell activation and bone destruction. Journal of Experimental Medicine, 203 (12): 2673-2682

282. Schaaf, M. and Cidlowski, J. (2002) Molecular mechanisms of glucocorticoid action and resistance. The Journal of Steroid Biochemistry and Molecular Biology, 83 (1-5): 37-48

283. Scheinman, R., Cogswell, P. and Lofquist, A. et al. (1995) Role of Transcriptional Activation of IkappaBalpha in Mediation of Immunosuppression by Glucocorticoids. Science, 270 (5234): 283-286

284. Schott, J., Reitter, S. and Philipp, J. et al. (2014) Translational Regulation of Specific mRNAs Controls Feedback Inhibition and Survival during Macrophage Activation. PLoS Genetics, 10 (6): e1004368

285. Schott, J., Reitter, S. and Philipp, J. et al. (2014) Translational Regulation of Specific mRNAs Controls Feedback Inhibition and Survival during Macrophage Activation. PLoS Genetics, 10 (6): e1004368

286. Schuster, D., Maurer, E. and Laggner, C. et al. (2006) The Discovery of New 11β-Hydroxysteroid Dehydrogenase Type 1 Inhibitors by Common Feature Pharmacophore Modeling and Virtual Screening. Journal of Medicinal Chemistry, 49 (12): 3454-3466

287. Semënov, M., Tamai, K. and Brott, B. et al. (2001) Head inducer Dickkopf-1 is a ligand for Wnt coreceptor LRP6. Current Biology, 11 (12): 951-961

288. Semënov, M., Tamai, K. and He, X. (2005) SOST Is a Ligand for LRP5/LRP6 and a Wnt Signaling Inhibitor. Journal of Biological Chemistry, 280 (29): 26770-26775

289. Semjonous, N.M., Sherlock, M., Jeyasuria, P., et al. (2011) Hexose-6-phosphate dehydrogenase contributes to skeletal muscle homeostasis independent of 11β-hydroxysteroid dehydrogenase type 1. Endocrinology, 152 (1): 93–102

290. Servaty, R., Schiller, J. and Binder, H. et al. (2001) Hydration of polymeric components of cartilage — an infrared spectroscopic study on hyaluronic acid and chondroitin sulfate. International Journal of Biological Macromolecules, 28 (2): 121-127

291. Sevilla, L., Jiménez-Panizo, A. and Alegre-Martí, A. et al. (2021) Glucocorticoid Resistance: Interference between the Glucocorticoid Receptor and the MAPK Signalling Pathways. International Journal of Molecular Sciences, 22 (18): 10049

292. Shah, S., Pishvaian, M. and Easwaran, V. et al. (2002) The Role of Cadherin, β-Catenin, and AP-1 in Retinoid-regulated Carcinoma Cell Differentiation and Proliferation. Journal of Biological Chemistry, 277 (28): 25313-25322

293. Silver, I. (1988) Microelectrode studies on the acid microenvironment beneath adherent macrophages and osteoclasts*1. Experimental Cell Research, 175 (2): 266-276

294. Silverstein, F., Faich, G. and Goldstein, J. et al. (2000) Gastrointestinal Toxicity With Celecoxib vs Nonsteroidal Anti-inflammatory Drugs for Osteoarthritis and Rheumatoid Arthritis. JAMA, 284 (10): 1247

295. Simonet, W., Lacey, D. and Dunstan, C. et al. (1997) Osteoprotegerin: A Novel Secreted Protein Involved in the Regulation of Bone Density. Cell, 89 (2): 309-319

296. Simpson, E. and Waterman, M. (1988) Regulation of the Synthesis of Steroidogenic Enzymes in Adrenal Cortical Cells by ACTH. Annual Review of Physiology, 50 (1): 427-440

297. Smoak, K. and Cidlowski, J. (2004) Mechanisms of glucocorticoid receptor signaling during inflammation. Mechanisms of Ageing and Development, 125 (10-11): 697-706

298. Smolen, J., Aletaha, D. and McInnes, I. (2016) Rheumatoid arthritis. The Lancet, 388 (10055): 2023-2038

299. Song, J., Pineault, K. and Dones, J. et al. (2020) Hox genes maintain critical roles in the adult skeleton. Proceedings of the National Academy of Sciences, 117 (13): 7296-7304

300. Spinedi, E., Hadid, R. and Daneva, T. et al. (1992) Cytokines Stimulate the CRH but Not the Vasopressin Neuronal System: Evidence for a Median Eminence Site of Interleukin-6 Action. Neuroendocrinology, 56 (1): 46-53

301. Stalmans, W. and Laloux, M. (1979) Glucocorticoids and Hepatic Glycogen Metabolism. Glucocorticoid Hormone Action, pp. 517-533

302. Stein, G., Lian, J. and Stein, J. et al. (1996) Transcriptional control of osteoblast growth and differentiation. Physiological Reviews, 76 (2): 593-629

303. Straub, R. and Cutolo, M. (2016) Glucocorticoids and chronic inflammation. Rheumatology, 55 (suppl 2): ii6-ii14

304. Stuart, J. and Dixon, F. (1983) Serum transfer of collagen-induced arthritis in mice. Journal of Experimental Medicine, 158 (2): 378-392

305. Subramaniam, N., Cairns, W. and Okret, S. (1998) Glucocorticoids Repress Transcription from a Negative Glucocorticoid Response Element Recognized by Two Homeodomain-containing Proteins, Pbx and Oct-1. Journal of Biological Chemistry, 273 (36): 23567-23574

306. Sugawara, Y., Suzuki, K. and Koshikawa, M. et al. (2002) Necessity of Enzymatic Activity of Alkaline Phosphatase for Mineralization of Osteoblastic Cells. Japanese Journal of Pharmacology, 88 (3): 262-269

307. Sun, K. and Myatt, L. (2003) Enhancement of Glucocorticoid-Induced 11β-Hydroxysteroid Dehydrogenase Type 1 Expression by Proinflammatory Cytokines in Cultured Human Amnion Fibroblasts. Endocrinology, 144 (12): 5568-5577

308. Swanson, C., Lorentzon, M. and Conaway, H. et al. (2006) Glucocorticoid Regulation of Osteoclast Differentiation and Expression of Receptor Activator of Nuclear Factor-κB (NF-κB) Ligand, Osteoprotegerin, and Receptor Activator of NF-κB in Mouse Calvarial Bones. Endocrinology, 147 (7): 3613-3622

309. Takayanagi, H., Ogasawara, K. and Hida, S. et al. (2000) T-cell-mediated regulation of osteoclastogenesis by signalling cross-talk between RANKL and IFN-γ. Nature, 408 (6812): 600-605

310. Takuma, A., Kaneda, T. and Sato, T. et al. (2003) Dexamethasone Enhances Osteoclast Formation Synergistically with Transforming Growth Factor-β by Stimulating the Priming of Osteoclast Progenitors for Differentiation into Osteoclasts. Journal of Biological Chemistry, 278 (45): 44667-44674

311. Tang, Y., Getzenberg, R. and Vietmeier, B. et al. (1998) The DNA-Binding and τ2 Transactivation Domains of the Rat Glucocorticoid Receptor Constitute a Nuclear Matrix-Targeting Signal. Molecular Endocrinology, 12 (9): 1420-1431

312. Tang, Y., Wu, X. and Lei, W. et al. (2009) TGF-β1–induced migration of bone mesenchymal stem cells couples bone resorption with formation. Nature Medicine, 15 (7): 757-765

313. Teelucksingh, S., Mackie, A. and Burt, D. et al. (1990) Potentiation of hydrocortisone activity in skin by glycyrrhetinic acid. The Lancet, 335 (8697): 1060-1063

314. Teitelbaum, S. (2007) Osteoclasts: What Do They Do and How Do They Do It?. The American Journal of Pathology, 170 (2): 427-435

315. Terrando, N., Monaco, C. and Ma, D. et al. (2010) Tumor necrosis factor- triggers a cytokine cascade yielding postoperative cognitive decline. Proceedings of the National Academy of Sciences, 107 (47): 20518-20522

316. Teti, A., Blair, H. and Teitelbaum, S. et al. (1989) Cytoplasmic pH regulation and chloride/bicarbonate exchange in avian osteoclasts. Journal of Clinical Investigation, 83 (1): 227-233

317. Tolar, J., Teitelbaum, S. and Orchard, P. (2004) Osteopetrosis. New England Journal of Medicine, 351 (27): 2839-2849i

318. Tominaga, T., Fukata, J. and Naito, Y. et al. (1991) Prostaglandin-Dependent in Vitro Stimulation of Adrenocortical Steroidogenesis by Interleukins*. Endocrinology, 128 (1): 526-531

319. Tu, J., Stoner, S. and Fromm, P. et al. (2017) Endogenous glucocorticoid signaling in chondrocytes attenuates joint inflammation and damage. The FASEB Journal, 32 (1): 478-487

320. Tuckermann, J., Kleiman, A. and Moriggl, R. et al. (2007) Macrophages and neutrophils are the targets for immune suppression by glucocorticoids in contact allergy. Journal of Clinical Investigation, 117 (5): 1381-1390

321. Turesson, C. (2013) Extra-articular rheumatoid arthritis. Current Opinion in Rheumatology, 25 (3): 360-366

322. Turner, J., Schote, A. and Keipes, M. et al. (2007) A New Transcript Splice Variant of the Human Glucocorticoid Receptor: Identification and Tissue Distribution of hGR 313-338, an Alternative Exon 2 Transactivation Domain Isoform. Annals of the New York Academy of Sciences, 1095 (1): 334-341

323. Uhlenhaut, N., Barish, G. and Yu, R. et al. (2013) Insights into Negative Regulation by the Glucocorticoid Receptor from Genome-wide Profiling of Inflammatory Cistromes. Molecular Cell, 49 (1): 158-171

324. Ulrich-Lai, Y., Arnhold, M. and Engeland, W. (2006) Adrenal splanchnic innervation contributes to the diurnal rhythm of plasma corticosterone in rats by modulating adrenal sensitivity to ACTH. American Journal of Physiology-Regulatory, Integrative and Comparative Physiology, 290 (4): R1128-R1135

325. Van der Goes, A., Hoekstra, K. and van den Berg, T. et al. (2000) Dexamethasone promotes phagocytosis and bacterial killing by human monocytes/macrophages in vitro. Journal of Leukocyte Biology, 67 (6): 801-807

326. van Staa, T. (2000) Use of oral corticosteroids in the United Kingdom. QJM, 93 (2): 105-111

327. Van Staa, T., Geusens, P. and Bijlsma, J. et al. (2006) Clinical assessment of the long-term risk of fracture in patients with rheumatoid arthritis. Arthritis & Rheumatism, 54 (10): 3104-3112

328. van Staa, T., Leufkens, H. and Cooper, C. (2002) The Epidemiology of Corticosteroid-Induced Osteoporosis: a Meta-analysis. Osteoporosis International, 13 (10): 777-787

329. Vassiliadi, D., Barber, T. and Hughes, B. et al. (2009) Increased 5α-Reductase Activity and Adrenocortical Drive in Women with Polycystic Ovary Syndrome. The Journal of Clinical Endocrinology & Metabolism, 94 (9): 3558-3566

330. Verheul, M., Fearon, U. and Trouw, L. et al. (2015) Biomarkers for rheumatoid and psoriatic arthritis. Clinical Immunology, 161 (1): 2-10

331. Villagra, A., Cruzat, F. and Carvallo, L. et al. (2006) Chromatin Remodeling and Transcriptional Activity of the Bone-specific Osteocalcin Gene Require CCAAT/Enhancer-binding Protein β-dependent Recruitment of SWI/SNF Activity. Journal of Biological Chemistry, 281 (32): 22695-22706

332. Waage, A., Slupphaug, G. and Shalaby, R. (1990) Glucocorticoids inhibit the production of IL 6 from monocytes, endothelial cells and fibroblasts. European Journal of Immunology, 20 (11): 2439-2443

333. Walker, B., Connacher, A. and Lindsay, R. et al. (1995) Carbenoxolone increases hepatic insulin sensitivity in man: a novel role for 11-oxosteroid reductase in enhancing glucocorticoid receptor activation. The Journal of Clinical Endocrinology & Metabolism, 80 (11): 3155-3159

334. Wang, D., Yin, Y. and Yang, Y. et al. (2014) Resveratrol prevents TNF-α-induced muscle atrophy via regulation of Akt/mTOR/FoxO1 signaling in C2C12 myotubes. International Immunopharmacology, 19 (2): 206-213

335. Watanabe, M., Yagi, M. and Omata, M. et al. (1991) Stimulation of neutrophil adherence to vascular endothelial cells by histamine and thrombin and its inhibition by PAF antagonists and dexamethasone. British Journal of Pharmacology, 102 (1): 239-245

336. Wei, S., Kitaura, H. and Zhou, P. et al. (2005) IL-1 mediates TNF-induced osteoclastogenesis. Journal of Clinical Investigation, 115 (2): 282-290

337. Wei, X., Zhang, X. and Zuscik, M. et al. (2005) Fibroblasts Express RANKL and Support Osteoclastogenesis in a COX-2-Dependent Manner After Stimulation With Titanium Particles. Journal of Bone and Mineral Research, 20 (7): 1136-1148

338. Weinstein, R. (2001) Glucocorticoid-induced osteoporosis. Reviews in Endocrine and Metabolic Disorders, 2 (1): 65-73

339. Weinstein, R., Jilka, R. and Parfitt, A. et al. (1998) Inhibition of osteoblastogenesis and promotion of apoptosis of osteoblasts and osteocytes by glucocorticoids. Potential mechanisms of their deleterious effects on bone. Journal of Clinical Investigation, 102 (2): 274-282

340. Westendorf, J., Kahler, R. and Schroeder, T. (2004) Wnt signaling in osteoblasts and bone diseases. Gene, 341: 19-39

341. Whorwood, C., Ricketts, M. and Stewart, P. (1994) Epithelial cell localization of type 2 11 beta-hydroxysteroid dehydrogenase in rat and human colon. Endocrinology, 135 (6): 2533-2541

342. Wikström, A., Okret, O. and Bakke, O. et al. (1986) Glucocorticoid mechanism of action: Monoclonal antibodies as experimental tools. Medical Oncology and Tumor Pharmacotherapy, 3 (3-4)

343. Winkler, D. (2003) Osteocyte control of bone formation via sclerostin, a novel BMP antagonist. The EMBO Journal, 22 (23): 6267-6276

344. Wise, J., Hendler, R. and Felig, P. (1973) Influence of Glucocorticoids on Glucagon Secretion and Plasma Amino Acid Concentrations in Man. Journal of Clinical Investigation, 52 (11): 2774-2782

345. Wolf, J., Kapral, T. and Grisar, J. et al. (2008) Glucocorticoid treatment in rheumatoid arthritis: low-dose therapy does not reduce responsiveness to higher doses. Clin Exp Rheumatol, 26 (1): 113-6

346. Woloski, B., Smith, E. and Meyer, W. et al. (1985) Corticotropin-releasing activity of monokines. Science, 230 (4729): 1035-1037

347. Wong, M., Rao, L. and Ly, H. et al. (2009) Long-term effects of physiologic concentrations of dexamethasone on human bone-derived cells. Journal of Bone and Mineral Research, 5 (8): 803-813

348. Wüst, S., van den Brandt, J. and Tischner, D. et al. (2008) Peripheral T Cells Are the Therapeutic Targets of Glucocorticoids in Experimental Autoimmune Encephalomyelitis. The Journal of Immunology, 180 (12): 8434-8443

349. Xian, L., Wu, X. and Pang, L. et al. (2012) Matrix IGF-1 maintains bone mass by activation of mTOR in mesenchymal stem cells. Nature Medicine, 18 (7): 1095-1101

350. Xiong, J., Piemontese, M. and Thostenson, J. et al. (2014) Osteocyte-derived RANKL is a critical mediator of the increased bone resorption caused by dietary calcium deficiency. Bone, 66: 146-154

351. Yang, C., Frei, H. and Burt, H. et al. (2009) Effects of continuous and pulsatile PTH treatments on rat bone marrow stromal cells. Biochemical and Biophysical Research Communications, 380 (4): 791-796

352. Yang-Yen, H., Chambard, J. and Sun, Y. et al. (1990) Transcriptional interference between c-Jun and the glucocorticoid receptor: Mutual inhibition of DNA binding due to direct protein-protein interaction. Cell, 62 (6): 1205-1215

353. Yavropoulou, M., Vafiadou, H. and Anastasiou, O. et al. (2008) Pioglitazone affects bone resorption but not bone formation. Bone, 42: S91

354. Yoshino, S., Schlipköter, E. and Kinne, R. et al. (1990) Suppression and prevention of adjuvant arthritis in rats by a monoclonal antibody to the α/β T cell receptor. European Journal of Immunology, 20 (12): 2805-2808

355. Yoshitake, F., Itoh, S. and Narita, H. et al. (2008) Interleukin-6 Directly Inhibits Osteoclast Differentiation by Suppressing Receptor Activator of NF-κB Signaling Pathways. Journal of Biological Chemistry, 283 (17): 11535-11540

356. Yu, K., Xu, J., Liu, Z., et al. (2003) Conditional inactivation of FGF receptor 2 reveals an essential role for FGF signaling in the regulation of osteoblast function and bone growth. Development, 130 (13): 3063–3074

357. Yuan, Q., Jiang, Y. and Zhao, X. et al. (2014) Increased Osteopontin Contributes to Inhibition of Bone Mineralization in FGF23-Deficient Mice. Journal of Bone and Mineral Research, 29 (3): 693-704

358. Yy, Y., Yang, D. and Qiu, L. et al. (2014) Tumor necrosis factor-α induces interleukin-34 expression through nuclear factor-κB activation in MC3T3-E1 osteoblastic cells. Molecular Medicine Reports, 10 (3): 1371-1376

359. Zabotti, A., Salvin, S. and Quartuccio, L. et al. (2016) Differentiation between early rheumatoid and early psoriatic arthritis by the ultrasonographic study of the synovio-entheseal complex of the small joints of the hands. Clin Exp Rheumatol, 34 (3): 459-65

360. Zaidi, M. (2007) Skeletal remodeling in health and disease. Nature Medicine, 13 (7): 791-801

361. Zhao, C., Irie, N. and Takada, Y. et al. (2006) Bidirectional ephrinB2-EphB4 signaling controls bone homeostasis. Cell Metabolism, 4 (2): 111-121

362. Zhao, Q., Wang, X. and Liu, Y. et al. (2010) NFATc1: Functions in osteoclasts. The International Journal of Biochemistry & Cell Biology, 42 (5): 576-579

363. Zhou, H., Mak, W. and Zheng, Y. et al. (2008) Osteoblasts Directly Control Lineage Commitment of Mesenchymal Progenitor Cells through Wnt Signaling. Journal of Biological Chemistry, 283 (4): 1936-1945

364. Zoorob, R. and Cender, D. (1998) A different look at corticosteroids. Am Fam Physician, 58 (2): 443-50

Appendix

mRNA genes	Assay Accession number/ ID
18S	Hs03003631_g1
GILZ	Hs00608272_m1
BGLAP	Hs01587814_g1
RANKL	Hs00243522_m1
ALPL	Hs01029144_m1
RUNX2	Hs01047973_m1
OPG	Hs00900358_m1
DKK-1	Hs00183740_m1
WNT 10B	Hs01045906_m1
WNT 11	Hs01045906_m1
IL1β	Hs01555410_m1
IL6	Hs00174131_m1

Appendix table 1: The table details the assay accession ID numbers for the genes used for mRNA work within the thesis.

Fenton et al. Arthritis Research & Therapy (2019) 21:188
https://doi.org/10.1186/s13075-019-1972-1

Arthritis Research & Therapy

RESEARCH ARTICLE Open Access

11ß-HSD1 plays a critical role in trabecular bone loss associated with systemic glucocorticoid therapy

C. G. Fenton[1,2], C. L. Doig[1], S. Fareed[2], A. Naylor[1], A. P. Morrell[3], O. Addison[4,5], C. Wehmeyer[1], C. D. Buckley[1], M. S. Cooper[6], G. G. Lavery[2], K. Raza[1,7] and R. S. Hardy[1,2*]

Abstract

Background: Despite their efficacy in the treatment of chronic inflammation, the prolonged application of therapeutic glucocorticoids (GCs) is limited by significant systemic side effects including glucocorticoid-induced osteoporosis (GIOP). 11β-Hydroxysteroid dehydrogenase type 1 (11β-HSD1) is a bi-directional enzyme that primarily activates GCs in vivo, regulating tissue-specific exposure to active GC. We aimed to determine the contribution of 11β-HSD1 to GIOP.

Methods: Wild type (WT) and 11β-HSD1 knockout (KO) mice were treated with corticosterone (100 μg/ml, 0.66% ethanol) or vehicle (0.66% ethanol) in drinking water over 4 weeks (six animals per group). Bone parameters were assessed by micro-CT, sub-micron absorption tomography and serum markers of bone metabolism. Osteoblast and osteoclast gene expression was assessed by quantitative RT-PCR.

Results: Wild type mice receiving corticosterone developed marked trabecular bone loss with reduced bone volume to tissue volume (BV/TV), trabecular thickness (Tb.Th) and trabecular number (Tb.N). Histomorphometric analysis revealed a dramatic reduction in osteoblast numbers. This was matched by a significant reduction in the serum marker of osteoblast bone formation P1NP and gene expression of the osteoblast markers *Alp* and *Bglap*. In contrast, 11β-HSD1 KO mice receiving corticosterone demonstrated almost complete protection from trabecular bone loss, with partial protection from the decrease in osteoblast numbers and markers of bone formation relative to WT counterparts receiving corticosterone.

Conclusions: This study demonstrates that 11β-HSD1 plays a critical role in GIOP, mediating GC suppression of anabolic bone formation and reduced bone volume secondary to a decrease in osteoblast numbers. This raises the intriguing possibility that therapeutic inhibitors of 11β-HSD1 may be effective in preventing GIOP in patients receiving therapeutic steroids.

Keywords: Glucocorticoids, Osteoporosis, 11β-HSD1, Trabecular bone

Introduction

Therapeutic glucocorticoids (GCs) show marked efficacy in the treatment of chronic inflammatory conditions. Unfortunately, prolonged exposure to GCs results in severe adverse metabolic side effects including osteoporosis, insulin resistance and obesity, severely limiting their long-term therapeutic application [1–3]. Glucocorticoid-induced osteoporosis (GIOP) is common in patients receiving therapeutic GCs with 30–50% of patients developing decreased bone mineral density and increased fracture risk within 6 months [4–6]. Several mechanisms have been proposed whereby GCs cause loss of bone mineral density and deterioration in bone architecture. Chief amongst these is the direct inhibition of the osteoid-forming osteoblasts within bone, as evidenced by a marked and rapid suppression of serum P1NP and osteocalcin in patients receiving the therapeutic GC prednisolone [7]. In addition, GCs cause increased

* Correspondence: r.hardy@bham.ac.uk
[1]Institute of Inflammation and Ageing, University of Birmingham, Birmingham, UK
[2]Institute of Metabolism and Systems Research, University of Birmingham, Birmingham, UK
Full list of author information is available at the end of the article

Therapeutic glucocorticoids prevent bone loss but drive muscle wasting when administered in chronic polyarthritis

Fenton, Chloe; Webster, Justine; Martin, Claire; Fareed, Syeda; Wehmeyer, C; Mackie, H; Jones, Rebecca; Seabright, Alex; Lewis, Jonathan; Lai, Yu-Chiang; Goodyear, C S; Jones, Simon; Cooper, M. S.; Lavery, Gareth; Langen, R; Raza, Karim; Hardy, Rowan

DOI:
10.1186/s13075-019-1962-3